Juuso Leskinen

Constraining inflationary scalar field models with CMB spectral distortions

Licentiate thesis

June 12, 2020

Department of Physics
Faculty of Mathematics and Science
UNIVERSITY OF JYVÄSKYLÄ 2020

ABSTRACT

Leskinen, Juuso
Constraining inflationary scalar field models with CMB spectral distortions
Jyväskylä: University of Jyväskylä, 2020, 86 p.(+included articles)
(Jyväskylä Licentiate Theses in Theoretical Physics)

The Cosmic Microwave Background (CMB) demonstrates extreme uniformity, with only small temperature anisotropies of the order of $\mathcal{O}\left(10^{-5}\right)$. These anisotropies are believed to originate from primordial density perturbations, caused by quantum fluctuations of scalar fields during the cosmic inflation. In the canonical scenario, the single-field slow-roll inflation, these perturbations are assumed to be sourced by one field, the inflaton. However, it is possible that there are multiple fields present during inflation, that give contribution to the perturbations.

In addition to the temperature anisotropies, the CMB spectrum encodes a wealth of information on the thermal history of the early universe. The measured frequency spectrum of the CMB is remarkably close to a black-body spectrum, meaning that the photons and electrons in the early universe plasma were extremely close to a thermal equilibrium. However, in the concordance model of cosmology, ΛCDM, there are mechanisms present that lead to unavoidable deviations from the black-body, dubbed as spectral distortions. The diffusion of the acoustic oscillations, that are created due to the initial perturbations, leads to mixing of photons of different temperatures, creating of spectral distortions, which are expected to be below the current observational sensitivity. In the literature, this mechanism is dubbed as the Silk damping.

In this thesis we study the formation of μ-type spectral distortions due to the Silk damping in models, where the primordial perturbations are sourced by multiple scalar fields. Our main task is to investigate the spectral distortion signal of inflationary two-field models. We find that generally, the μ-signal can be greatly enhanced compared to the single-field model value. We further show that in a specific two-field model, the mixed inflaton-curvaton model, the μ-distortion testable by future CMB surveys in conjunction with bounds on the tensor-to-scalar ratio r, can efficiently constrain the curvaton model parameter space.

Keywords: inflation, many field models, curvaton, primordial perturbations, cosmic microwave background, spectral distortions, μ-distortion

Author

Juuso Leskinen
Department of Physics
University of Jyväskylä
Finland

Supervisor

Sami Nurmi, Senior Lecturer
Department of Physics
University of Jyväskylä
Finland

Reviewers

Syksy Räsänen, Title of Docent
Department of Physics
University of Helsinki
Finland

Kimmo Tuominen, Title of Docent
Department of Physics
University of Helsinki
Finland

PREFACE

“Minä olen valvonut tuhat yötä
Tehnyt työtä tyhjää niin kuin kuolemaa”

— Timo Turunen (Tenavatähti 1990),
“Minä olen muistanut” (san. E. Kettunen)

ACKNOWLEDGEMENTS

I would like to express my gratitude to my friends, colleagues and family both inside and outside of academia. Especially I want to thank my supervisor Sami Nurmi, my professor Kimmo Kainulainen and my fellow students Olli Koskivaara and Laura Laulumaa, with whom I've had the pleasure of discussing the intricacies of physics and beyond (most importantly weight-lifting and cinema), and who have been an important part of my life for the better part of a decade.

I also want to thank the staff and students in the Department of Physics, who have all contributed to the warm atmosphere and humanity present in the daily life of the department. I also thank the Jenny and Antti Wihuri Foundation for keeping me financially afloat during the last three years of my studies.

CONTENTS

LIST OF PUBLICATIONS

PI Kimmo Kainulainen, Juuso Leskinen, Sami Nurmi and Tomo Takahashi. "CMB spectral distortions in generic two-field models". JCAP **1711**, 11, 002 (2017). doi: 10.1088/1475-7516/2017/11/002.

The author has contributed significantly to the analysis, theoretical calculations and the numerical code of the joint publication. The basis of the numerical code was written by Kimmo Kainulainen and thereafter substantially modified and extended by the author. The author wrote the first draft of the publication with Sami Nurmi, while the published version was finalized jointly by all authors.

1 INTRODUCTION

Modern cosmology gives a description of the history of the universe that spans from the time when the universe was only picoseconds old to 14 billion years later, the present day. The concordance model of cosmology, ΛCDM, describes how the light elements such as hydrogen and helium were formed, the formation of the observed cosmic microwave background (CMB), and the distribution of large-scale structures in our expanding universe. There are still open questions on its foundations such as the microscopic nature of dark matter and dark energy, and the exact mechanism for the baryon asymmetry, i.e. how the abundance of matter overwhelms antimatter in our universe.

Cosmic inflation, i.e. a very early universe epoch of accelerated expansion, appears to be a key element of large-scale structure and the evolution of the universe. The inflationary paradigm can explain the temperature anisotropies seen in the CMB, that are believed to originate from the primordial density perturbations. These perturbations are in turn assumed to be caused by the quantum fluctuations of scalar fields during the cosmic inflation, but the microscopic nature of these fields is still not known. In addition to the temperature anisotropies, the primordial curvature perturbations can leave an imprint on the CMB as deviations from the pure black-body, dubbed as the spectral distortions. The prediction for the spectral distortions depends on details of the inflationary model: for example, whether the primordial perturbations are sourced by a single or multiple scalar fields.

The thesis is organized as follows. We start by giving a brief introduction of the generalities of the standard model of cosmology: we discuss thermal history of the universe and the formation of the CMB, the inflationary paradigm and the primordial perturbations. In Chapters 2 and 3, we concentrate on the computation of primordial curvature power spectrum due to the fluctuations of scalar fields. We will use both the linear order cosmological perturbation theory and the ΔN formalism in the computation. Chapter 4 is devoted to the discussion on the CMB spectral distortions: we give a review on the literature and compute the prediction for μ-distortion in the canonical single-field slow-roll inflation. In Chapter 5, we discuss the scientific work related to this thesis, where we study the formation of μ-type spectral distortions due to the diffusion of primordial perturbations in models, where the primordial perturbations are sourced by two scalar fields. We conclude the thesis in Chapter 6.

1.1 The Friedmann—Lemaître—Robertson—Walker Cosmology

On large distance scales, i.e. distances larger than $\mathcal{O}(100)$ Mpc, the universe seems to be rather homogeneous and isotropic, i.e. all places and directions look the same [1, 2]. For smaller scales one obviously sees structures such as galax-

ies and super clusters, but to a first approximation these can be neglected. In the early universe — before the structure formation — the homogeneous and isotropic universe is even better approximation. In the standard model of cosmology one thus adopts the Robertson—Walker metric, which is the most general metric that describes a homogeneous and isotropic universe [3]:

$$\mathrm{d}s^2 = -\mathrm{d}t^2 + a^2(t)\left(\frac{\mathrm{d}r^2}{1-Kr^2} + r^2\mathrm{d}\theta^2 + r^2\sin^2(\theta)\,\mathrm{d}\phi^2\right), \tag{1}$$

where t is the physical time, $a(t)$ is the scale factor that describes the evolution of distances and thereof the expansion of the universe, and the three-metric part represents the spatial line element in comoving spherical coordinates. The parameter K describes the geometry of the universe: positive, negative and zero — or values $K = \{1, -1, 0\}$ — curvature indicate closed, open and flat universe [3]. Note that in this work we use the natural units, i.e. we set $\hbar = c = k_\mathrm{B} = 1$.

The evolution of the scale factor $a(t)$ depends on the energy content of the universe. The equations of motion for the scale factor can be derived by starting from the Einstein equations [1]

$$G_{\mu\nu} = R_{\mu\nu} - \frac{1}{2}g_{\mu\nu}R = M_\mathrm{Pl}^{-2}T_{\mu\nu}, \tag{2}$$

where $G_{\mu\nu}$ is the Einstein tensor, $g_{\mu\nu}$ is the metric tensor, $R_{\mu\nu}$ and R are respectively the Ricci tensor and Ricci scalar, the reduced Planck mass is defined as $M_\mathrm{Pl} = (8\pi G_\mathrm{N})^{-1/2}$, where G_N is the Newton gravitational constant and $T_{\mu\nu}$ is the energy-momentum tensor. The information of the geometry of the universe is encoded on the left-hand side of eq. (2), while the information about the energy content of the universe is described by the energy-momentum tensor $T_{\mu\nu}$ on the right-hand side of eq. (2). In the concordance model of cosmology one assumes that the matter content of the universe is described by ideal fluids. In the comoving coordinates, the energy-momentum tensor can be written as

$$T_{\mu\nu} = \mathrm{diag}\left(\rho, p\,\frac{a^2}{1-Kr^2}, p\,a^2r^2, p\,a^2r^2\sin^2(\theta)\right), \tag{3}$$

where ρ and p are the fluid energy density and pressure, respectively. The energy-momentum tensor satisfies the continuity equations $\nabla_\mu T^{\mu\nu} = 0$, which can now be written as

$$\dot{\rho} + 3H(\rho + p) = 0, \tag{4}$$

where $H = \mathrm{d}a/\mathrm{d}t/a = \dot{a}/a$ is the Hubble parameter that measures the expansion rate. For a fluid with a constant equation of state, $p = w\rho$, the scaling of the fluid energy density can be written as

$$\rho(t) \propto a(t)^{-3(1+w)}. \tag{5}$$

[1] Note that we do not include the cosmological constant term $g_{\mu\nu}\Lambda$ on the right-hand side of eq. (2). However, we allow the existence of a vacuum energy ρ_Λ, which has the same effect as the inclusion of the cosmological constant term (one would then define $\rho_\Lambda \equiv M_\mathrm{Pl}^2\Lambda$.

For example, for radiation we have that $w_r = p_r/\rho_r = 1/3$, i.e. $\rho \propto a^{-4}$, while for pressureless non-relativistic matter ($w_m = 0$) we have $\rho_m \propto a^{-3}$. The equation of state parameter w can also be a dynamical quantity, as we will see in Section 1.3, where we discuss the evolution of the inflaton field.

The evolution eqs. for the scale factor $a(t)$ can then be derived by computing the left-hand side of eq. (2) from the metric (1). These eqs. are referred to as the Friedmann equations and are usually written in the following form [3]

$$H^2 = \frac{\rho}{3M_{\rm Pl}^2} - \frac{K}{a} \tag{6}$$

$$\frac{\ddot{a}}{a} = -\frac{\rho + 3p}{6M_{\rm Pl}^2}. \tag{7}$$

From the Friedmann eqs. it is quite straightforward to see how the energy content of the universe affects the evolution of the scale factor and thus the expansion of the universe. We can see that while the energy stored in the matter fluid and the curvature affect the rate of expansion in eq. (6), in the acceleration eq. (7) also the pressure of the fluid contributes to the acceleration of $a(t)$, and thus the overall evolution.

The equation for the Hubble parameter can also be written in terms of the different energy components. In the ΛCDM matter consists of radiation ρ_r, non-relativistic matter (both baryonic and dark matter) ρ_m, vacuum energy which we refer to as the dark energy $\rho_{\rm DE}$ and the energy stored in the curvature ρ_K, hence we have

$$H^2 = H_0^2 \left[\Omega_{r,0} \left(\frac{a_0}{a} \right)^4 + \Omega_{m,0} \left(\frac{a_0}{a} \right)^3 + \Omega_{\rm DE} + \Omega_{K,0} \left(\frac{a_0}{a} \right)^2 \right], \tag{8}$$

where $a_0 = a\,(t_0)$ (it is customary to choose that t_0 refers to the present time), and we defined the density parameter $\Omega_{i,0} = \rho_i/\rho_{\rm cr,0}$, where $\rho_{\rm cr,0} = 3M_{\rm Pl}^2 H_0^2$ is the critical density, which describes the critical value of the energy density related to the curvature of the universe. Note that we defined the curvature density to be $\Omega_{K,0} = -K/a_0^2 H_0^2$. The total energy density can be written as

$$\Omega = 1 + \frac{K}{a^2 H^2} = 1 - \Omega_K. \tag{9}$$

That is, the flat universe with $K = 0$ corresponds to $\Omega = 1$ (or $\rho = \rho_{\rm cr}$), while $\Omega > 1$ to corresponds to closed geometry and $\Omega < 1$ to open geometry. Physically this roughly means that in the case $\rho > \rho_{\rm cr}$ the gravitational pull is strong enough to curve the universe into a closed and finite form, while for $\rho < \rho_{\rm cr}$ the universe is left open and finite. From observations we know that the total energy density of the universe is extremely close to the critical value $\Omega_0 \approx 1$, i.e. the geometry of the universe seems to be flat, and as $|\Omega_K| = |\Omega - 1| \propto t^{2/3}$ (t) in the matter (radiation) dominated epoch, at earlier times $t < t_0$ we would have that $|\Omega - 1|$ would be even closer to zero. In the ΛCDM-model it is then assumed that $\Omega_{K,0} = 0$ [4]. Assuming the base-ΛCDM model, at present the current best-fit values for the different energy components are roughly $\Omega_{m,0} \approx 0.315$, $\Omega_{\rm DE} \approx 0.685$, $\Omega_{r,0} \approx 10^{-5}$ and $H_0 \approx 67.4\,{\rm kms}^{-1}{\rm Mpc}^{-1}$ [4].

1.2 Thermal history and the Cosmic Microwave Background

In this section we give a brief review of the thermal history of the universe. We mainly focus on the creation of the cosmic microwave background and its anisotropies. The given presentation follows closely the refs. [5, 6, 7].

1.2.1 Brief thermal history of the universe

The very early universe was in a very hot and dense state. After the inflationary and reheating epochs (the exponential expansion of space and the creation of particles present in the universe — see Section 1.3), the early universe plasma was in a thermodynamic equilibrium, i.e. the different elementary particles present shared the same temperature T. As the universe expanded, the plasma cooled down, and different particle species started to decouple from plasma as their interaction rates Γ could not keep up with the changing equilibrium due to the expansion described by the Hubble rate H.

In the following we will briefly describe the key events in the thermal history of the universe:

- **Baryogenesis**. During this event the observed over-abundance of matter (baryons) over antimatter was generated. The exact mechanism for the creation of the asymmetry is not known, and the baryogenesis models try to derive the observed baryon-to-photon ratio $\eta = n_b/n_\gamma \sim 10^{-9}$.
- **Electroweak transition** . At $T \sim \mathcal{O}(100)$ GeV, the elementary particles receive their masses via the Higgs mechanism. The corresponding time and redshift are $t \sim 10^{-12}$ s and $z \sim 10^{15}$.
- **QCD phase transition**. At the temperature $T \approx 150$ MeV the previously free quarks and gluons are bound into hadrons (i.e. baryons, three-quark configurations, and mesons, quark-antiquark configurations). In terms of time and redshift this transition happens at $t \sim 10^{-9}$ s and $z \sim 10^{12}$.
- **Neutrino decoupling**. Neutrinos, which only interact via weak interactions, decouple from the thermal bath at $T \sim 1$ MeV $\left(1\text{ s},\ 6 \times 10^9\right)$.
- **Electron-positron annihilation**. Electrons and positrons annihilate shortly after the decoupling of neutrinos (0.5 MeV$, 6$ s$, 2 \times 10^9$), i.e. $e^- + e^+ \rightarrow \gamma + \gamma$. Due to the neutrino decoupling, the annihilation mostly heats up photons, but not the neutrinos, which is why the photon temperature today T_0 is greater than the neutrino temperature $T_{\nu,0}$.
- **(Big Bang) Nucleosynthesis**. The light elements (hydrogen, helium, lithium and beryllium) are formed, when the reactions between neutrons and protons fall out of equilibrium. This happens roughly at $T \sim 100$ keV (10 min$, 10^8$).
- **Matter-radiation equality**. After $z \approx 3400$ (60 000 yr, 0.8 keV), the non-relativistic matter starts to dominate over the radiation.
- **Recombination**. Free protons and electrons combine to form neutral hydrogen via the process $e^- + p \rightarrow H + \gamma$, when the reverse reaction is not efficient. Recombination happens when the universe is roughly 400 000 years

old ($z \sim 1300$, $T \sim 0.3$ eV).

- **Photon decoupling**. Before the recombination the Thomson/Compton scattering , $e^- + \gamma \to e^- + \gamma$, binds the photons to the electrons and rest of the plasma. As the recombination starts the number of free electrons rapidly drops, and the universe becomes electrically neutral. As the Compton scattering becomes inefficient, the photons decouple from the plasma (at the redshift $z \approx 1100$) and start to stream freely through the universe. This is observed as the cosmic microwave background (CMB).
- **Reionization**. The radiation from the formed stars reionizes the interstellar gas when the universe was roughly $\mathcal{O}\left(10^6\right)$ years old ($z \sim \mathcal{O}\left(10\right)$).
- **Dark energy-matter equality**. Dark energy starts to dominate over matter when the universe is 9×10^9 years old ($z \sim 0.4$).

In the next section we will discuss the CMB and its temperature anisotropies.

1.2.2 The Cosmic Microwave Background

As discussed above, the photons decoupled from electrons and baryonic matter at $t_{\text{dec}} \approx 3.8 \times 10^5$ yr, and this last-scattering surface at t_{dec} is referred to as the cosmic microwave background. The temperature of the CMB photons has cooled to the present day value $T_0 = 2.725$ K, and their distribution is extremely close to a black-body distribution (see Chapter 4). The CMB has been mapped to a very high precision, and observed to be highly isotropic with small temperature anisotropies: $T\left(\theta, \varphi\right) = T_0 + \delta T\left(\theta, \varphi\right)$, where the anisotropies are $\delta T \sim \mathcal{O}\left(10^{-5} T_0\right)$ [8, 9]. This great uniformity also introduces a problem, as during the photon decoupling, the scale of causal horizon (i.e. how far information could have propagated, effectively described by the Hubble scale H^{-1}) was such that the CMB consisted of over $\mathcal{O}\left(10^3\right)$ distinct causal patches — the problem being, that how the whole CMB could have thermalized to the same temperature, as there could not have been particle interactions between different causal patches. We will come back to this problem in next section, where we will discuss how the inflation can bring the different patches to causal contact at the very early universe epoch.

These anisotropies are believed to originate from the primordial density fluctuations, which in turn are believed to be generated during inflation from the quantum fluctuations of scalar fields. Due to gravity, these small overdensities grew to form the structures, e.g. galaxies, that we see today. The imprint left on the CMB acts then as a probe to the primordial physics. Quite obviously, a thorough discussion on both the theoretical and experimental side of CMB physics and its connection to the primordial perturbations is well beyond the scope of this work, and in the following we choose to go through some chosen points.

The temperature perturbation today can be decomposed to two different sources [7]

$$\left.\frac{\delta T}{T}\right|_{t_0} = \left.\frac{\delta T}{T}\right|_{\text{intrinsic}} + \left.\frac{\delta T}{T}\right|_{\text{journey}}, \tag{10}$$

where T is the all-sky average temperature, and the first term on the right-hand side describes the original anisotropies in the baryon-photon fluid at $t = t_{\rm dec}$, while the second term describes the possible anisotropies generated as the photons have traveled in the expanding universe from the decoupling time $t_{\rm dec}$ to the present time t_0. The observed anisotropy is usually expanded in spherical harmonics:

$$\frac{\delta T\left(\theta,\varphi\right)}{T} = \sum_{l=1}^{\infty}\sum_{m=-l}^{l} a_{lm} Y_{lm}\left(\theta,\varphi\right), \tag{11}$$

where the information of the primordial density perturbations is encoded in the coefficients a_{lm}. It is customary to define the two-point function[2] of the anisotropies in terms of the angular power spectrum:

$$\left\langle \left(\frac{\delta T\left(\theta,\varphi\right)}{T}\right)^2 \right\rangle = \sum_{l} \frac{2l+1}{4\pi} \widehat{C}_l, \tag{12}$$

where we sky-averaged (over θ and φ) and $\widehat{C}_l$ is the observed angular power spectrum, which is measured per multipole l (larger the multipole, smaller the distance scale). One can also define and compute the theoretical angular power spectrum C_l, and find that the squared difference is

$$\left\langle \left(\widehat{C}_l - C_l\right)^2 \right\rangle = \frac{2}{2l+1} C_l^2, \tag{13}$$

which is dubbed as the cosmic variance, which limits the accuracy in comparing the observed CMB data to the theoretical prediction (there is only one universe/CMB that we can observe). This is also seen in Figure 1, where the scaled angular power spectrum $D_l = \widehat{C}_l T_0^2\, l\left(l+1\right)/2\pi$ is plotted. On the small multipoles, i.e. large distance scales, the statistical error grows. We can also see that the angular power spectrum in Figure 1 has different behaviour on different multipoles. In the following we would like to briefly describe the main effects in the creation of the observed spectrum.

In the case of a instantenous recombination, the evolution of the temperature anisotropy can be approximated as [5]

$$\Theta|_{t=t_0} \approx \left(\Theta+\Psi\right)|_{t=t_{\rm dec}} - \left(\hat{\mathbf{n}}\cdot\mathbf{v}_e\right)|_{t=t_{\rm dec}} + \int_{t_{\rm dec}}^{t_0} \left(\dot{\Psi}+\dot{\Phi}\right) {\rm d}t, \tag{14}$$

where $\Theta = \delta T/T$, Ψ and Φ are gravitational Bardeen potentials, that are related to metric perturbations and are discussed in Chapter 3; as discussed there, one can usually assume that $\Psi = \Phi$. The second term on right-hand side, where $\mathbf{v}_e$ is the electron velocity and $\hat{\mathbf{n}}$ the direction, is dubbed as the Doppler term, that describes the shift in the photon energy as photons scatter off moving electrons. The first term is the Sachs-Wolfe (SW) term, that is combination of the intrinsic

[2] The CMB anisotropies are nearly Gaussian, and for a Gaussian distribution all the information is stored in the two-point correlator.

temperature anisotropy at $t = t_{\rm dec}$ and the gravitational redshift of photons due to the potential wells in the photon-baryon fluid. The last term is referred to as the Integrated Sachs-Wolfe (ISW) term, which takes into account the evolution of gravitational potentials along the line-of-sight — see more details in refs. [5, 7].

On distance scales larger than the Hubble horizon at decoupling, $H^{-1}\left(t_{\rm dec}\right)$, the causal interactions do not affect the primordial density perturbations $\delta\rho/\rho$. On these scales, the SW-term dominates the CMB anisotropies in eq. (14), and one can write $\delta T/T \sim \Phi \sim -\delta\rho_\gamma/\rho_\gamma$ at $t = t_{\rm dec}$ [5]. Note also that the gravitational redshifting SW-term dominates over the intrinsic temperature fluctuations [5]. In Figure 1, these large scales corresponds to the so-called Sachs-Wolfe plateu at multipoles $l < \mathcal{O}\left(100\right)$.

On subhorizon scales, the primordial density fluctuations are affected by the causal interactions in the photon-baryon plasma. Before the decoupling, $t < t_{\rm dec}$, the master evolution equation for the temperature perturbation can be written in the Fourier k-space as [5]

$$\ddot{\Theta}_k + \frac{\mathcal{H}R_{b,\gamma}}{1+R_{b,\gamma}}\dot{\Theta}_k + c_{\rm s}^2 k^2 \Theta_k = -\frac{1}{3}k^2\Psi_k + \ddot{\Phi}_k + \frac{\dot{R}_{b,\gamma}}{1+R_{b,\gamma}}\dot{\Phi}_k, \tag{15}$$

where the comoving Hubble parameter is $\mathcal{H} = aH$, the baryon fraction is $R_{b,\gamma} = 3\rho_b/4\rho_\gamma$ and the sound speed is defined as $c_{\rm s}^2 = \left(3\left(1+R_{b,\gamma}\right)\right)^{-1}$. The sound speed $c_{\rm s}$ is related to the sound horizon $r_{\rm s} = c_{\rm s}\mathcal{H}^{-1}$, which describes the scale on which the causal interactions affect the photon fluctuations. At early times $R_{b,\gamma} \ll 1$ and $c_{\rm s} \approx 1/\sqrt{3}$, i.e. the sound horizon is nearly equal to the comoving Hubble radius $\mathcal{H}^{-1}$. However, just before the photon decoupling the baryon ratio $R_{b,\gamma}$ becomes significant and the sound horizon $r_{\rm s}$ is significantly smaller than the Hubble radius [5].

The photon fluctuations are effectively frozen until they cross the sound horizon $r_{\rm s}$. After the crossing, they start to oscillate according to eq. (15), and this oscillatory behaviour is usually referred to as the acoustic oscillations. As the photons decouple, these oscillations leave an imprint on the CMB sky, which can be seen in Figure 1 at multipoles $l > \mathcal{O}\left(100\right)$. The seen acoustic peaks allow one to probe the early universe physics: for example, the gravitional potentials are probe to the baryonic matter and dark matter, and the sound speed probes the ratio of baryons and photons. See e.g. ref. [5] for solutions to eq. (15), and more detailed discussion.

There is still an important effect that is seen in Figure 1 that we have not discussed: the damping of the CMB acoustic oscillations on small scales. The effect stems from the finite mean free path for the photons and the (finite) duration of recombination, where the former is often referred to as the Silk damping. The non-zero mean free path means that photons can diffuse out the perturbations. The small scales are especially damped, as these are the scales that become subhorizon before the larger scales, and have spend longer time in the diffusive regime. In this heurestic picture, on these small scales the photons have more time to diffuse to surroundings and thus damp the initial fluctuations, as seen in Figure 1 on multipoles $l > \mathcal{O}\left(1000\right)$. An important consequence of the diffusion

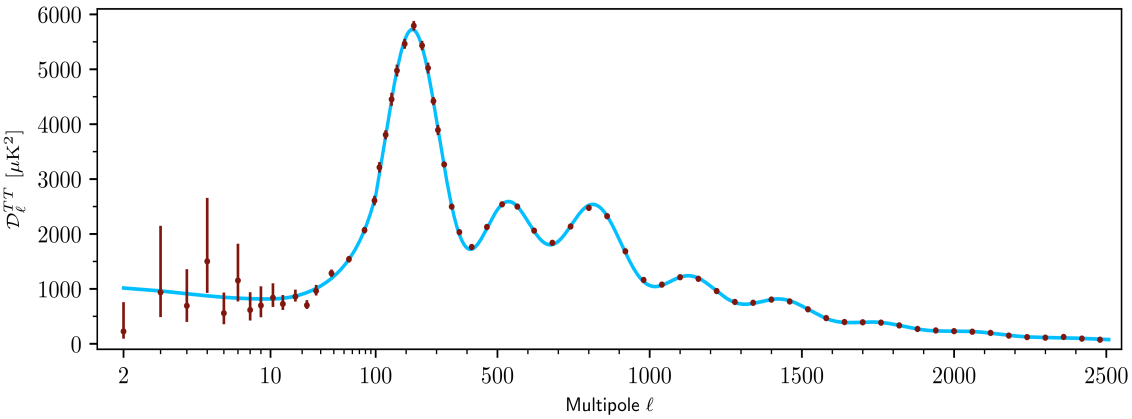

FIGURE 1 The Planck 2018 angular power spectrum, $D_l = \widehat{C}_l T_0^2 \, l\,(l+1)\,/2\pi$. On the small multipoles one can see the Sachs-Wolfe plateu (see text), while the acoustic oscillations are present on multipoles $l \sim \mathcal{O}\,(100 - 1000)$. For larger multipoles we can see the effect of diffusion damping, which damps the seen acoustic peaks. Figure from ref. [10].

is the creation of small deviations from the black-body spectrum, due to energy release and mixing of photons from different regions having different temperatures — we will discuss this in Chapter 4. A more in depth study of the photon diffusion is beyond the scope of this work, and we will refer e.g. to refs. [5, 7] for more detailed introduction to the CMB physics.

1.3 Inflationary cosmology

In the previous section we briefly discussed the known key events of thermal history of the universe. This time-line is usually referred to as the hot big bang model, and it describes the abundances of light elements and explains the formation of the CMB. However, it leaves open the question of initial values of the model of the universe: why is the universe initially in such a homogeneous and isotropic state? One way to tackle this question is inflation, that is, an early universe epoch when the expansion of the universe was accelerating [3].

Historically the inflationary epoch was proposed as an solution to the horizon problem (why is CMB so homogeneous?), flatness problem (why is Ω_K so close to zero) and the lack of certain relics, such as topological monopoles and domain walls, that might have been produced in the very early universe. However, the most important prediction of inflation is the formation of nearly scale-invariant primordial perturbations, from which the structure of the universe grew: these initial perturbations and their evolution can explain the source of the small

[3] The introduction of an inflationary period does not exactly remove the initial value problem, but in reality pushes the problem to even further in the past. See for example refs. [11, 12], where the low-entropy state of the universe and the inflation are discussed.

temperature fluctuations observed in the CMB that were discussed in the previous section. Let us then next briefly discuss these initial condition problems, and then move on to the discussion on how we actually define the inflationary period and from there continue to discuss the most studied model of inflation — the slow-roll inflation. Most of the discussion in this section follows ref. [13]. Historically, the inflation as a solution to the aforementioned problems and the slow-roll inflation were first discussed e.g. in refs. [14, 15, 16, 17, 18, 19].

1.3.1 Initial condition problems

As discussed, the inflationary paradigm can provide a setting that to some extent resolves the initial condition problems of the hot big bang model. Let us then start by discussing the horizon problem. It has been experimentally verified that the CMB temperature is extremely uniform – the temperature fluctuations are at most of the order of $\delta T/T \sim \mathcal{O}\left(10^{-5}\right)$. However, we know that the causal interactions that would thermalize the plasma in the very early universe have a finite distance horizon (when $\ddot{a} < 0$), that is, the CMB seems to consist of roughly $\mathcal{O}\left(10^3\right)$ causally disconnected regions at the time of recombination, and thus the thermalization should not be a viable scenario. It is of course possible, that the initial conditions resulted in such a uniform configuration that the right degree of uniformity and fluctuations are observed today in the CMB. However, this level of fine-tuning might be a somewhat of a turn-off. This problem is resolved by inflation, which gives dynamical mechanism, in which all the disconnected patches at recombination are brought into causal contact in a earlier phase of the universe.

Observationally we know that the total energy density seems to be close to unity, that is $|\Omega_0 - 1| < 0.005$ [20]. As discussed earlier, this means that the curvature is extremely close to zero, and the geometry of the universe seems to be flat. The curvature energy density was defined as $|\Omega_K| = |K|/a^2H^2$, and therefore in the matter dominated epoch it scales as $|\Omega_K| \propto t^{2/3}$ and in the radiation dominated epoch $|\Omega_K| \propto t$. This means that the curvature has to have been even smaller in the earlier universe! It is quite straightforward to show that at the big bang nucleosynthesis the total energy density was approximately

$$|\Omega - 1|_{\mathrm{BBN}} \lesssim 10^{-17}, \tag{16}$$

that is, the universe is extremely close to a flat geometry. This seems to again be a fine-tuning problem, as for random initial conditions it seems somewhat unnatural-ish to end up in a universe, where the total energy density is right at the critical value ρ_{cr}. Again, inflation allows a dynamic mechanism for driving the curvature to the observed extremely small values.

Inflation has also been seen as a solution for the problem of unwanted relics. In certain theories such as the supersymmetric grand unified theories, the high energy behaviour of symmetry breaking allows the formation of topological defects such as magnetic monopoles. However, these configurations have not been observed in the universe, and one would like a mechanism to remove these kinds

of (model-dependent) objects. A long enough inflationary epoch in the very early universe can effectively remove these symmetry breaking remnants due to dilution via the rapid expansion of space [21]. If these relics are produced after inflation, one needs to take them into account in the hot big bang cosmology — this is a possible scenario for example in axion scalar dark matter models, where the breaking of global $U(1)$ symmetry can induce the creation of strings and domain walls (see e.g. ref. [22]).

1.3.2 Conditions for inflation

Let us then define more quantitatively, what we mean by inflation. We start by defining inflation simply as an era of accelerated expansion, i.e.

$$\ddot{a} > 0. \tag{17}$$

What are then the requirements for the energy fluid content of the universe to achieve this? The second Friedmann eq. (7) turns the requirement of an accelerated expansion to the following relation:

$$\ddot{a} > 0 \rightarrow \rho + 3p < 0 \rightarrow \frac{p}{\rho} < -\frac{1}{3}. \tag{18}$$

That is, the equation of state of the fluid needs to be such that $w = p/\rho < -1/3$, which is the condition for gravity being repulsive — as for the so-called ordinary matter the gravity is always attractive, $\rho + 3p \geq 0$. Inflation then requires a matter fluid that has a negative pressure, $p < -\rho/3$. Important examples of this type of matter are vacuum energy $p_\Lambda = -\rho_\Lambda$ and certain type of scalar models, such as the slowly-rolling inflaton field that is discussed in the next section. The latter is important for the inflationary physics, while the former is important for the current and future evolution of the universe (see eq. (8)).

We can also write the requirement (17) as

$$\ddot{a} > 0 \leftrightarrow \frac{\mathrm{d}}{\mathrm{d}t}\frac{1}{aH} < 0, \tag{19}$$

which tells us that the curvature density is driven to zero during inflation, i.e.

$$|\Omega - 1| = |\Omega_K| = \frac{|K|}{a^2 H^2} \rightarrow 0. \tag{20}$$

What is then the amount of inflation needed, i.e. the elapsed time of accelerated expansion, to solve the flatness problem? It is customary to measure the amount of inflation in terms of e-folds, i.e.

$$N_k \equiv \log\left(\frac{a_{\mathrm{end}}}{a_k}\right), \tag{21}$$

where a_k and a_{end} are the values of the scale factor at some point during and at the end of inflation, respectively. It is straightforward to estimate the amount of

e-folds needed, and in a typical estimation one ends up needing roughly $N_k \approx 60$ e-folds to drive the value of Ω_K to meet to current observational constraints [5].

It happens that the estimated growth of $a_k/a_{\text{end}} \approx \text{e}^{60}$ needed to solve the flatness problem coincides with the value needed to solve the horizon problem [13]. As discussed, to explain the homogeneity of CMB the observed universe needs to originate from a single causal patch. If we have a phase of decreasing comoving Hubble horizon, i.e.

$$\frac{\mathrm{d}}{\mathrm{d}t}\mathcal{H}^{-1} = \frac{\mathrm{d}}{\mathrm{d}t}\left(aH\right)^{-1} < 0, \tag{22}$$

that lasts long enough, one can bring all the observed scales within the same causal patch [6]. As we saw above, eq. (22) is condition for $\ddot{a} > 0$, which means that during inflation the comoving Hubble horizon $\mathcal{H}^{-1} = (aH)^{-1}$ shrinks, and allows one to bring the last-scattering surfaces to causal contact during inflation. See e.g. refs. [6, 13] for more in-depth discussion.

The value $N \sim 60$ e-folds is regarded loosely as the target value for the different inflation models. The exact value needed to explain the aforementioned problems and other details involving for example the primordial perturbations, is dependent on the inflationary model details, in particular, the reheating of the universe (see e.g. refs [6, 13]).

1.3.3 Slow-roll scalar field inflation

In the previous section we saw how the inflation requires the inflation driving matter to have an equation of state parameter $w < -1/3$. A classic example of this kind of behaviour can be found by considering a scalar field model, where the potential of the field dominates over the kinetic term and the friction of the expanding universe dominates over the field acceleration, i.e. the field is slowly-rolling. In this kind of setup, the scalar field dominates the whole energy density of the universe and as it drives the inflationary dynamics it is referred to as the inflaton field.

We can start by considering a scalar field in a curved space. The action is then given by [3]

$$S_\phi = -\int \mathrm{d}^4x\, \sqrt{-g}\left[\frac{1}{2}\nabla_\mu\phi\nabla^\mu\phi + V\left(\phi\right)\right], \tag{23}$$

where ∇_μ is the covariant derivative, $\sqrt{-g}$ is the determinant of the metric tensor and $V\left(\phi\right)$ is the potential of the field which we for now leave unspecified. For a homogeneous scalar field, $\phi = \phi\left(t\right)$, in a flat FLRW universe one can easily find the pressure p_ϕ and the energy density ρ_ϕ to be [6]

$$p_\phi = \frac{1}{2}\dot{\phi}^2 - V\left(\phi\right),\ \rho_\phi = \frac{1}{2}\dot{\phi}^2 + V\left(\phi\right). \tag{24}$$

The dynamics of the FLRW universe dominated by the inflaton are then described

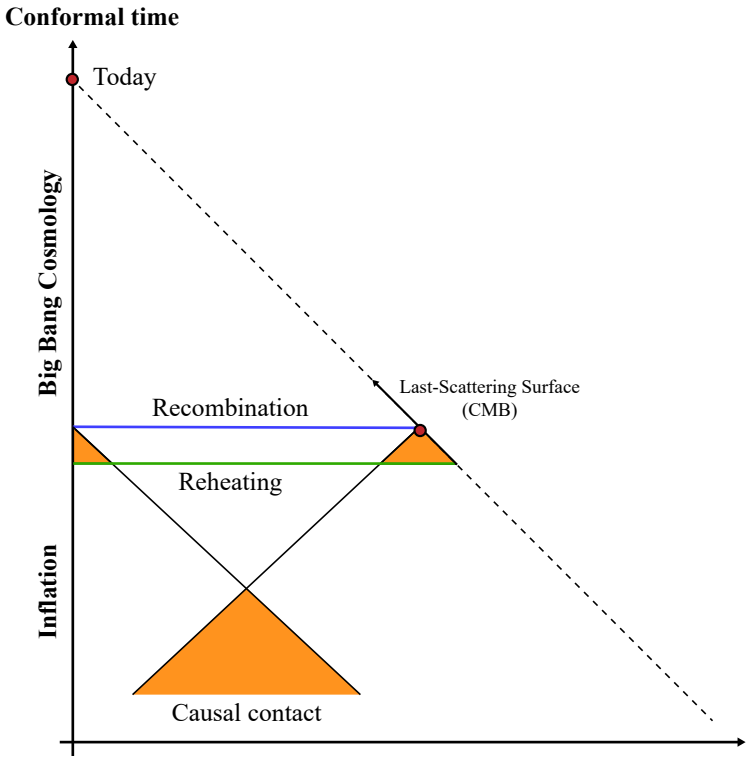

FIGURE 2 A conformal time diagram of the the last-scattering light-cones. The causally separated light-cones are brought into contact if the inflation lasts long enough. Figure remade and adapted from ref. [13].

by the following equation of motion for ϕ and the ϕ-dependent Hubble parameter

$$\ddot{\phi} + 3H\dot{\phi} + V_{,\phi}(\phi) = 0 \tag{25}$$

$$3M_{\mathrm{Pl}}^2 H^2 = \rho_\phi = \frac{1}{2}\dot{\phi}^2 + V(\phi), \tag{26}$$

where the subscript $_{,\phi} = \mathrm{d}/\mathrm{d}\phi$. We can then see, that if we have $\dot{\phi}^2 \ll V(\phi)$, the inflaton equation of state parameter w_ϕ is

$$w_\phi = \frac{p_\phi}{\rho_\phi} = \frac{\frac{1}{2}\dot{\phi}^2 - V(\phi)}{\frac{1}{2}\dot{\phi}^2 + V(\phi)} \approx -1, \tag{27}$$

which is the desired value for the accelerated expansion (18). The requirement $\dot{\phi}^2 \ll V(\phi)$ means that the slope of the potential is shallow enough, that the scalar field rolls slowly towards the minimum of its potential while keeping its kinetic term small enough to allow $\ddot{a} > 0$. The slow-roll state ends when the field reaches and starts to oscillate around the minimum its potential and decays into radiation — see Figure 3.

It is customary to define the dimensionless slow-roll parameter $\epsilon_H \equiv -\dot{H}/H^2$, which allows us to turn the acceleration requirement $\ddot{a} > 0$ to the condition

$$\epsilon_H < 1. \tag{28}$$

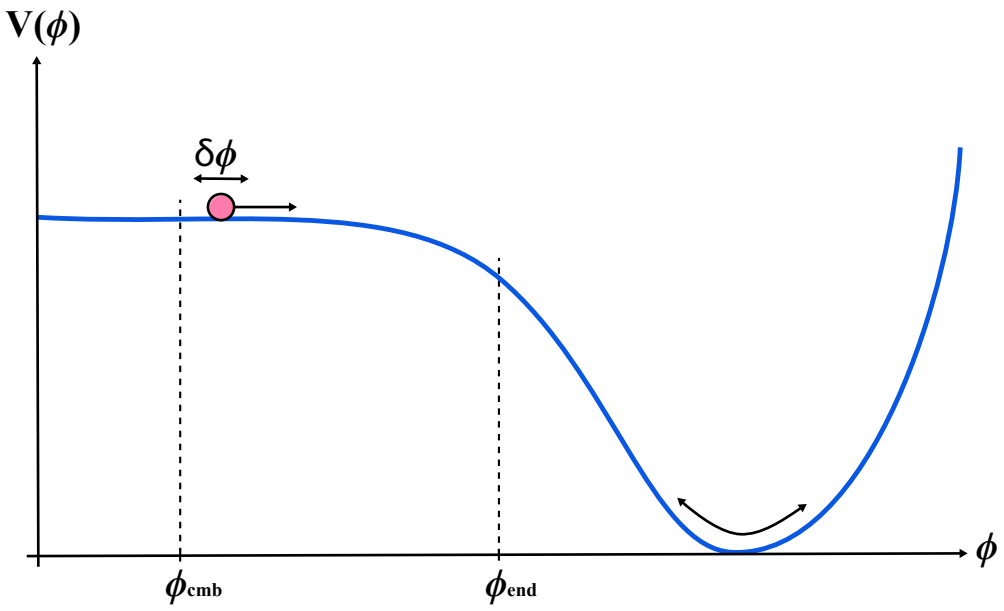

FIGURE 3 Sketch of the inflaton potential, that shows an example potential and mechanism of the slow-roll inflation. The field starts from a certain initial value and starts to roll towards the minimum of its potential. The fluctuations observed at the CMB are created at ϕ_{cmb}, which needs to be roughly $N \sim 60$ e-folds before the end of inflation at ϕ_{end}. As the inflation ends, the scalar field starts to oscillate around its minimum, and decays into radiation, which is usually referred to as the reheating of the universe. Figure remade and adapted from ref. [13].

This requirement can also be written as $\dot{\phi}^2 < V(\phi)$, and $\epsilon_H < 1$ implies that the kinetic energy must be smaller than the potential of the field. Inflation ends by definition when $\ddot{a} < 0 \leftrightarrow \epsilon_H > 1$.

In the limit $\epsilon_H \ll 1$, one an also see how does the Hubble parameter evolve during slow-roll inflation,

$$\epsilon_H \ll 1 \rightarrow H = \frac{\dot{a}}{a} = H_* \left(1 - \mathcal{O}\left(\epsilon_H\right)\right) \tag{29}$$

$$\rightarrow a(t) \propto \mathrm{e}^{H_* t\left(1-\mathcal{O}\left(\epsilon_H\right)\right)}, \tag{30}$$

where H_* is the value of Hubble parameter during inflation and the scale factor grows exponentially during inflation. If $\epsilon_H = 0$, the Hubble parameter is constant and the universe is described by the de Sitter spacetime, $a = \exp\left(H_* t\right)$. Most of the studied models of inflation predict $\epsilon_H \ll 1$, and therefore are described by a nearly de Sitter spacetime.

In the standard slow-roll approximation, one then requires that

$$\dot{\phi}^2 \ll V(\phi), \; |\ddot{\phi}| \ll 3H|\dot{\phi}|, \tag{31}$$

where the latter condition constrains $\ddot{\phi}$ to be small so that the ϕ field is in the slow-roll state long enough for the universe to inflate the required $N_k \sim 60$ e-

folds. Assuming these requirements the slow-roll eqs. are then

$$\dot{\phi} = -\frac{V_{,\phi}}{3H}\ ,\ H^2 = \frac{V}{3M_{\rm Pl}^2}. \tag{32}$$

These allow us to write the standard slow-roll parameters that only depend on the scalar potential $V(\phi)$ and its derivatives

$$\epsilon_V = \frac{M_{\rm Pl}^2}{2}\left(\frac{V_{,\phi}}{V}\right)^2 \tag{33}$$

$$\eta_V = M_{\rm Pl}^2 \frac{V_{,\phi\phi}}{V}. \tag{34}$$

A necessary condition for the shape of the potential in slow-roll approximation is then

$$\epsilon_V \ll 1,\ |\eta_V| \ll 1. \tag{35}$$

We can see that for small values the two ϵ-parameters coincide, $\epsilon_H \approx \epsilon_V$.

The slow-roll parameters (33) and (34) are usually descriptive enough when studying the leading-order behaviour in slow-roll. For example, the spectral index that describes to first-order the scale-dependency of the curvature power spectrum (that is, if there is change in the perturbation on different distance scales), can be written in terms of eqs. (33) and (34). However, if one wants to compute the prediction of the studied inflation model for the running of the spectral index (scale-dependency of the spectral index), one needs to take into account next-to-leading order slow-roll parameters, such as $\xi_V = M_{\rm Pl}^4\left(V_{,\phi}V_{,\phi\phi\phi}/V^2\right)$. For a more thorough formalization of the slow-roll treatment, see for example ref. [23].

1.4 Primordial perturbations

We have briefly mentioned the formation of the primordial density fluctuations, that act as a seed of structure growth and have left an imprint on the CMB map (see Section 1.2). The inflation provides a mechanism for the creation of these initial perturbations. During inflation the quantum fluctuations of the scalar fields are expanded to large scales: as the comoving $\mathcal{H}^{-1}$ shrinks, the different scales of the quantum fluctuations become classical perturbations as they become larger than the horizon. The evolution of these superhorizon fluctuations is effectively frozen. After the inflation ends, and the universe transitions to the standard hot big bang era via the reheating, and the horizon starts to grow (first in the radiation dominated epoch, then in the matter and vacuum/dark energy dominated epochs), and the scales of cosmological interest come back within the Hubble horizon. As the fluctuations of the initial scalar fields become subhorizon, they start to evolve according to the causal physics, and thus can be related to observable quantities. This mechanism is depicted in Figure 4. In the following

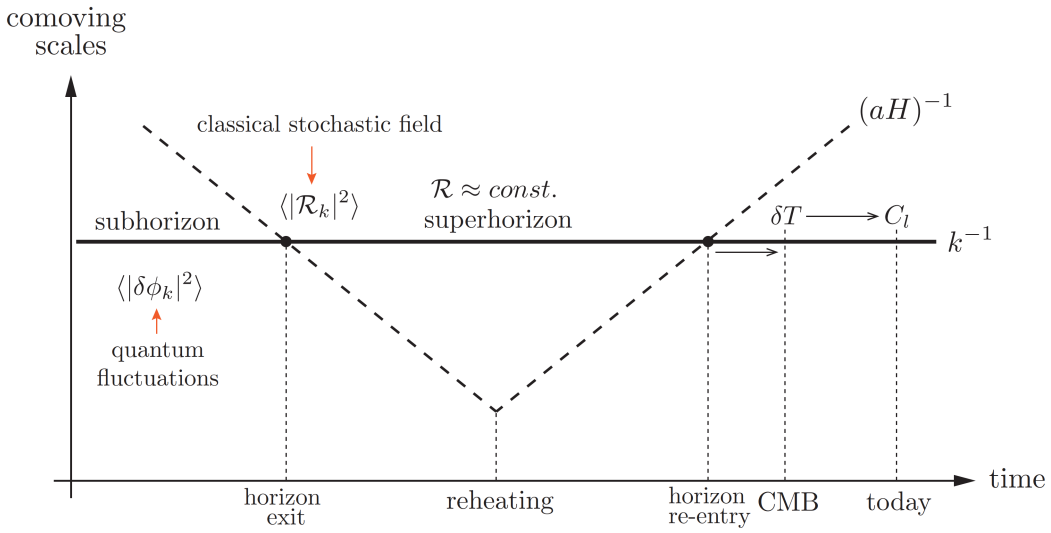

FIGURE 4 The evolution of the primordial perturbations. During inflation the quantum fluctuations of scalar field $\delta\phi$, are translated into curvature perturbations $\mathcal{R}$, that become classical stochastic quantities on superhorizon scales. As they re-enter the Hubble horizon, the density perturbations are related to the observed temperature anisotropies δT, that are measured in terms of the CMB angular power spectrum C_l. Figure from. ref. [5].

chapters we will discuss the formation and evolution of the quantum fluctuations, the primordial perturbation theory needed to quantify the perturbations and their power spectrum. We will also discuss different scalar field models, where the primordial perturbations are sourced by multiple fields, in contrast to the standard single-field slow-roll inflation, where the inflaton is responsible for the inflationary dynamics and the perturbations.

2 QUANTUM FLUCTUATIONS OF SCALAR FIELDS

In this chapter we study the quantum fluctuations of nearly massless scalar fields in (quasi) de Sitter spacetime. We start by considering small fluctuations of the field, and follow to quantize the field and finally to define the power spectrum of the scalar field fluctuations. The discussion given in this chapter follows mostly refs. [24, 25, 26].

2.1 Fluctuations of a generic light scalar in de Sitter

2.1.1 Action and equation of motion

We start by considering a test scalar field $\sigma(\tau, \mathbf{x})$ in a de Sitter space, i.e. $a = \mathrm{e}^{Ht} = -1/H\tau$, where $H \simeq$ constant and the conformal time is $\mathrm{d}t = a\mathrm{d}\tau$, and $\sqrt{-g} = a^3$. The action of the scalar field can then be written as

$$S_\sigma = -\int \mathrm{d}\tau \mathrm{d}^3\mathbf{x} \left[\frac{1}{2}a^2\left(\left(\sigma'\right)^2 - \left(\nabla\sigma\right)^2\right) + a^4 V(\sigma)\right], \tag{36}$$

where the superscript $' = \mathrm{d}/\mathrm{d}\tau$. Note that we assume that the scalar field σ is both light, $V_{,\sigma\sigma} = \partial^2 V/\partial\sigma^2 < H^2$, and subdominant during inflation, i.e. $\rho_\sigma \ll \rho_\phi$, where ρ_ϕ is the inflaton energy density. In this case the field does not contribute to the overall spacetime dynamics, and one can consider the scalar σ in this fixed background. For the inflaton field this is generally not true, as one needs to take into account the metric fluctuations in the calculation. We will discuss the inflaton spectrum and the perturbations generated during inflation in Section 3.2.1.

As we are interested in the quantum fluctuations of the field, it is customary to divide the scalar field σ to the background field $\bar{\sigma}(\tau)$ and to the small perturbed part $\delta\sigma(\tau, \mathbf{x})$

$$\sigma(\tau, \mathbf{x}) \to \bar{\sigma}(\tau) + \delta\sigma(\tau, \mathbf{x}) = \bar{\sigma}(\tau) + \frac{\chi(\tau, \mathbf{x})}{a(\tau)}, \tag{37}$$

where we also defined the scaled field $\chi = a\delta\sigma$, which will be useful in the calculation and it allows us to use the results derived in this chapter in Section 3.2.1, where we will compute the primordial power spectrum in the single-field slow-roll inflation.

To find the linearized equation of motion for the scalar field, one needs to expand eq. (36) to second order in fluctuations, and then use the equations of motion for the background field $\bar{\sigma}$. One can then write the action for the perturbed field $\chi = a\delta\sigma$ as

$$S_\chi = \frac{1}{2}\int \mathrm{d}\tau \mathrm{d}^3\mathbf{x} \left[\left(\chi'\right)^2 - \left(\nabla\chi\right)^2 + \left(\frac{a''}{a} - a^2 V_{,\sigma\sigma}\right)\chi^2\right]. \tag{38}$$

With the Euler-Lagrange equation one can compute the equation of motion for χ which now reads

$$\chi'' + \left[-\nabla^2 - \frac{a''}{a} + a^2 V_{,\sigma\sigma} \right] \chi = 0, \tag{39}$$

where a''/a can also be written in the de Sitter space as $a''/a = 2a^2H^2$.

As we are interested in the information encoded in the different distance scales of the fluctuations, we perform the following Fourier decomposition

$$\chi(\tau) = a(\tau)\,\delta\sigma(\tau, \mathbf{x}) = \int \frac{\mathrm{d}^3\mathbf{x}}{(2\pi)^3}\, \mathrm{e}^{\mathrm{i}\mathbf{k}\cdot\mathbf{x}}\, \chi_k(\tau), \tag{40}$$

and the equations of motion for the mode functions χ_k read

$$\chi_k'' + \left[k^2 + a^2 \left(V_{,\sigma\sigma} - 2H^2 \right) \right] \chi_k = 0. \tag{41}$$

We can see, that if the field is light, $V_{,\sigma\sigma} \ll H^2$, eq. (41) has two different asymptotic limits: for $k \gg aH$ the solution is $\chi_k \propto \mathrm{e}^{\mathrm{i}k\tau}$, and for $k \ll aH$ we have $\chi_k \propto a$. In terms of the non-scaled mode functions $\sigma_k = \chi_k/a$, we have that $\sigma_k(k \gg aH) \propto \mathrm{e}^{\mathrm{i}k\tau}/a$ and $\sigma_k(k \ll aH) \propto$ constant. For a light scalar the mode functions then behave like plane waves within the horizon ($k \gg aH$), while outside the horizon in the superhorizon limit ($k \ll aH$) the fluctuations approach a constant value — see Figure 4.

Eq. (41) can be cast in a Bessel equation form

$$\chi_k'' + \left(k^2 - \frac{\nu^2 - \frac{1}{4}}{\tau^2} \right) \chi_k = 0, \tag{42}$$

where $\nu^2 = 9/4 - V_{,\sigma\sigma}/H^2$. Eq. (42) has a general solution that can be expressed in terms of the Hankel functions of first and second kind $H_\nu^{(1,2)}$ [24]

$$\chi_k(\tau) = \sqrt{-\tau} \left[c_{1,k}\, H_\nu^{(1)}(-k\tau) + c_{2,k}\, H_\nu^{(2)}(-k\tau) \right], \tag{43}$$

where the coefficients $c_{1,k}$ and $c_{2,k}$ are constant in time. The value chosen for the coefficients is equivalent to the freedom of choosing the vacuum on which the fluctuations are interpreted. We will come back to this below, after we quantize the scalar field.

As above, we are interested in the asymptotical behaviour of the mode functions. Assuming that $\sqrt{V_{,\sigma\sigma}/H} < 3/2$ (which is fulfilled in the case of light scalar), the Hankel functions have the following asymptotical behaviour [25]

$$H_\nu^{(1)}(-k\tau) \to \sqrt{\frac{2}{\pi(-k\tau)}}\, \mathrm{e}^{-\mathrm{i}k\tau - \pi(\nu+1/2)/2} \tag{44}$$

$$H_\nu^{(2)}(-k\tau) \to \sqrt{\frac{2}{\pi(-k\tau)}}\, \mathrm{e}^{\mathrm{i}k\tau + \pi(\nu+1/2)/2}, \tag{45}$$

when $-k\tau \gg 1 \rightarrow k \gg aH$, i.e. in the subhorizon limit the mode functions behave as positive/negative plane waves. In the superhorizon limit, $-k\tau \ll 1 \rightarrow k \ll aH$, the asymptotic behaviour is [25]

$$H_\nu^{(1)}(-k\tau) \rightarrow -\mathrm{i}\sqrt{\frac{2}{\pi}} 2^{\nu-3/2} \frac{\Gamma(\nu)}{\Gamma(3/2)} (-k\tau)^{-\nu} \tag{46}$$

$$H_\nu^{(2)}(-k\tau) \rightarrow \mathrm{i}\sqrt{\frac{2}{\pi}} 2^{\nu-3/2} \frac{\Gamma(\nu)}{\Gamma(3/2)} (-k\tau)^{-\nu}, \tag{47}$$

i.e. in the superhorizon limit $\sigma_k = \chi_k/a \propto (-\tau)^{3/2-\nu} \propto$ constant, when $\nu \approx 3/2$.

2.1.2 Quantization of the field and choosing the vacuum

As we are studying the quantum fluctuations of the field, we want to quantize the field. To quantize the scalar field σ, we promote

$$\widehat{\delta\sigma}(\tau, \mathbf{x}) = \int \frac{\mathrm{d}^3\mathbf{k}}{(2\pi)^3} \left(\mathrm{e}^{\mathrm{i}\mathbf{k}\cdot\mathbf{x}} u_k(\tau) \hat{a}_\mathbf{k} + \mathrm{e}^{-\mathrm{i}\mathbf{k}\cdot\mathbf{x}} u_k^*(\tau) \hat{a}_\mathbf{k}^\dagger \right), \tag{48}$$

where $\hat{a}_\mathbf{k}$ and $\hat{a}_\mathbf{k}^\dagger$ are respectively the annihilation and creation operators, the mode functions $u_k(\tau)$ satisfy the equation of motion eq. (41) ($\chi_k \propto u_k/a$). When we impose the canonical equal-time commutation relations for $\widehat{\delta\sigma}(t, \mathbf{x})$ and its canonical momentum $\widehat{\Pi}_{\delta\sigma}$,

$$\left[\widehat{\delta\sigma}(\mathbf{x}), \widehat{\Pi}_{\delta\sigma}(\mathbf{y}) \right] = \mathrm{i}\delta(\mathbf{x} - \mathbf{y}) \tag{49}$$

$$\left[\widehat{\delta\sigma}(\mathbf{x}), \widehat{\delta\sigma}(\mathbf{y}) \right] = \left[\widehat{\Pi}_{\delta\sigma}(\mathbf{x}), \widehat{\Pi}_{\delta\sigma}(\mathbf{y}) \right] = 0, \tag{50}$$

we can also write the equivalent commutator relations for the creation and annihilation operators:

$$[\hat{a}_\mathbf{k}, \hat{a}_{\mathbf{k}'}] = \left[\hat{a}_\mathbf{k}^\dagger, \hat{a}_{\mathbf{k}'}^\dagger \right] = 0 \tag{51}$$

$$\left[\hat{a}_\mathbf{k}, \hat{a}_{\mathbf{k}'}^\dagger \right] = (2\pi)^3 \delta(\mathbf{k} - \mathbf{k}'), \tag{52}$$

with the normalization condition [24, 26]

$$u_k u_k^{*\prime} - u_k^* u_k' = \mathrm{i}a^{-2}, \tag{53}$$

where the conformal time derivatives originate from the canonical momentum.

The problem of choosing the vacuum still lingers. In quantum field theory in curved spacetime there is in general no unique or preferred choice of vacuum: the dynamical spacetime leads to a time-dependent minimum-energy state, i.e. in Schrödinger picture, the state Ψ_0 which we define to have zero particle number at a certain time τ_0 can generally have a non-zero particle number at time $\tau_1 > \tau_0$ (see for example ref. [27]). However, in the context of inflation we have a natural choice for the vacuum, as in the beginning of inflation all relevant modes of the

fluctuations were deep inside the horizon (assuming that the total amount of e-folds is $N_{\rm tot} \gg 60$). In this limit, eq. (41) tells us that

$$k \gg aH \rightarrow \chi_k'' + k^2 \chi_k = 0, \tag{54}$$

for $V_{,\sigma\sigma} \approx 0$, i.e. the modes have time-independent frequencies and the result coincides with that of a Minkowski space. From eqs. (43), (44) and (45), we have that the mode function in the limit $-k\tau \gg 1$ reads

$$\chi_k \rightarrow \sqrt{\frac{2}{\pi k}} \left(c_{1,k}\, \mathrm{e}^{-\mathrm{i}k\tau - \pi(\nu+1/2)/2} + c_{2,k}\, \mathrm{e}^{\mathrm{i}k\tau + \pi(\nu+1/2)/2} \right). \tag{55}$$

As we define particles in the Minkowski space as positive frequency plane waves, we choose the vacuum such that χ_k matches the Minkowski result (54) in this limit. This then corresponds to setting

$$c_{2,k} = 0 \rightarrow \chi_k = \sqrt{\frac{2}{\pi k}} \left(c_{1,k}\, \mathrm{e}^{-\mathrm{i}k\tau - \pi(\nu+1/2)/2} \right). \tag{56}$$

The coefficient $c_{1,k}$ is fixed by the normalization condition (53) for the non-scaled mode functions u_k, which yields

$$c_{1,k} = \frac{\sqrt{\pi}}{2}. \tag{57}$$

The vacuum choice (56) and (57) is referred to as the Bunch-Davies vacuum [28]. To recap, this choice corresponds to defining particles as positive frequency plane waves, and in the context of inflation this means that the modes deep within the horizon coincide with the flat space interpretation of particles.

And finally, we can write the mode function u_k as

$$u_k(\tau) = \frac{\chi_k(\tau)}{a(\tau)} = (-\tau)^{3/2} H \frac{\sqrt{\pi}}{2} H_\nu^{(1)}(-k\tau), \tag{58}$$

and we can also write the field operator $\widehat{\delta\sigma}(\tau, \mathbf{x})$ as

$$\widehat{\delta\sigma}(\tau, \mathbf{x}) = \int \frac{\mathrm{d}^3\mathbf{k}}{(2\pi)^3} \left(\mathrm{e}^{\mathrm{i}\mathbf{k}\cdot\mathbf{x}}\, u_k \hat{a}_{\mathbf{k}} + \mathrm{e}^{-\mathrm{i}\mathbf{k}\cdot\mathbf{x}}\, u_k^* \hat{a}_{\mathbf{k}}^\dagger \right) \tag{59}$$

$$= \int \frac{\mathrm{d}^3\mathbf{k}}{(2\pi)^3}\, \mathrm{e}^{\mathrm{i}\mathbf{k}\cdot\mathbf{x}} \left(u_k \hat{a}_{\mathbf{k}} + u_k^* \hat{a}_{-\mathbf{k}}^\dagger \right) \tag{60}$$

$$\equiv \int \frac{\mathrm{d}^3\mathbf{k}}{(2\pi)^3}\, \mathrm{e}^{\mathrm{i}\mathbf{k}\cdot\mathbf{x}} \widehat{\sigma}_{\mathbf{k}}(\tau), \tag{61}$$

where we used the isotropy condition $u_{\mathbf{k}} = u_k$.

We are then ready to compute any n-point correlator of the field. For example, the two-point function between modes k and k', which gives the power spectrum that is to be discussed more in the next section, is given by

$$\langle \widehat{\sigma}_{\mathbf{k}}(\tau)\, \widehat{\sigma}_{\mathbf{k}'}(\tau) \rangle = \langle 0 | \widehat{\sigma}_{\mathbf{k}}(\tau)\, \widehat{\sigma}_{\mathbf{k}'}(\tau) | 0 \rangle = u_k u_{k'}^* \langle 0 \left| \widehat{a}_{\mathbf{k}} \widehat{a}_{-\mathbf{k}'}^\dagger \right| 0 \rangle \tag{62}$$

$$= (2\pi)^3 \delta(\mathbf{k} + \mathbf{k}')\, u_k u_{k'}^* = (2\pi)^3 \delta(\mathbf{k} + \mathbf{k}')\, |u_k|^2. \tag{63}$$

As discussed in the previous section, the mode functions of the field fluctuations behave like plane waves within the horizon. Therefore, deep within the horizon the field behaviour is in a quantum state. However, when the corresponding wavelength crosses the Hubble horizon, the quantum state becomes a squeezed state, which essentially corresponds to a classical stochastic configuration, after the decaying mode is neglected [29, 30, 31]. One can then compute the expectation value of the quantum field, which at later times (when the corresponding scale has exited the horizon) is then matched with the variance of a classical stochastic variable. See for example refs. [29, 30, 31].

2.1.3 Power spectrum of fluctuations

The power spectrum P_σ is usually defined as the Fourier transformation of the real space equal-time two-point correlator, i.e.

$$\left\langle 0 \left| \widehat{\delta\sigma}\left(\tau,\mathbf{x}\right), \widehat{\delta\sigma}\left(\tau,\mathbf{y}\right) \right| 0 \right\rangle = \int \frac{\mathrm{d}^3\mathbf{k}}{\left(2\pi\right)^3} \frac{\mathrm{d}^3\mathbf{k}'}{\left(2\pi\right)^3} \langle \widehat{\sigma}_{\mathbf{k}}\left(\tau\right) \widehat{\sigma}_{\mathbf{k}'}\left(\tau\right) \rangle \mathrm{e}^{\mathrm{i}\mathbf{k}\cdot\mathbf{x}} \mathrm{e}^{\mathrm{i}\mathbf{k}'\cdot\mathbf{y}} \tag{64}$$

$$= \int \frac{\mathrm{d}^3\mathbf{k}}{\left(2\pi\right)^3} \left|u_k\right|^2 \mathrm{e}^{\mathrm{i}\mathbf{k}\cdot\left(\mathbf{x}-\mathbf{y}\right)} = \int \frac{\mathrm{d}^3\mathbf{k}}{\left(2\pi\right)^3} P_\sigma\left(k\right) \mathrm{e}^{\mathrm{i}\mathbf{k}\cdot\left(\mathbf{x}-\mathbf{y}\right)}. \tag{65}$$

In the literature one usually defines the scaled power spectrum $\mathcal{P}_\sigma = k^3 P_\sigma / 2\pi^2$, which has the following solution with the Bunch-Davies vacuum choice

$$\mathcal{P}_\sigma\left(k\right) \equiv \frac{k^3}{2\pi^2} P_\sigma\left(k\right) = \frac{k^3}{2\pi^2} \left|u_k\right|^2 \tag{66}$$

$$= \left(\frac{H}{2\pi}\right)^2 \frac{\pi}{2} \left(-k\tau\right)^3 \left| H_\nu^{(1)}\left(-k\tau\right) \right|^2, \tag{67}$$

where we used the result (58). We can then use the late-time asymptotic limit expressions for the Hankel function given in eq. (46). For the light scalar, the power spectrum $\mathcal{P}_\sigma$ in the superhorizon limit $-k\tau \ll 1$ is then

$$\mathcal{P}_\sigma\left(k\right) \approx \left(\frac{H}{2\pi}\right)^2 \times \left(\frac{k}{aH}\right)^{3-2\nu}, \tag{68}$$

where the index ν can be written as

$$\nu = \frac{3}{2}\sqrt{1 - \frac{4}{9}\frac{V_{,\sigma\sigma}}{H^2}} \approx \frac{3}{2} - \frac{V_{,\sigma\sigma}}{3H^2} = \frac{3}{2} - \eta_\sigma, \tag{69}$$

where we used the condition $V_{,\sigma\sigma} \ll H^2$, and defined the second slow-roll parameter η_σ for the field σ.

The power spectrum of the fluctuations that the scalar field acquires is then

$$\mathcal{P}_\sigma\left(k\right) \approx \left(\frac{H}{2\pi}\right)^2 \times \left(\frac{k}{aH}\right)^{2\eta_\sigma}, \tag{70}$$

or in the massless case $V_{,\sigma\sigma} = 0$,

$$\mathcal{P}_\sigma(k) \approx \left(\frac{H}{2\pi}\right)^2. \tag{71}$$

This demonstrates that the light scalar field acquires nearly scale-invariant perturbations for the modes that have exited the horizon in de Sitter space. As we can see, for the massless case (71) the power spectrum is scale-invariant. However, before discussing the fluctuations of the inflaton field, we need to take into account the fact that due to the need to end inflation at some point, the spacetime cannot be a pure de Sitter space. We will discuss how this affects the calculations in the next section.

2.2 Fluctuations of a generic light scalar in quasi de Sitter

So far we have studied the evolution of the light scalar field in pure de Sitter space, i.e. the Hubble rate is assumed to be constant and the expansion follows $a = \mathrm{e}^{Ht}$. However, during inflation the Hubble rate is not constant, as we saw in Section 1.3.3, the change of Hubble rate is described by the parameter $\epsilon_H = -\dot{H}/H^2$. Luckily, the inclusion of this quasi de Sitter behaviour does not drastically alter the computation that was described in the previous section. There are two ways we can introduce the time-dependent H or ϵ into the analysis. In the first one we assume that there is ϵ dependency in the scale factor, and in the second one we take the pure de Sitter result (70) and then reinstate the time-dependency in the Hubble rate and compute the spectral index, which describes the scale-dependency of the spectrum.

2.2.1 Effect of quasi de Sitter spacetime

First, we can write the scale factor as

$$a(\tau) = \frac{-1}{H\tau^{1+\epsilon_H}}. \tag{72}$$

For small values of ϵ_H, which are required for a successful inflationary period, the only change is that in eq. (39), the term a''/a acquires ϵ_H proportional term, $a''/a \approx (2+3\epsilon_H)/\tau^2$. We can then write eq. (42) as before, but replace the previous index ν with

$$\nu = \sqrt{\frac{9}{4} - \frac{V_{,\sigma\sigma}}{H^2}} \;\rightarrow\; \nu = \sqrt{\frac{9}{4} + 3\epsilon_H - \frac{V_{,\sigma\sigma}}{H^2}}. \tag{73}$$

Assuming that the field is light, and that ϵ_H remains small, we can use the result (68) for the power spectrum $\mathcal{P}_\sigma$, except now

$$\nu \approx \frac{3}{2} + \epsilon_H - \eta_\sigma. \tag{74}$$

The power spectrum for the light scalar field in the quasi de Sitter space, in the superhorizon limit, is then given by [24]

$$\mathcal{P}_\sigma(k) \approx \left(\frac{H}{2\pi}\right)^2 \times \left(\frac{k}{aH}\right)^{-2\epsilon_H+2\eta_\sigma}. \tag{75}$$

Where we can see that the scale-dependency (k-dependency) of the spectrum changed due to the spacetime being non-pure de Sitter.

2.2.2 Alternative approach and parametrization of the spectrum

Alternatively, we can take the pure de Sitter solution (70)

$$\mathcal{P}_\sigma(k) \approx \left(\frac{H}{2\pi}\right)^2 \times \left(\frac{k}{aH}\right)^{2\eta_\sigma}, \tag{76}$$

and consider that there is a scale-dependency in the Hubble rate. In this case, reinstate that there is a small time- or scale-dependency in the Hubble rate $H \to H_{\mathbf{k}}$. The value of the Hubble rate then corresponds to the given wavelength k^{-1} that exits the horizon during inflation, and from thereon remains frozen due to the superhorizon behaviour discussed previously.

It is customary to define the scale-dependency in the spectrum in terms of the spectral index [4]:

$$n_\sigma - 1 = \frac{\mathrm{d}\log\mathcal{P}_\sigma}{\mathrm{dlog}\, k}. \tag{77}$$

As we assume that the scalar field is in slow-roll, we can then compute eq. (77). First, we note that $\mathrm{dlog}\, k = \mathrm{dlog}\, a + \mathrm{dlog}\, H \approx \mathrm{dlog}\, a$, as we work first-order in slow-roll. We can then write [5, 24]

$$n_\sigma - 1 = \frac{\mathrm{d}}{\mathrm{dlog}\, k}\log\left(\frac{H_{\mathbf{k}}}{2\pi}\right)^2 + \frac{\mathrm{d}}{\mathrm{dlog}\, k}\log\left(\frac{k}{aH}\right)^{2\eta_\sigma} \tag{78}$$

$$= \frac{2}{H}\frac{\mathrm{d}H}{\mathrm{dlog}\, k} + 2\eta_\sigma = \frac{2}{H}\frac{\mathrm{d}H}{\mathrm{d}t}\frac{\mathrm{d}t}{\mathrm{dlog}\, a} + 2\eta_\sigma \tag{79}$$

$$= 2\frac{\dot{H}}{H^2} + 2\eta_\sigma = -2\epsilon_H + 2\eta_\sigma, \tag{80}$$

which reproduces our result (75). We can then write

$$\mathcal{P}_\sigma(k) = \left(\frac{H}{2\pi}\right)^2 \left(\frac{k}{aH}\right)^{n_\sigma-1}, \tag{81}$$

and we can see, that for small slow-roll values $n_\sigma - 1 \approx 0$.

We have now seen that the fluctuations of a light scalar field yield a power spectrum that is nearly scale-invariant. It is customary to approximate this weakly scale-dependent power spectrum $\mathcal{P}$ by a power-law form. In the literature the standard parametrization is [4]

$$\mathcal{P}_\sigma(k) = \mathcal{P}_\sigma(k_{\mathrm{ref}}) \left(\frac{k}{k_{\mathrm{ref}}}\right)^{n_\sigma-1+\frac{1}{2}\alpha_\sigma\log\left(\frac{k}{k_{\mathrm{ref}}}\right)+\frac{1}{6}\beta_\sigma\log^2\left(\frac{k}{k_{\mathrm{ref}}}\right)+\ldots}, \tag{82}$$

where k_{ref} is the reference or pivot scale which, i.e. the scale $k_{\text{ref}} = a_{\text{ref}} H_{\text{ref}}$ that crosses the horizon during inflation, and $\mathcal{P}_\sigma\left(k_{\text{ref}}\right)$ is the amplitude of the spectrum at the pivot scale. The parameters α_σ and β_σ are referred to as the running of the spectral index and running of the running, respectively. They describe the scale-dependency of the spectrum in next-leading orders in slow-roll. The spectral index, running and running of the running are defined as [4]

$$n_\sigma = 1 + \left.\frac{\mathrm{d}\log\mathcal{P}_\sigma}{\mathrm{dlog}\,k}\right|_{k=k_{\text{ref}}} \tag{83}$$

$$\alpha_\sigma = \left.\frac{\mathrm{d}^2\log\mathcal{P}_\sigma}{\mathrm{dlog}\,k^2}\right|_{k=k_{\text{ref}}} \tag{84}$$

$$\beta_\sigma = \left.\frac{\mathrm{d}^3\log\mathcal{P}_\sigma}{\mathrm{dlog}\,k^3}\right|_{k=k_{\text{ref}}}, \tag{85}$$

where the quantities are evaluated at the horizon crossing $k = k_{\text{ref}}$. We will come back to the discussion on the power spectrum in Section 3.2, where we will study the spectrum of primordial perturbations.

3 PRIMORDIAL PERTURBATIONS

In this chapter, we will give a brief review on the primordial perturbations, the small deviations from the homogeneous and isotropic universe, that allow the emergence of the growth of structures that are seen today. These perturbations are believed to originate from the initial fluctuations of the scalar fields present during inflation. We start by going through the linear order cosmological perturbation theory in Section 3.1, that is needed in quantifying and computing the curvature perturbations, and their relation to the matter content of the universe. In Section 3.2.1, we compute the primordial curvature perturbation power spectrum in the single-field slow-roll inflation, i.e. perturbations that originate from the fluctuations of the inflation-driving inflaton field. We also give a brief review on an alternative approach to perturbation theory, the separate universe approach or ΔN formalism [32, 33, 34, 35] in Section 3.3. The ΔN formalism allows us to compute the primordial curvature perturbation in multifield scenarios, where the perturbations are sourced by multiple scalar fields. As a case-example, we study the curvaton scenario [36, 37, 38] in Section 3.4, which is a two-field model, where the inflaton is responsible for the inflationary dynamics, while the primordial perturbations originate from a spectator field dubbed as the curvaton.

3.1 Cosmological perturbation theory

In this section we study the cosmological perturbation theory, that is needed in the computation of primordial perturbations. We start by discussing the scalar-vector-tensor decomposition of the perturbed metric, and move on to discuss the different gauge-invariant quantities. We briefly touch on the matter of adiabatic and non-adiabatic perturbations and their evolution on superhorizon scales. This section is mostly based on the presentation of cosmological perturbation theory given in refs. [13, 25, 39].

3.1.1 Metric perturbations and SVT-decomposition

We start by writing the perturbed metric $g_{\mu\nu}$ as

$$g_{\mu\nu} = \bar{g}_{\mu\nu}(\tau) + \delta g_{\mu\nu}(\tau, \mathbf{x}), \quad \delta g_{\mu\nu} \ll \bar{g}_{\mu\nu}, \tag{86}$$

where $\bar{g}_{\mu\nu} = a^2(\tau)\ \mathrm{diag}(-1,1,1,1)$, is the standard unperturbed FRW-metric (in conformal time) and $\delta g_{\mu\nu}$ is the small perturbation on the FRW-background. As before, the barred quantities refer to the background values, and quantities without bars are the perturbed quantities. We know the form of the metric on the homogeneous and isotropic FRW-background, but what is the general form for the perturbed part? It happens that the metric perturbations can be decomposed according to the their transformation properties under spatial rotations. First,

the spacetime is sliced into homogeneous constant-time spacelike slices (referred to as the (3 + 1) -split). Then the rotations on these hypersurfaces of constant time leads to three different perturbations: scalar, vector and tensor perturbations. This is referred to as the SVT-decomposition. [25]

In SVT-decomposition one usually starts by writing the components of the metric perturbation as [25]

$$\delta g_{\mu\nu} = a^2(t) \begin{pmatrix} -2A & -B_i \\ -B_i & h_{ij} \end{pmatrix}, \tag{87}$$

where $A = A(\tau, \mathbf{x})$, $B_i = B_i(\tau, \mathbf{x})$ and $h_{ij} = h_{ij}(\tau, \mathbf{x})$. The quantity h_{ij} is usually further decomposed into the trace and traceless parts $h_{ij} = -2D\delta_{ij} + 2E_{ij}$. The full metric then reads

$$g_{\mu\nu} = a^2(\tau) \begin{pmatrix} -1-2A & -B_i \\ -B_i & (1-2D)\delta_{ij} + 2E_{ij} \end{pmatrix}. \tag{88}$$

It is then straightforward to show that under constant rotation $g_{\alpha\beta} = \Lambda^{\mu}{}_{\alpha}\Lambda^{\nu}{}_{\beta} g_{\mu\nu}$, where $\Lambda^{\mu}{}_{\nu} = \mathrm{diag}\left(1, \Lambda^{i}{}_{j}\right)$ is the rotation matrix, the components of $g_{\mu\nu}$ transform such that A and D transform as scalars, B_i transforms as a vector and E_{ij} transforms as a $(0,2)$-tensor. It is customary to further decompose the B_i and E_{ij}:

$$B_i = \partial_i B + B_i^V \tag{89}$$

$$E_{ij} = \left(\partial_i\partial_j - \frac{1}{3}\delta_{ij}\nabla^2\right) E + \frac{1}{2}\left(\partial_i E_j + \partial_j E_i\right) + E_{ij}^T, \tag{90}$$

where B and E transform as scalars, B_i^V and E_i transform as vectors and E_{ij}^T transforms as a tensor.

In the SVT-decomposition the perturbed metric has all in all ten degrees of freedom: four scalars A, B, D and E (1 degree of freedom for each), two vectors B_i and E_i (2 degrees for freedom for each) and one tensor E_{ij}^T (2 degrees of freedom). In linear order perturbation theory the scalar, vectorial and tensorial degrees of freedom decouple from each other, i.e. their evolution can be studied independently [25]. The vector perturbations are decaying solutions, and not much of interest in the context of this thesis, as they are not excited during inflation [25]. The tensor perturbation E_{ij}^T is gauge-invariant quantity and corresponds to gravitational waves [25]. The interest of this thesis are scalar perturbation degrees of freedom, as they couple to the matter density and the curvature perturbation. In the following sections we will focus on the scalar perturbations.

3.1.2 Scalar perturbations and gauge freedom

The line-element of the scalar part of the metric reads [13, 25]

$$\mathrm{d}s^2 = a^2\left[-(1+2A)\,\mathrm{d}\tau^2 - 2\partial_i B \mathrm{d}\tau \mathrm{d}x^i + \left((1-2\psi)\delta_{ij} + 2\partial_i\partial_j E\right)\mathrm{d}x^i\,\mathrm{d}x^j\right], \tag{91}$$

where we defined the quantity ψ as

$$\psi = D + \frac{1}{3}\nabla^2 E, \tag{92}$$

which is referred to as the curvature perturbation, as the scalar curvature ${}^3R$, the spatial part of the Ricci scalar, can be written in terms of it, ${}^{(3)}R = \left(4/a^2\right)\nabla^2\psi$ [25].

As expected, there are certain gauge-freedom in the computation. Although we start from a configuration with scalar perturbations, for a general gauge-transformation generated by the vector field $\tilde{\xi}^\mu\left(\tau, x^i\right)$, it is possible that the transformation induces vector perturbations. These remnants are not physical, as they are only effects of a badly chosen gauge. To avoid these pure gauge effects, it is then customary to divide the spatial part of the vector $\tilde{\xi}^i$ to the scalar and vectorial part

$$\tilde{\xi}^i = \chi^i + \partial^i\xi, \tag{93}$$

and only consider the following gauge transformations

$$\tilde{x}^0 = x^0 + \tilde{\xi}^0\left(\tau, \mathbf{x}\right), \; \tilde{x}^i = x^i + \delta^{ij}\partial_j\xi\left(\tau, \mathbf{x}\right). \tag{94}$$

With these choices and with the requirement that the line-element (91) is invariant under the above gauge-transformation, one can check how the scalar quantities in eq. (91) transform: [25]

$$\tilde{A} = A - \partial_0\tilde{\xi}^0 - \mathcal{H}\tilde{\xi}^0, \; \tilde{B} = B + \tilde{\xi}^0 - \partial_0\tilde{\xi} \tag{95}$$

$$\tilde{D} = D + \frac{1}{3}\nabla^2\tilde{\xi} + \mathcal{H}\tilde{\xi}^0, \; \tilde{E} = E - \tilde{\xi} \tag{96}$$

$$\tilde{\psi} = \psi + \mathcal{H}\tilde{\xi}^0. \tag{97}$$

In the perturbed metric (91) we have four different scalar quantities A, B, E, ψ, and if we take into account the inflaton ψ, that dominates the energy density of the universe during inflation, there are five different scalar degrees of freedom in total. If one fixes the two gauge degrees of freedom (94), and takes into account the constraint eqs. coming from the continuity conditions $\nabla_\mu G^{\mu\nu} = 0$ and $\nabla_\mu T^{\mu\nu} = 0$, there is one scalar degree of freedom left — assuming that only one scalar field contributes to $T^{\mu\nu}$. Next we then identify different gauge-invariant scalar quantities, that are used in the computation of primordial perturbations.

Let us first define the Bardeen potentials [40]

$$\Phi \equiv A - \mathcal{H}\left(B + E'\right) - \left(B + E'\right)', \; \Psi \equiv \psi + \mathcal{H}\left(B + E'\right), \tag{98}$$

one can check using the transformation of A, B, E and ψ that Φ and Ψ are indeed gauge-invariant quantities. In the conformal Newtonian gauge one sets the scalar perturbations B and E to zero, which is achieved from any gauge that has $E, B \neq 0$ by choosing $\tilde{\xi}^0 = E' + B$ and $\tilde{\xi} = E$. In the Newtonian gauge we then have that

$$\tilde{A} = A - \partial_0\tilde{\xi}^0 - \mathcal{H}\tilde{\xi}^0 = A - \left(B + E'\right)' - \mathcal{H}\left(B + E'\right) \tag{99}$$

$$\tilde{\psi} = \psi + \mathcal{H}\tilde{\xi}^0 = \psi + \mathcal{H}\left(B + E'\right), \tag{100}$$

i.e. the Bardeen potentials Φ and Ψ coincide with the scalar perturbations A and ψ. In the conformal Newtonian gauge the metric is then simply just

$$g_{\mu\nu} = a^2 \begin{pmatrix} -1-2\Phi & 0 \\ 0 & (1-2\Psi)\,\delta_{ij} \end{pmatrix}. \tag{101}$$

In the case, where the perturbed system is described by an ideal fluid which anisotropic stress vanishes, the Bardeen potentials are equivalent $\Phi = \Psi$ [25]. The conformal Newtonian gauge is useful when computing structure formation from the perturbed Einstein eqs. $\delta G^{\mu}_{\nu} = M_{\mathrm{Pl}}^{-2}\delta T^{\mu}_{\nu}$. In the subhorizon limit the conformal Newtonian gauge approaches the standard Newtonian description, and in this limit one can understand the Bardeen potential as a Newtonian gravitational potential due to density perturbations. The Bardeen potentials are then often used when the subhorizon evolution of perturbations are studied, but due to non-trivial time evolution, different gauge-invariant measures of the scalar perturbations are used on the superhorizon levels.

In the context of inflation, one of the most used quantities is the curvature perturbation on uniform-density hypersurfaces [39]

$$-\zeta = \psi + \frac{\mathcal{H}}{\bar{\rho}'}\delta\rho = \psi|_{\delta\rho=0}\,, \tag{102}$$

where $\delta\rho$ is the perturbation of the energy density. The name refers to working in a uniform-density gauge, where $\delta\rho = 0$. In this gauge, by construction, it is ζ that represents the gravitational potential ψ on uniform energy density slices. We know that the scalar quantities transform as $\delta\widetilde{S}\left(x^{\mu}\right) = \delta S\left(x^{\mu}\right) - \xi^0\bar{S}'\left(t\right)$ [25], and it is then clear from eq. (97), that eq. (102) is obtained by setting $\xi^0 = \delta\rho/\bar{\rho}'$. In the literature ζ is often written as

$$-\zeta = \psi - \frac{\delta\rho}{3\left(\bar{\rho}+\bar{p}\right)}, \tag{103}$$

where we used the continuity equation for the background field $\bar{\rho}' + 3\mathcal{H}\left(\bar{\rho}+\bar{p}\right) = 0$. The advantage of using ζ in the computation of the scalar perturbations is its superhorizon evolution: in the single-field slow-roll inflation ζ is conserved on superhorizon scales [39]. We will discuss the evolution of ζ in Section 3.1.3. We will encounter ζ also in Section 3.3, where we will discuss the separate universe method of computing perturbations.

Another often used gauge-invariant quantity is the curvature perturbation on comoving slices $\mathcal{R}$. It is defined in terms of ψ and the inflaton field ϕ (single-field case), as for the observers on the comoving slices the expansion is isotropic, and thus there is no measured energy flux, $T_{0i} = 0$ [13]. During inflation $T_{0i} \propto \partial_i\delta\phi$, which means that these observes measure $\delta\phi = 0$ on comoving slices [13]. We know that the perturbation of the scalar field transforms as $\delta\tilde{\phi} = \delta\phi - \bar{\phi}'\xi^0$, i.e. we choose $\xi^0 = \delta\phi/\bar{\phi}'$ on the comoving slice. The definition for the comoving curvature perturbation $\mathcal{R}$ is then

$$\mathcal{R} = \psi + \mathcal{H}\xi^0 = \psi + \mathcal{H}\frac{\delta\phi}{\bar{\phi}'} = \psi + H\frac{\delta\phi}{\dot{\bar{\phi}}}. \tag{104}$$

Perturbations ζ and $\mathcal{R}$ can be related via the linearized Einstein equations, and in Fourier space this reads [13]

$$-\zeta_{\mathbf{k}} = \mathcal{R}_{\mathbf{k}} + \left(\frac{k}{\mathcal{H}}\right)^2 \frac{2\bar{\rho}}{3\left(\bar{\rho}+\bar{p}\right)}\Psi_{\mathbf{k}}, \tag{105}$$

where Ψ is one of the Bardeen potentials. We can see, that on superhorizon levels, $k \ll \mathcal{H}$, the two quantities coincide $-\zeta_{\mathbf{k}} \approx \mathcal{R}_{\mathbf{k}}$. Also, ζ and $\mathcal{R}$ are equal during (single-field) slow-roll [13]. This means that as ζ is conserved in the superhorizon limit, so is $\mathcal{R}$. In the Newtonian gauge, the curvature $\mathcal{R}$ can be written in terms of the Bardeen potential Φ:

$$\mathcal{R} = \Phi + \frac{2}{3\mathcal{H}\left(1+w\right)}\left(\Phi' + \mathcal{H}\Phi\right), \tag{106}$$

where $w = \bar{p}/\bar{\rho}$ [25]. For $w = $ const., as is for the single-field case, where perturbations are adiabatic, the superhorizon result for eq. (4) in Fourier space reads [39]

$$\mathcal{R}_{\mathbf{k}} = \frac{5+3w}{3+3w}\Phi_{\mathbf{k}}. \tag{107}$$

Therefore, the superhorizon value of the gravitational potential is related to the conserved curvature perturbation $\mathcal{R}$.

One can also consider a spatially flat gauge $\tilde{\psi} = 0$. Starting from a non-flat gauge, this gauge choice corresponds to fixing $\xi^0 = -\psi/\mathcal{H}$. This of course fixes also the perturbation of the inflaton field, i.e.

$$\delta\tilde{\phi} = \delta\phi - \bar{\phi}'\xi^0 = \delta\phi + \bar{\phi}'\frac{\psi}{\mathcal{H}}. \tag{108}$$

We then define the so-called Sasaki-Mukhanov variable Q as [13, 41, 42]

$$Q = \delta\phi + \bar{\phi}'\frac{\psi}{\mathcal{H}} = \frac{\bar{\phi}'}{\mathcal{H}}\mathcal{R} = \frac{\dot{\bar{\phi}}}{H}\mathcal{R}, \tag{109}$$

where we used the definition (104) for $\mathcal{R}$. This gauge-invariant quantity describes the inflaton fluctuations on a spatially flat slicing, i.e. $Q = \delta\phi|_{\psi=0}$. This allows us to connect the curvature perturbation $\mathcal{R}$ to the inflaton fluctuations, $\mathcal{R} = \left(H/\dot{\bar{\phi}}\right)\delta\phi$. We are going to come back to this result in Section 3.2, where we compute the power spectrum of the curvature perturbation $\mathcal{R}$.

3.1.3 Evolution of ζ & adiabatic and non-adiabatic perturbations

Generally, to study the evolution of the perturbations one needs to start from the Einstein eqs. (2). On the left-hand side of eq. (2) one computes the Einstein tensor from the perturbed metric (86), by first computing the Christoffel connections and then proceeds to compute the Riemann tensor and Ricci scalar etc. On the right-hand side of eq. (2), one also perturbs the matter content in $T_{\mu\nu}$, i.e. $\rho \to \bar{\rho} + \delta\rho$

and $p \to \bar{p} + \delta p$. This is straightforward albeit laborious. In the end, one ends up with four Einstein equations and two continuity equations for the perturbed quantities.

However, as we are now interested in the superhorizon evolution of the perturbations, we do not need to perform the laborous process of going through the full perturbed Einstein equations. The local conservation of $\nabla_\mu T^\mu_\nu = 0$ can be used to derive the result for the time-evolution of ζ [43]. Assuming that all gradients vanish at large enough scales, the superhorizon result reads [43]

$$\zeta' \approx -\frac{\mathcal{H}}{\bar{\rho} + \bar{p}} \left(\delta p - \frac{\bar{p}'}{\bar{\rho}'} \delta\rho \right) = -\frac{\mathcal{H}}{\bar{\rho} + \bar{p}} \delta p_{\mathrm{nad}}, \tag{110}$$

where p_{nad} is the referred to as the non-adiabatic component of the pressure. For adiabatic perturbations $\delta p_{\mathrm{nad}} = 0$, which implies that ζ is conserved on superhorizon scales. For non-adiabatic perturbations the curvature perturbation ζ evolves on the superhorizon scales.

The adiabatic perturbations correspond to a change in the total energy density ρ. Adiabatic perturbations have the property, that the value or state of the matter at $(\tau, \mathbf{x})$ in the perturbed universe is the same as in the background universe at some different shifted time $(\tau + \delta\tau, \mathbf{x})$. For example, we have that for the energy density and pressure the adiabatic condition says that [6]

$$\delta\rho(\tau, \mathbf{x}) = \bar{\rho}(\tau + \delta\tau(\mathbf{x})) - \bar{\rho}(\tau) = \bar{\rho}'\delta\tau(\mathbf{x}) \tag{111}$$

$$\delta p(\tau, \mathbf{x}) = \bar{p}(\tau + \delta\tau(\mathbf{x})) - \bar{p}(\tau) = \bar{p}'\delta\tau(\mathbf{x}). \tag{112}$$

As the shift is common for both of the scalar quantities, we get the adiabatic condition

$$\frac{\delta\rho}{\bar{\rho}'} = \frac{\delta p}{\bar{p}'}, \tag{113}$$

which is fulfilled for barotropic fluids, which have the equation of state $p = p(\rho) = w\rho$, where w is constant, i.e. $\delta p = w\delta\rho$. We can then see, that for adiabatic perturbations (113) the non-adiabatic pressure δp_{nad} in eq. (110) vanishes, that is, for adiabatic perturbations the curvature perturbation ζ is constant on superhorizon scales:

$$\zeta' = 0, \tag{114}$$

if $\delta p_{\mathrm{nad}} = 0$ on superhorizon scales during inflation. It is then justified to compute the value of ζ at the horizon exit and to ignore the superhorizon evolution. This effect is essentially just the conservation of entropy, as there are no perturbations between different fluid components.

If the universe contains multiple fluids I, J, and there is no energy transfer between the fluids at the background level, we can write the above condition (113) as

$$\frac{\delta_I}{1 + w_I} = \frac{\delta_J}{1 + w_J}, \tag{115}$$

where $\delta_I = \delta\rho_I/\bar{\rho}_I$, and where we used the continuity eq. $\bar{\rho}_I' + 3\mathcal{H}\left(1+w_I\right)\bar{\rho}_I = 0$. For example, in the case universe contains matter ($w_m \approx 0$) and radiation ($w_r = 1/3$), we have that for adiabatic perturbations $\delta_r = 4\delta_m/3$.

While the adiabatic perturbations respect the conservation of entropy, this is not true for the non-adiabatic perturbations that are usually referred to as entropy or isocurvature perturbations. Isocurvature perturbations correspond to perturbations between the different fluid components. Following eq. (115) it is customary to define the isocurvature perturbations as [6]

$$S_{IJ} = \frac{\delta_I}{1+w_I} - \frac{\delta_J}{1+w_J} = -3\mathcal{H}\left(\frac{\delta\rho_I}{\bar{\rho}_I'} - \frac{\delta\rho_J}{\bar{\rho}_J'}\right), \tag{116}$$

which vanishes for adiabatic perturbations, i.e. $S_{IJ} = 0$. In the uniform-density gauge $\psi = 0$, eq. (116) can also be written as $S_{IJ}\big|_{\psi=0} = 3\left(\zeta_I - \zeta_J\right)$ [43]. We can also define the isocurvature perturbation in terms of $\delta p_{\rm nad}$:

$$\delta S = \frac{\mathcal{H}}{\bar{\rho}'}\delta p_{\rm nad} = \mathcal{H}\left(\frac{\delta p}{\bar{p}'} - \frac{\delta\rho}{\bar{\rho}'}\right), \tag{117}$$

which also allows us to write eq. (110) as $\zeta' = 3\mathcal{H}\delta S$.

In the single-field slow-roll inflation, the perturbations generated during inflation are adiabatic [44, 45] (see also ref. [13]). On the superhorizon scales the curvature perturbation ζ is thus conserved. If there are multiple fields involved in the inflationary dynamics, one generally can have isocurvature (or entropy) perturbations. With multiple fields, it is possible to redefine the fields such that one field is responsible for the adiabatic perturbations, while other fields can be either purely isocurvature perturbation or a mixture of both [46]. If there are multiple fields present during inflation, the evolution of both the adiabatic and non-adiabatic perturbations is non-trivial, as the entropy perturbations (that can also have superhorizon evolution) can be transformed into adiabatic ones. Importantly, current observations are consistent with purely adiabatic perturbations [4]. See e.g. refs. [39, 46] for more details.

3.2 Curvature perturbation in singe-field slow-roll

We are finally ready to discuss the primordial perturbation originating from the inflaton field. In principle, there are various different ways how to proceed on computing the emerging perturbations. First, one can start from the full Einstein-Hilbert action

$$S = \int \mathrm{d}^4x\sqrt{-g}\left(\frac{M_{\rm Pl}^2}{2}R + \mathcal{L}_\phi\right), \tag{118}$$

where R is the Ricci scalar and $\mathcal{L}_\phi$ is the Lagrangian of the inflaton field. From here one then proceeds to expand the perturbed Ricci scalar etc. Another way

is to compute the perturbed Einstein and energy-momentum tensor in a gauge-invariant way and find the evolution equations. Both of these methods are quite labourious, and we will not go through them in this present work — see e.g. refs. [13, 25, 39] for details.

In this work, we first compute the power spectrum of curvature perturbation $\mathcal{R}$ by identifying that the quadratic action for $\mathcal{R}$ coincides in the comoving gauge, that was discussed in Section 3.1.2, with the action for a massless test scalar discussed in Chapter 2, where we did not have to take into account the metric perturbations in the computation. We can therefore use the already derived results in computing the power spectrum $\mathcal{P}_{\mathcal{R}}$.

One can also use the separate universe approach or ΔN formalism, to compute the primordial perturbations. This approach is especially helpful when studying scenarios involving multiple scalar fields in the very universe. We will discuss the ΔN formalism in Section 3.3.

3.2.1 Power spectrum of curvature perturbations generated by the inflaton

The quadratic action for $\mathcal{R}$ can be written as [13, 47]

$$S_{\mathcal{R}} = \frac{1}{2}\int \mathrm{d}\tau \mathrm{d}^3\mathbf{x}\, \left(\frac{a\bar{\phi}'}{\mathcal{H}}\right)^2 \left[\mathcal{R}'^2 - (\nabla\mathcal{R})^2\right]. \tag{119}$$

We can write eq. (119) in a more familiar form, if we define $q = z\mathcal{R}$, where $z = a\bar{\phi}'/\mathcal{H}$. The action for q reads [13]

$$S_q = \frac{1}{2}\int \mathrm{d}\tau \mathrm{d}^3\mathbf{x} \left[(q')^2 - (\nabla q)^2 + \frac{z''}{z}q^2\right], \tag{120}$$

which has the same form as the action for the scaled test scalar $\chi = a\delta\sigma$ in eq. (38), except the effective mass term $a''/a - a^2 V_{,\sigma\sigma}$ is replaced by z''/z. In the pure de Sitter limit, where $H \simeq$ const., we have $z''/z = a''/a = 2/\tau^2$, i.e. eq. (120) describes a massless scalar field that was already discussed in Chapter 2. In the quasi de Sitter limit, where the time-dependency of H is described the slow-roll parameter ϵ_H, the field acquires a small effective mass that depends on the slow-roll parameters (as was the case in the quasi de Sitter limit discussed in Chapter 2).

In the spatially flat gauge we have that the scaled Sasaki-Mukhanov variable (109) is

$$q|_{\psi=0} = \frac{a\dot{\bar{\phi}}}{H}\,\mathcal{R}|_{\psi=0} = a\,Q|_{\psi=0} = a\,\delta\phi|_{\psi=0}\,, \tag{121}$$

i.e. we can write the gauge-invariant curvature perturbation $\mathcal{R}$ in the Fourier space as

$$\mathcal{R}_{\mathbf{k}} = \frac{H}{\dot{\bar{\phi}}}\delta\phi_{\mathbf{k}}, \tag{122}$$

where we dropped the subscript $\psi = 0$ referring to spatially flat gauge. We can then follow to define the curvature power spectrum $\mathcal{P}_\mathcal{R}$ to be

$$\langle \mathcal{R}_\mathbf{k} \mathcal{R}_{\mathbf{k}'} \rangle = \left(\frac{H}{\dot{\bar{\phi}}} \right)^2 \langle \delta\phi_\mathbf{k} \delta\phi_{\mathbf{k}'} \rangle = (2\pi)^3 \, \delta\left(\mathbf{k} + \mathbf{k}'\right) \frac{2\pi^2}{k^3} \mathcal{P}_\mathcal{R}\left(k\right). \tag{123}$$

The curvature spectrum $\mathcal{P}_\mathcal{R}$ is then the scalar spectrum multiplied by the factor coming from the Sasaki-Mukhanov variable:

$$\mathcal{P}_\mathcal{R}\left(k\right) = \left(\frac{H}{\dot{\bar{\phi}}} \right)^2 \mathcal{P}_{\delta\phi}\left(k\right). \tag{124}$$

We can then use the slow-roll eqs. (32) to write $(H/\dot{\bar{\phi}})^2 = \left(2\epsilon_\phi M_{\rm Pl}^2\right)^{-1}$. As discussed, the action for $q = a\delta\phi$ describes fluctuations of a light scalar field, and as we know that the curvature perturbations $\mathcal{R}$ freeze on superhorizon scales in single-field slow-roll inflation, we can evaluate $\mathcal{P}_{\delta\phi}$ at the horizon crossing $k = aH$ and use the result (71). The primordial curvature spectrum $\mathcal{P}_\mathcal{R}$ is then given by

$$\mathcal{P}_\mathcal{R}\left(k\right) = \frac{1}{2\epsilon_\phi M_{\rm Pl}^2} \times \left(\frac{H}{2\pi} \right)^2 \Bigg|_{k=aH}, \tag{125}$$

which is the main result of this section.

We can find the scale-dependency of the curvature spectrum $\mathcal{P}_\mathcal{R}$ as we did in Sec. 2.2.2, by considering that the Hubble rate H is not exactly constant. The spectral index n_s for the primordial curvature perturbation is then

$$\begin{aligned} n_s - 1 &= \left. \frac{\mathrm{d}\log\mathcal{P}_\mathcal{R}}{\mathrm{d}\log k} \right|_{k=aH} && (126) \\ &= \left(-\frac{1}{\epsilon_\phi} \frac{\mathrm{d}\epsilon_\phi}{\mathrm{d}\log k} + \frac{2}{H} \frac{\mathrm{d}H}{\mathrm{d}\log k} \right)_{k=aH} && (127) \\ &= -4\epsilon_\phi + 2\eta_\phi - 2\epsilon_\phi = -6\epsilon_\phi + 2\eta_\phi, && (128) \end{aligned}$$

where we used the slow-roll equations (32) and set $\epsilon_H = \epsilon_\phi$. Note that all quantities are evaluated at the horizon crossing $k = aH$. Note that compared to the power spectrum of test scalar (80), the spectral tilt for curvature perturbations is more tilted due to the extra ϵ_ϕ terms.

3.2.2 Current constraints on $\mathcal{P}_\mathcal{R}$ and testing inflationary models

Let us then briefly discuss the constraints on the power spectrum (125) and how they are used in constraining the inflationary models. As discussed previously, it is customary to parameterize the spectrum as [4]

$$\mathcal{P}_\mathcal{R}\left(k\right) = A_s \left(\frac{k}{k_{\rm ref}} \right)^{n_{\rm s} - 1 + \frac{1}{2}\alpha_{\rm s} \log\left(\frac{k}{k_{\rm ref}}\right)} \tag{129}$$

where we took the parameterization only to second-order in slow-roll, and $A_s = \mathcal{P}_{\mathcal{R}}(k_{\rm ref})$ is the amplitude of the spectrum at the pivot scale. In terms of the slow-roll parameters, the running of the spectral index α_s is given by [39]

$$\alpha_s = -24\epsilon_\phi^2 + 16\epsilon_\phi\eta_\phi - 2\xi_\phi. \tag{130}$$

The Planck 2018 best-fit values for the spectral index and its running are $n_s = 0.9641 \pm 0.0044$, $\alpha_s = -0.0045 \pm 0.0067$, where the Planck pivot scale is $k_{\rm ref} = 0.05\,{\rm Mpc}^{-1}$ [4]. The Planck 2018 data is then consistent with a vanishing running of the scalar spectral index n_s. The scale-invariant Harrison-Zeldovich spectrum, $n_s - 1 = 0$, is also ruled out in a great accuracy [48]. At the Planck pivot scale $k_{\rm ref} = 0.05\,{\rm Mpc}^{-1}$, the amplitude of the primordial perturbations is observed to be $A_s \approx 2.09 \times 10^{-9}$ [4].

Given the inflaton potential $V(\phi)$, one can compute the slow-roll parameters and the spectrum (125) in terms of the model parameters. These need to satisfy the observed values for the amplitude and and the scale-dependency of $\mathcal{P}_{\mathcal{R}}$. The exact details depend on the model details, such as how the end of inflation and reheating (decay of inflaton) affect the amount of e-folds between the horizon exit of the observed CMB scale and the end of inflation.

Another important observable quantity is the spectrum of tensor perturbations $\mathcal{P}_T$, which measures the primordial gravitational waves coming from inflation — see for example refs. [13, 25] for more information. The power spectrum is given by [13]

$$\mathcal{P}_T(k) = \frac{8}{M_{\rm Pl}^2} \times \left(\frac{H}{2\pi}\right)^2 \Bigg|_{k=aH}, \tag{131}$$

that is, the amplitude of tensor perturbations depends only on the inflationary scale H, and not on the inflaton model details. The amplitude of the tensorial perturbations is usually characterized in terms of the tensor-to-scalar ratio r, which is defined as [13]

$$r = \frac{P_T}{P_{\mathcal{R}}}. \tag{132}$$

In the single-field slow-roll inflation the tensor-to-scalar ratio (132) is then given by

$$r = 16\epsilon_\phi, \tag{133}$$

where ϵ_ϕ is evaluated at the horizon crossing. The current observational limit for the tensor-to-scalar ratio is $r < 0.06$ at the pivot scale $k_{\rm ref} = 0.002\,{\rm Mpc}^{-1}$ [4]. The upper-bound on r is then also a direct constraint for the slow-roll ϵ_ϕ. Eq. (133) also acts as a consistency relation for single-field inflation: if the relation is observationally found to be violated, the inflation is not driven by a single scalar field.

3.3 Alternative approach to perturbations: ΔN formalism

We have now seen how in the linear perturbation theory one can straightforwardly compute the spectrum of adiabatic perturbations, for which the curvature perturbation is conserved on the superhorizon scales. In short, one can choose the preferred slicing in which to do the computation, as the different gauges coincide at the large-scale limit. However, if one wants to study higher-order effects, such as non-Gaussianities (which involve higher-order field correlators), one is required to use higher-order perturbation theory. Albeit straightforward, the non-linearities in the calculation become labourious already in the second-order. This problem is also present in the case, where one wants to consider multifield models, where one needs to take into account the effect of non-adiabatic (isocurvature) perturbations. Fortunately, there is an alternative approach, the ΔN formalism or the separate universe approach, which we will discuss in this section, before moving on to discuss multifield models in Section 3.4. We mostly follow refs. [32, 33, 34, 35, 49].

3.3.1 Separate universes and gradient expansion

The gist of the separate universe approach [32, 33, 34, 35] is to consider the result of gradient expansion [32, 33], that each super-horizon sized region of the universe evolves like a separate FLRW universe. The matter content, i.e. energy density and pressure, can be have different values in each patch, but these patches are still homogeneous and isotropic. The idea is then that in this approach the perturbation is not defined as a deviation from a background value, as in the linear perturbation theory, but as a difference between different separate patches.

For these patches to evolve independently without causal contact, they need to be separated by scales larger that $\mathcal{H}^{-1} = (aH)^{-1}$. Also, as we assume that the different patches are individual FLRW universes, there needs to exist a smoothing scale $\lambda_s \gtrsim \mathcal{H}^{-1}$, that allows to treat the patch as a homogeneous region free of gradients — see for example Figure 1 in ref. [43]. One then needs to consider a local (FLRW) region, which is significantly smaller than the smoothing scale λ_s, but also larger than the Hubble horizon, as we are interested in the superhorizon evolution of the curvature quantities, that is, the treatment applies on scales $\mathcal{H}^{-1} < k^{-1} < \lambda_s$. [33, 34, 43]

One then starts from a generic metric (in the ADM formalism [50]), and deals with the resulting inhomogeneities in the Einstein eqs. by expanding the spatial gradients in some expansion parameter $\tilde{\epsilon}$, i.e. the gradient quantities are multiplied by $\tilde{\epsilon}$ and it is assumed that $\tilde{\epsilon} \ll 1$ [32]. Assuming that the smoothing scale is large enough, in the first-order gradient expansion the Einstein eqs. reduce in leading-order to the standard homogeneous Friedmann equations, and the gradient terms yield an additional term, that acts as a momentum constraint equation of general relativity [32, 33].

3.3.2 The metric and local scale factor

In the separate universe approach the metric is parameterized as in the Arnowitt-Deser-Misner formalism [50], and to first order in gradient expansion it can be shown to be [32]

$$\mathrm{d}s^2 = -\mathcal{N}^2\mathrm{d}t^2 + \gamma_{ij}\mathrm{d}t\left(N^i\mathrm{d}x^j + N^j\mathrm{d}x^i\right) + \gamma_{ij}\mathrm{d}x^i\mathrm{d}x^j, \tag{134}$$

where $\mathcal{N}$ is the lapse function, N^i is the shift-function and γ_{ij} is the spatial metric. The three-metric is then written as $\gamma_{ij} = \mathrm{e}^{2\alpha}\tilde{\gamma}_{ij}$, and the locally-defined scale factor $\tilde{a}$ is then defined as [32]

$$\tilde{a} = \mathrm{e}^{\alpha} = a\left(t\right)\mathrm{e}^{-\psi(t,\mathbf{x})}, \tag{135}$$

where the coordinate $\mathbf{x}$ refers to the coarse-grained quantities, and the global scale factor $a\left(t\right)$ and the quantity ψ were factored out. We can then see that the difference between the evolution of the different patches described by the local scale factors $\tilde{a}$, is encoded in the quantity ψ. If the perturbation ψ vanishes for example at our location of the observable universe, we have that $a\left(t\right)$ is the scale factor of our part of the universe. The local Hubble parameter is then given by [32]

$$\tilde{H} = \frac{1}{\mathcal{N}}\frac{\mathrm{d}\alpha}{\mathrm{d}t} = \frac{1}{\mathcal{N}}\frac{\mathrm{d}}{\mathrm{d}t}\log\left(a\left(t\right)\mathrm{e}^{-\psi(t,\mathbf{x})}\right) = \frac{1}{\mathcal{N}}\left(\frac{\dot{a}}{a} - \dot{\psi}\right). \tag{136}$$

As expected, we would like to relate the scale factor $\tilde{a}$ to the matter content of the universe, as we are interested in the perturbations coming from the inflaton or other scalar fields. In the gradient expansion the evolution equations reduce to the FLRW ones point by point, the continuation equation is just [32]

$$\frac{\mathrm{d}\rho}{\mathrm{d}t} = -3\tilde{H}\mathcal{N}\left(\rho + p\right), \tag{137}$$

which allows us to relate the derivative of the local scale factor to the matter content:

$$\frac{\dot{a}}{a} - \dot{\psi} = -\frac{1}{3}\frac{\dot{\rho}}{\rho + p}, \tag{138}$$

which we are going to use in the next section where we will define the quantity ΔN. Note that we have not discussed the mentioned constraint eqs. coming from the gradient expansion. We refer the interested readers to (the appendix of) ref. [32] and references therein for a detailed discussion on the matter.

3.3.3 Definition of ΔN

The number of e-foldings of expansion along a comoving worldline between initial time t_1 to final time t_2 is then defined to be [32]

$$N\left(t_2, t_1; \mathbf{x}\right) = \int_{t_1}^{t_2}\tilde{H}\mathcal{N}\mathrm{d}t = \int_{t_1}^{t_2}\frac{\mathrm{d}}{\mathrm{d}t}\log\left(a\left(t\right)\mathrm{e}^{-\psi(t,\mathbf{x})}\right)\mathrm{d}t \tag{139}$$

$$= \log\left(\frac{a\left(t_2\right)\mathrm{e}^{-\psi(t_2,\mathbf{x})}}{a\left(t_1\right)\mathrm{e}^{-\psi(t_1,\mathbf{x})}}\right) = -\frac{1}{3}\int_{t_1}^{t_2}\frac{\dot{\rho}}{\rho + p}\mathrm{d}t, \tag{140}$$

where we used eq. (138). We can then write that the difference in ψ, when one goes from a slicing to another, is given by the difference of the perturbed and "background" universe e-folds:

$$-\psi\left(t_2,\mathbf{x}\right)+\psi\left(t_1,\mathbf{x}\right)=N\left(t_2,t_1;\mathbf{x}\right)-\log\left(\frac{a\left(t_2\right)}{a\left(t_1\right)}\right). \tag{141}$$

Note that this is still a general result as we have not fixed the gauge. Here the background universe refers to the value of e-folds determined by the global scale factor $a\left(t\right)$. We can see, that in a flat gauge $\psi=0$ the number of e-folds $N\left(t_2,t_1;\mathbf{x}\right)$ coincides with the background value $\log\left(a\left(t_2\right)/a\left(t_1\right)\right)$, as expected.

Let us then choose the time-slicing to be such that the initial hypersurface is spatially flat, $\psi\left(t_1=t',\mathbf{x}\right)=0$, and that the final hypersurface at $t_2=t$ is uniform in density, i.e. $\rho=\rho\left(t\right)$. With this choice we can write eq. (141) as [32]

$$\zeta\left(t,\mathbf{x}\right)=-\psi\left(t,\mathbf{x}\right)=N\left(t,t',\mathbf{x}\right)-\log\left(\frac{a\left(t\right)}{a\left(t'\right)}\right)\equiv\Delta N\left(t,t',\mathbf{x}\right), \tag{142}$$

where we used that on uniform-density slices $-\zeta=\psi$. We then have, that the defined quantity ΔN measures the shift in the e-foldings between the flat and the uniform density hypersurfaces.

If the universe is filled by an ideal fluid with $p=p\left(\rho\right)$ (i.e. we can change the variable $\mathrm{d}t\rightarrow\mathrm{d}\rho$ in eq. (140)), it is straightforward to show that eq. (142) can be written as [32]

$$\zeta\left(t,\mathbf{x}\right)=\frac{1}{3}\int_{\rho\left(t'\right)}^{\rho\left(t',\mathbf{x}\right)}\frac{\mathrm{d}\rho}{\rho+p}, \tag{143}$$

where $\rho\left(t'\right)$ is the background energy density value, and $\rho\left(t',\mathbf{x}\right)$ is the perturbed value on the initial spatially flat hypersurface. As ζ does not explicitly depend on the time-coordinate t, it is therefore conserved quantity for adiabatic perturbations (to the first order in gradient expansion) [32]. We can see, that the first order result (102) is obtained by linearizing eq. (143) [32].

3.3.4 ΔN in terms of scalar field content

We know that in the single-field slow-roll inflation the amount of e-folds is determined by the inflaton field, $N=N\left(\phi\right)$. Starting from eq. (143), and as $\rho=\rho\left(\phi\right)$ and $p=p\left(\phi\right)$, one integrates ϕ from the initial spatially flat hypersurface, where the are no scalar metric perturbations, but only fluctuations of the matter fields, i.e. $\bar{\phi}+\delta\phi$, to the final uniform-energy hypersurface, where the energy density ρ, i.e. inflaton field is unperturbed. The curvature perturbation ζ can be written as [49]

$$\zeta\left(t,\mathbf{x}\right)=\int_{\bar{\phi}+\delta\phi}^{\bar{\phi}}\frac{H}{\dot{\phi}}\mathrm{d}\phi=N_{,\phi}\left(\bar{\phi}\right)\delta\phi\left(\mathbf{x}\right)+\frac{1}{2}N_{,\phi\phi}\left(\bar{\phi}\right)\delta\phi\left(\mathbf{x}\right)^2+\ldots, \tag{144}$$

where the field derivatives are $N_{,\phi}\left(\bar{\phi}\right)=\mathrm{d}N\left(\phi\right)/\mathrm{d}\phi|_{\phi=\bar{\phi}}$ etc., $\delta\phi\left(\mathbf{x}\right)$ is the inflaton perturbation on the spatially flat slicing, and we Taylor expanded to the second order in $\delta\phi$.

As ζ is conserved on superhorizon scales for adiabatic perturbations, we can compute the spectrum $\mathcal{P}_\zeta$ at the horizon exit of a scale $k = aH$. Following the standard definition power spectrum in Fourier space (123), the spectrum for ζ is given by

$$\mathcal{P}_\zeta(k) = \left(N_{,\phi}\right)^2 \mathcal{P}_{\delta\phi}(k), \tag{145}$$

where the derivative of the amount of background e-folds $N(\bar{\phi})$ is

$$N_{,\phi} = -\frac{H}{\dot{\bar{\phi}}}. \tag{146}$$

It is then clear that eq. (145) reduces to

$$\mathcal{P}_\zeta(k) = \left(\frac{H}{\dot{\bar{\phi}}}\right)^2 \left(\frac{H}{2\pi}\right)^2 \Bigg|_{k=aH}, \tag{147}$$

which coincides with the result (125) for $\mathcal{P}_\mathcal{R}$ in the single-field slow-roll inflation.

The ΔN formalism generalizes easily to computing the primordial curvature ζ in models where there are multiple scalar fields present. If we consider a set of scalars ϕ_i, one can show that the linear combination of these fields corresponds to the adiabatic field, i.e. the inflaton, while the remaining fields are the entropy fields (non-adiabatic perturbations) — see for example ref. [46]. Let us then first evolve the unperturbed fields $\bar{\phi}_i$ from the initial spatially flat hypersurface to the uniform-energy density slice with $\delta\rho = 0$. And let us denote the corresponding amount of expansion in e-folds as $N(\rho(t), \bar{\phi})$. We can then proceed to perform the same for the perturbed fields $\bar{\phi}_i + \delta\phi_i$, i.e. evolve them from the flat (unperturbed) slice to the final hypersurface, and denote the corresponding amount of e-folds as $N(\rho(t), \bar{\phi}_i + \delta\phi_i)$, where the $\rho(t)$ corresponds to evolving both of the unperturbed and perturbed field configurations to the same hypersurface. Note, that in the single-field case the final hypersurface corresponds to $\delta\phi = 0$ slicing (as seen above), due to the fact that that $\rho = \rho(\phi)$. However, in the scenario where multiple fields are present, this is generally not the case. It is also clear, that with multiple fields, one generally cannot write $p = p(\rho)$ and therefore eq. (143) is not applicable.

In the multifield setting we can then write ζ or ΔN as [49]

$$\zeta(t, \mathbf{x}) = \Delta N = N(\rho(t), \bar{\phi}_i + \delta\phi_i) - N(\rho(t), \bar{\phi}_i) \tag{148}$$

$$= \sum_i N_{,i}\delta\phi_i(\mathbf{x}) + \frac{1}{2}\sum_{i,j} N_{,ij}\delta\phi_i(\mathbf{x})\,\delta\phi_j(\mathbf{x}) + \ldots, \tag{149}$$

where $N_{,i} = \partial_i N = \partial N/\partial\phi_i$, $N_{ij} = \partial_i\partial_j N$, and we again Taylor expanded assuming that the perturbation $\delta\phi$ is small. We can see that eq. (149) allows the curvature perturbation ζ to have two two different sources of deviations from the Gaussian distribution: the intrinsic non-Gaussianity of the fields on the initial slice $\delta\phi_i$, and the non-Gaussianity arising from the non-linear relation between ζ

and the fields $\delta\phi_i$ [39]. One often assumes that the initial field distributions are gaussian, while the non-gaussianities arise from the following non-linear evolution after the horizon crossing [39]. The discussion of non-Gaussianities is beyond the scope of this present work, and we refer to e.g. ref. [39] for more detailed discussion.

Assuming that the fields are initially purely Gaussian and do not have correlations with each other, we can write the power spectrum $\mathcal{P}_\zeta$ as a sum of nearly massless scalar fields [39]

$$\mathcal{P}_\zeta(k) = \mathcal{P}_{\delta\phi}\left(\sum_i N_{,i}^2\right) = \left(\frac{H}{2\pi}\right)^2 \left(\sum_i N_{,i}^2\right)\Bigg|_{k=aH}, \tag{150}$$

where the derivatives of the number of e-folds depend on the details of the model. We can also follow to decompose eq. (150) to the adiabatic and non-adiabatic parts

$$\mathcal{P}_\zeta(k) = \mathcal{P}_\zeta^{\mathrm{ad}}(k) + \left(\frac{H}{2\pi}\right)^2 \left(\sum_j N_{,j}^2\right)\Bigg|_{k=aH}, \tag{151}$$

where the adiabatic part $\mathcal{P}_\zeta^{\mathrm{ad}}$ follows the standard (inflaton) paradigm that was discussed in Section 3.2.1 [39].

3.4 Curvaton model

So far we have mainly concentrated on inflationary models where the inflationary dynamics and primordial perturbations are sourced by only a one field, the inflaton. However, it is possible that there are multiple scalar fields present in the very early universe. These fields can have multiple different roles: they can act as drivers of the inflationary dynamics, e.g. there can be double inflationary scenario with two acceleration phases [51], or they can be subdominant spectator fields that do not affect the dynamics of inflation, but after inflation can for example lead to creation of curvature perturbations [36, 37, 38] or contribute to the energy density as a dark matter component (see e.g. refs. [52, 53, 54]).

As we have discussed previously, as soon as there are multiple scalar fields present, one needs to consider how the possible non-adiabatic fluctuations affect the evolution of the universe. We know the non-adiabatic entropy perturbations can alter the evolution of curvature perturbations on superhorizon scales, as given by eq. (110). In a setting, where there are multiple scalar fields present during inflation, one can generally perform such a field rotation that the arbitrary field perturbation can be decomposed into the adiabatic and entropy components. [46]

The evolution of the entropy modes is model-dependent, and the production of the primordial isocurvature perturbation depends for example on the details of reheating [55]. In certain cases, the initial isocurvature mode can be converted into adiabatic curvature perturbations well after the inflationary epoch.

This is the case in the curvaton scenario [36, 37, 38], which we will discuss in more detail below, where the initial light spectrator field (and thus isocurvature mode) decays to radiation after the field has become massive. We will then leave the general discussion of the details of adiabatic and non-adiabatic perturbations out of this work, and refer to the detailed discussion e.g. in refs. [46, 56]

3.4.1 Curvaton scenario

In the curvaton scenario [36, 37, 38] there are two scalar fields present during inflation: the inflaton ϕ, which is responsible of the dynamics of inflation, and a spectator field referred to as the curvaton σ, which is at least partly responsible for the primordial perturbations. In the simplest curvaton models (see e.g. [36, 37, 38]), the primordial perturbations generated by the inflaton are assumed to be negligible, and that the observed adiabatic perturbations originate from the conversion of the initial isocurvature perturbations of the curvaton field as it decays into radiation after inflation. In the literature there are various different curvaton models discussed (see e.g. [57, 58, 59]), but in this section we will mainly mention the main points of the simplest models.

We assume that during the inflation there are only the two scalars present, i.e. the inflaton ϕ and the curvaton σ, and that they are uncoupled, that is

$$V(\phi, \sigma) = V(\phi) + U(\sigma), \tag{152}$$

where $V(\phi)$ and $U(\sigma)$ are the inflaton and curvaton potentials, respectively. The curvaton field is assumed to act as a spectator field during inflation, i.e. it does not take part into the inflationary dynamics. Therefore it is required that the curvaton is subdominant, $\rho_\sigma \ll \rho_\phi$. We also assume that the curvaton is light during inflation, $U_{,\sigma\sigma} < H^2$. As discussed, a light scalar acquires perturbations via the quantum fluctuations $\delta\sigma$ around it's classical background value $\bar{\sigma}$ with the nearly scale-invariant spectrum:

$$\mathcal{P}_{\delta\sigma} = \left(\frac{H}{2\pi}\right)^2 \Bigg|_{k=aH}, \tag{153}$$

where the Hubble rate is evaluated during the horizon crossing. From the discussion in Section 2 we know that the spectral index of this kind of light scalar is $n_\sigma - 1 = 2\epsilon_\phi - 2\eta_\sigma$.

After the inflaton has decayed to its decay products and the thermalization of said particles, the universe enters a radiation dominated epoch. We assume that the inflaton produced curvature perturbation is negligible, and therefore the radiation filled universe is highly homogeneous $\rho_r \approx \rho_r(t)$. On the superhorizon scales the still subdominant curvaton evolves according to the standard equation of motion [60]

$$\ddot{\sigma} + 3H\dot{\sigma} + U_{,\sigma} = 0, \tag{154}$$

where the Hubble parameter is $H = 1/2t$ during radiation domination. We can further decompose this to the equations for the background field and the perturbation, i.e. $\sigma = \bar{\sigma} + \delta\sigma$ [60]:

$$\ddot{\bar{\sigma}} + 3H\dot{\bar{\sigma}} + U_{,\sigma} = 0 \tag{155}$$

$$\ddot{\delta\sigma} + 3H\dot{\delta\sigma} + U_{,\sigma\sigma}\delta\sigma = 0. \tag{156}$$

We can see that the fractional perturbation, $\delta\sigma/\sigma$, does not change if the potential $U(\sigma)$ is quadratic $U(\phi) = \frac{1}{2}m_\sigma^2\sigma^2$ or is flat enough $U_{,\sigma}, U_{,\sigma\sigma} \approx 0$, as the background and perturbations follow the same equations of motion [60]. This result allows us to connect the value of the curvaton field at the end of the inflation σ_* to the computed curvature perturbation ζ.

During the curvaton slow-roll, the field value remains roughly constant. The evolution changes as the Hubble friction no longer dominates, $U_{,\sigma\sigma} \approx H_{\text{osc}}^2$, and the curvaton σ starts to oscillate around the minimum of its potential. The scaling behaviour of the field amplitude, denoted now by σ_{amp}, is determined by the shape of the potential. If the potential is quadratic, the field behaves like non-relativistic matter, and the curvaton energy density scales like $\rho_\sigma = \frac{1}{2}m_\sigma^2\sigma_{\text{amp}}^2 \propto a^{-3}$. If the curvaton has self-interaction term in its potential, e.g. the potential is of the form $U(\sigma) = \frac{1}{2}m_\sigma^2\sigma^2 + \frac{1}{4}\lambda_\sigma\sigma^4$, the field can first enter a phase in which it oscillates according to its self-interaction term and scales like radiation ($\rho_\sigma \propto a^{-4}$), and then proceeds to oscillate in the quadratic phase like non-relativistic matter (see e.g. ref. [57]). For simplicity, in the following we will assume, that the curvaton is a free massive field with the potential $U(\sigma) = \frac{1}{2}m_\sigma^2\sigma^2$.

So far we have assumed that the universe is radiation dominated at least until the quadratic field oscillations start. The gist of the curvaton mechanism is that with respect to radiation the curvaton energy density grows, i.e. $\rho_\sigma/\rho_r \propto a$, when $m^2 > H^2$ and $\rho_\sigma/\rho_r \propto a^4$, when $m^2 \ll H^2$. This means, that while the curvaton might be a subdominant component at the start of field oscillations, it can have a significant contribution to the total energy density at some later time, and therefore the perturbation of the curvaton field can generate curvature perturbations. Following the definition of eq. (103), we can define the curvature perturbation ζ_i for individual fluid components as [60]

$$\zeta_i = -\psi + \frac{\delta\rho_i}{3(\bar{\rho}_i + \bar{p}_i)}, \tag{157}$$

which allows us to write the total curvature perturbation ζ in this two fluid configuration $\rho = \rho_r + \rho_\sigma$ as [60]

$$\zeta = \left(1 - \frac{3\rho_\sigma}{4\rho_r + 3\rho_\sigma}\right)\zeta_r + \frac{3\rho_\sigma}{4\rho_r + 3\rho_\sigma}\zeta_\sigma, \tag{158}$$

where we used that for non-relativistic curvaton $p_\sigma = 0$ and for radiation $p_r = \rho_r/3$. The individual curvature perturbations ζ_i have their individual evolution following eq. (110), and according to the adiabatic condition (113) they are conserved, if the fluids do not interact. In this section we approximate that the curvaton field and the radiation only interact at the time when the curvaton instantaneously decays into radiation.

As we assume that the radiation is almost homogeneous, we can neglect the curvature perturbation resided in the radiation, $\zeta_r \approx 0$, and the curvature perturbation ζ is given by [60]

$$\zeta \approx \left.\frac{3\rho_\sigma}{4\rho_r + 3\rho_\sigma}\right|_{\rm dec} \zeta_\sigma = r_{\rm dec}\zeta_\sigma. \tag{159}$$

Here we assumed that the produced curvature perturbation ζ is evaluated at the time of the curvaton decay, and defined the parameter $r_{\rm dec}$. We can see, that the evolution and produced amount of ζ is determined by the evolution of the energy densities ρ_r and ρ_σ, as we have that $\zeta_\sigma =$ constant in the case of quadratic potential. On the spatially flat slicing, the curvaton perturbation ζ_σ can be written in the first order perturbation theory as [60]

$$\zeta_\sigma = \frac{1}{3}\frac{\delta\rho_\sigma}{\bar{\rho}_\sigma} = \frac{2}{3}\frac{\delta\sigma}{\sigma} = \frac{2}{3}\left(\frac{\delta\sigma}{\sigma}\right)_*, \tag{160}$$

where in the last equality the subscript refers to the value of the field and its perturbation at the end of inflation, and we used the result that $\delta\sigma/\sigma$ is conserved with the quadratic potential. Note that eq. (160) can receive large second order corrections that lead to significant non-Gaussianities [60].

The curvature perturbation ζ then becomes

$$\zeta = \frac{2}{3}\frac{r_{\rm dec}}{\sigma_*}\delta\sigma_*. \tag{161}$$

And using eq. (153) we can write the power spectrum of curvature perturbations as

$$\mathcal{P}_\zeta(k) = \left.\frac{4}{9}\frac{r_{\rm dec}^2}{\sigma_*^2}\left(\frac{H}{2\pi}\right)^2\right|_{k=aH}. \tag{162}$$

We can see that the power spectrum (162) depends on the initial value of the curvaton field and the fractional energy density $r_{\rm dec}$. In the limit where the curvaton is dominant at the time of its decay, $r_{\rm dec} \to 1$. If the curvaton is subdominant during the decay, the $r_{\rm dec}$ is heavily suppressed, and the quantity $\delta\sigma_*/\sigma_*$ needs to accommodate for the observed curvature perturbation $\zeta \sim 10^{-5}$. This means, that second-order effects might become important, which leads to creation of large non-Gaussianities (which can be computed with the ΔN formalism) [60].

A comprehensive study of the simplest curvaton model and the observational constraints can be found in ref. [61] (see also references therein). A systematic analysis of single-field slow-roll inflation with an extra light scalar field (that can act as a curvaton), where different inflaton potentials and reheating scenarios are studied can be found in ref. [58]. While the simplest model can be in mild tension with the observations, it is generally not ruled out [61]. In cases where the curvaton is highly suppressed at the time of its decay, the constraints on the non-Gaussianities can be used to rule out certain parts of the model parameter space [61]. Generally, the tension is alleviated if the inflaton perturbations are allowed

to be non-negligible [61]. Deviations from the simplest models, where the curvaton is allowed to have self-interactions, alter the model predictions and typically have a rich structure of non-Gaussianities, which can be used in constraining the models — see for example refs. [57, 59, 62] and references therein.

3.4.2 Curvaton and ΔN formalism

We can also use the ΔN formalism to compute the curvature perturbation ζ, i.e. we compute the field-derivative of e-folds, $N_{,\sigma}$. In the curvaton generated primordial perturbations setup, we can compute the amount of e-folds from the end of inflation, where the curvaton has a inital value σ_*, to the time when the curvaton decays into radiation, $N = \log\left(a_{\rm dec}/a_{\rm end}\right)$. However, as the field σ is assumed to be very subdominant before the field oscillations start at $V_{,\sigma\sigma} \sim H^2_{\rm osc}$, we can safely neglect the e-folds coming from this era and write [49]

$$N = \log\left(\frac{a_{\rm dec}}{a_{\rm osc}}\right) = \frac{1}{3}\log\left(\frac{\rho_{\sigma,\rm osc}}{\rho_{\sigma,\rm dec}}\right), \tag{163}$$

where we used that after the field oscillations start the curvaton energy density scales likes non-relativistic matter, $\rho_\sigma \sim a^{-3}$. As we assume the potential to be $U(\sigma) = \frac{1}{2}m_\sigma^2\sigma^2$, we can write that $\rho_{\sigma,\rm osc} \approx \frac{1}{2}m_\sigma^2\sigma_*^2$. We would then like to compute

$$\frac{\partial}{\partial\sigma_*}N \approx \frac{1}{3}\frac{\partial}{\partial\sigma_*}\log\left(\frac{\rho_{\sigma,\rm osc}}{\rho_{\sigma,\rm dec}}\right) = \frac{1}{3}\left(\frac{\partial_{\sigma_*}\rho_{\sigma,\rm osc}}{\rho_{\sigma,\rm osc}} - \frac{\partial_{\sigma_*}\rho_{\sigma,\rm dec}}{\rho_{\sigma,\rm dec}}\right). \tag{164}$$

As we are dealing with a two-fluid system, $\rho = \rho_r + \rho_\sigma$, it is straightforward to show that

$$\frac{\partial}{\partial\sigma_*}\rho_{\sigma,\rm dec} = \frac{8}{3}\frac{1}{\sigma_*}\rho_{r,\rm dec}r_{\rm dec}. \tag{165}$$

And therefore eq. (164) is [49]

$$\frac{\partial}{\partial\sigma_*}N \approx \frac{1}{3}\left(\frac{2}{\sigma_*} - \frac{2}{\sigma_*}\frac{4\rho_{r,\rm dec}r_{\rm dec}}{3\rho_{\sigma,\rm dec}}\right) = \frac{2}{3}\frac{r_{\rm dec}}{\sigma_*}, \tag{166}$$

i.e. we see that the ΔN formalism reproduces the result (161) obtained in previous section:

$$\zeta = N_{,\sigma}\delta\sigma_* = \frac{2}{3}\frac{r_{\rm dec}}{\sigma_*}\delta\sigma_*. \tag{167}$$

The ΔN formalism is especially useful when computing higher-order quantities that are used in the computation of non-Gaussianities. These quantities correspond to calculating higher-order derivatives of the amount of e-folds, i.e. $N_{,\sigma\sigma}$ etc. Note also that, in models where the field value at the start of quadratic oscillations $\sigma_{\rm osc}$ is not exactly the initial value, but non-trivial function of if, i.e. $\sigma_{\rm osc}(\sigma_*) \neq \sigma_*$, the above results are modified. See for example refs. [49, 62]

3.4.3 Mixed curvaton-inflaton model

In the above discussion on curvaton scenario we assumed that the adiabatic curvature perturbations are sourced solely by the curvaton field σ. It is of course interesting also to study two-field models, where both the inflaton and curvaton can source the perturbations[1]. Assuming that the scalar potential is separable, we can write the full curvature power spectrum according to eq. (151) in leading order in slow-roll as

$$\mathcal{P}_\zeta(k) = N_{,\phi}^2(k)\,\mathcal{P}_\phi(k) + N_{,\sigma}^2(k)\,\mathcal{P}_\sigma(k) = \left(N_{,\phi}^2 + N_{,\sigma}^2\right)\left(\frac{H}{2\pi}\right)^2\Bigg|_{k=aH}, \tag{168}$$

where we still maintain the assumption that the field σ is energetically subdominant and light during inflation.

In this double field setup we are interested in the amount of e-folds between the initial time t_* during inflation and the final decay of the curvaton to radiation at time $t_{\rm dec}$, i.e. $N = \log(a_{\rm dec}/a_*)$. As the amount e-folds is determined by the dominant inflaton between a_* and the end of inflation at $a_{\rm end}$ we can write

$$N_{,\phi}^2 = \left(\frac{H}{\dot{\bar{\phi}}}\right)^2 = \frac{1}{2\epsilon_\phi(k)\,M_{\rm Pl}^2}. \tag{169}$$

While the the value of $N_{,\sigma}$ depends on the specific model.

We can parameterize the scale-dependency of the spectra by defining the individual spectral index, its running and the running of running. We have shown that the spectral index of the inflaton is $n_\phi - 1 = -6\epsilon_\phi + 2\eta_\phi$, while the spectral tilt for a light and subdominant scalar is $n_\sigma - 1 = -2\epsilon_\phi + 2\eta_\sigma$. In the scientific work of this thesis [74], we study the spectral distortion signals of these kinds of two-field models, where the curvature perturbations can be sourced by both of the fields.

[1] See e.g. refs. [63, 64, 65, 66, 67, 68, 69, 70, 71, 72, 73] for studies on the mixed inflaton-curvaton models

4 CMB BLACK-BODY SPECTRUM AND SPECTRAL DISTORTIONS

In addition to the anisotropies, the CMB holds another observable that encodes a wealth of information of the thermal history of the early universe: the frequency-spectrum. The spectrum of the CMB is known to be remarkably close to a perfect black-body spectrum, with deviations from it being at most to one part in 10^5 [8, 9]. These departures from the black-body spectrum are referred to as spectral distortions, and they occur when the photons and electrons are not in equilibrium in the early universe plasma. The deviations from equilibrium can be caused by many processes: for example, energy can ne dumped into the CMB by dissipation of the energy stored in the density fluctuations, evaporating primordial black holes and annihilating particles — see e.g. ref. [75] and references therein. Some of the non-equilibrium processes are unavoidable effects in the standard ΛCDM cosmology, while some are deviations from the concordance model requiring new physics [75].

The current constraints for the spectral distortions date back to the measurements by COBE/FIRAS in the early 90's [8, 9], and while the COBE/FIRAS measurement of a perfect black-body can exclude certain cosmological models, the proposed next-generation experiments can achieve several orders of magnitude improvement in sensivity, and can offer a complementary probe of the very early physics, such as the primordial perturbations and inflationary physics [75].

In this chapter we give a brief review of the CMB spectral distortions. While we start from the discussion on the different types of distortions, we choose to limit our discussion on the μ-type spectral distortion, which is interesting in the scope of this work, i.e. as a probe of the inflationary models. We briefly go through the interactions that affect the creation of μ-distortion and then move on to give analytical expression for the μ-distortion derived in the literature: in this work we concentrate on the μ-distortion created by the dissipation of the energy in the density perturbations, where the μ-distortion depends on the shape of the primordial power spectrum $\mathcal{P}_\zeta$. The literature on CMB spectral distortions spans over five decades, see e.g. ref. [76] for a reference list of significant contributions to the study of CMB spectral distortions, and in this chapter we choose to mostly follow refs. [76, 77, 78, 79] and references therein (most of these are either reviews or comprehensive analyses on the CMB spectral distortions).

4.1 Photon black-body spectrum and spectral distortions

4.1.1 Photon black-body spectrum

In Section 1.2, we discussed the formation of the cosmic microwave background from the photon decoupling shortly after the time of recombination. The formed

CMB is remarkably close to a black-body spectrum, meaning that the universe was extremely close to thermal equilibrium at the time of decoupling. The intensity of the black-body photon spectrum can written as [76]

$$I(E) = \frac{2E^3}{h^2c^2}\frac{1}{e^{E/T}-1} = \frac{2E^3}{h^2c^2}\frac{1}{e^x-1} = \frac{2E^3}{h^2c^2}\, f_{\rm bb}(x) \tag{170}$$

where the photon energy is $E = |p| = p = h\nu$, where ν is the photon frequency, $f_{\rm bb}$ is the black-body spectrum (with zero chemical potential μ) and the redshift-independent variable is $x = p/T$. We note that black-body spectrum is characterized by one number, its temperature T. The COBE/FIRAS measurement tells us that the variations in the intensity cannot be larger than $\delta I/I \sim 10^{-4}\ldots 10^{-5}$ [8, 9]. The photon energy density ρ_γ and number density n_γ, in the case of a pure black-body, read

$$n_{\gamma,{\rm bb}} = g_\gamma \int \frac{{\rm d}^3\mathbf{p}}{(2\pi)^3} f_{\rm bb} = \frac{2\zeta(3)}{\pi^2}T^3 \tag{171}$$

$$\rho_{\gamma,{\rm bb}} = g_\gamma \int \frac{{\rm d}^3\mathbf{p}}{(2\pi)^3} E f_{\rm bb} = \frac{\pi^2}{15}T^4. \tag{172}$$

As we are interested in the deviations from the black-body, we would like to know what effects can distort the spectrum. As the temperature T characterizes the shape of the spectrum, we can find out what happens when we perform a small change in the temperature, i.e. consider shift $T \to T' = T + \Delta T$. Let us assume, that the temperature change comes from a energy injection/extraction to/from the photon side $\Delta\rho_\gamma$, which allows us to write

$$\frac{\Delta T}{T} \approx \frac{1}{4}\frac{\Delta\rho_\gamma}{\rho_{\gamma,{\rm bb}}}, \tag{173}$$

where we used the above result $\rho_{\gamma,{\rm bb}} \propto T^4$. It is quite clear, that to keep the black-body spectrum, we need to also change the photon number density, as the change in temperature ΔT does not retain the black-body relation $n_{\gamma,{\rm bb}} \propto T^3$. To keep the black-body spectrum, the change in the number density can be written as [78]

$$\frac{\Delta n_\gamma}{n_{\gamma,{\rm bb}}} \approx 3\frac{\Delta T}{T} \to \frac{\Delta n_\gamma}{n_{\gamma,{\rm bb}}} - \frac{3}{4}\frac{\Delta\rho_\gamma}{\rho_{\gamma,{\rm bb}}} = 0, \tag{174}$$

where we gave the condition between the change in the number density and the energy density. We then have the necessary condition, which states that in the event of energy injection/extraction, the number of photons needs to change in the system to keep the black-body spectrum. However, the above consideration does not tell us how the added/removed photons are distributed in energy — it is clear that if one adds photons of only one frequency/energy, the distribution does not follow a black-body distribution albeit the above condition is satisfied. There is then inherently need for a frequency-dependent processes, where the number-changing processes need in addition energy redistributing processes to

thermalize the possible energy or photon injections — see e.g. ref. [78] for more details. If we require that the spectrum at the temperature T' is also a black-body spectrum, we get that the change between the two black-bodies is [78]

$$\Delta f_{\rm bb} = f_{\rm bb}\left(T'\right) - f_{\rm bb}\left(T\right) \approx \frac{x\mathrm{e}^{x}}{\left(e^{\mathrm{x}}-1\right)^{2}}\frac{\Delta T}{T} = -x\frac{\partial f_{\rm bb}}{\partial x}\frac{\Delta T}{T}, \tag{175}$$

which gives the change as a function of derivative of the black-body and temperature, and the function $-x\partial_x f_{\rm bb}$, is usually in the literature referred as the temperature shift function — see e.g. ref. [78] for its spectral shape.

We have now seen, that an energy injection/extraction or addition/destruction of photons can cause deviations from the black-body spectrum. We know, that there are some unavoidable effects that can perturb the equilibrium between the electrons(/baryons) and photons in the CMB. For the CMB this means, that there must be number-changing and energy redistributing processes, that can thermalize these perturbations to the level observed today. In the following sections we proceed to discuss the evolution of the photon spectrum under the different interaction processes, and give a brief review of the different types of deviations from the black-body spectrum that are usually studied in the literature.

4.1.2 The Photon Boltzmann equation

As we are interested in the formation and evolution of the CMB spectrum, we need to study the evolution of the photon phase space distribution, $f\left(x^{\mu}, p^{\mu}\right)$, where p^{μ} are the components of the four-momentum, which evolves according to the Boltzmann equation [76, 77]

$$\frac{\mathrm{d}f}{\mathrm{d}t} = C\left[f\right], \tag{176}$$

where the left-hand side accounts the effects of gravity, and collision terms $C\left[f\right]$ account the interactions of photons with other particle species in the universe. On a FLRW background, where $f = f\left(t, p\right)$, the left-hand side of eq. (176) can be written as [7, 77]

$$\frac{\mathrm{d}f\left(t,p\right)}{\mathrm{d}t} = \frac{\partial f\left(t,p\right)}{\partial t} - Hp\,\frac{\partial f\left(t,p\right)}{\partial p}, \tag{177}$$

where the second term describes the cosmological redshift.

The right-hand side of eq. (176) encodes all the possible photon interactions. However, in this context, the most important processes for the photon interactions are the Compton scattering (CS), double Compton scattering (DC) and Bremmstrahlung (BR) [77, 78], which we will discuss below. It is also possible to have non-standard processes, as decaying particles, that add a source term for the photons [77, 78]. We then write the photon collision term $C\left[f\right]$ as

$$C\left[f\right] = C\left[f\right]|_{\rm CS} + C\left[f\right]|_{\rm DC} + C\left[f\right]|_{\rm BR} + C\left[f\right]|_{\rm source}, \tag{178}$$

where we decomposed the collision term to the individual collision terms. We can see, that if we neglect the collisions, i.e. $C[f] = 0$, the solution to eq. (176) is

$$\frac{\partial f}{\partial t} = \frac{\dot{a}}{a} p \frac{\partial f}{\partial p} \rightarrow f(t,p) = f\left(t_0, p\frac{a(t)}{a(t_0)}\right), \tag{179}$$

which means that the shape of the photon spectrum is conserved while the momenta is redshifted according to $p \propto a^{-1}$ [76].

It is convenient to switch to the variable $x = p/T(t)$, where the photon/CMB temperature is $T(t) = T_0(1+z) \propto a^{-1}$ and T_0 is the observed CMB temperature today. This change of variables allows us to write the Boltzmann equation in a compact form for the spectrum $f = f(t,x)$ [76]:

$$\frac{\partial f(t,x)}{\partial t} = C[f(t,x)], \tag{180}$$

where it is easy to see that for $C[f] = 0$ the shape of the spectrum is conserved. In the literature one often changes the time-coordinate to the Thomson optical depth $\mathrm{d}\tau = n_e \sigma_{\mathrm{T}} \mathrm{d}t$, where n_e is the electron number density and σ_{T} is the Thomson cross-section, and also writes eq. (180) as

$$\frac{\partial f(\tau,x)}{\partial \tau} = \left.\frac{\partial f(\tau,x)}{\partial \tau}\right|_{\mathrm{CS}} + \left.\frac{\partial f(\tau,x)}{\partial \tau}\right|_{\mathrm{DC}} + \left.\frac{\partial f(\tau,x)}{\partial \tau}\right|_{\mathrm{BR}} + S(\tau,x), \tag{181}$$

where $S(\tau,x)$ is an additional photon source term — see for example refs. [77, 78, 79] and references therein. Before discussing the solutions to eq. (181), we need to find the forms of the collision terms for the different interactions.

4.1.3 Compton scattering

The most important interaction process between CMB photons and free electrons is the Compton scattering, i.e.

$$e^-(k) + \gamma(p) \rightleftharpoons e^-(k') + \gamma(p'), \tag{182}$$

where the kinematic conditions is $p + k = p' + k'$. The Compton scattering efficiently distributes energy between the photons and electrons, and is the primary mechanism for the CMB thermalization [77]. Important thing to note is, that while the Compton scattering is efficient in redistributing energy, it is non-number-changing process, i.e. in the event that that extra photons are dumped into a thermalized configuration, it by itself cannot maintain a black-body.

The calculation of the Compton scattering collision term is beyond the scope of this work — see for example ref. [77] and references therein for the computation. The Compton scattering term appearing in eq. (181) can be written as [78]

$$\left.\frac{\partial f}{\partial \tau}\right|_{\mathrm{CS}} \approx \frac{\theta_e}{x^2}\frac{\partial}{\partial x}\left\{x^4\left[\frac{\partial f}{\partial x} + \frac{T}{T_e} f(1+f)\right]\right\}, \tag{183}$$

where one has averaged over the scattering cross-section and the electron velocity distribution [77], and expanded to first order in $\theta_e = T_e/m_e$ and $h\nu/m_e$,

where ν is the photon frequency and m_e and T_e are the electron mass and temperature, respectively [76]. Note that the (fine structure) coupling α is absorbed in the time-variable τ as it depends on the Thomson cross-section $\sigma_{\rm T}$. The first term in eq. (183) describes the Doppler boosting (diffusion of photons in energy due to Doppler effect) and the second term accounts for the recoil effect, where photons are downward scattered in frequency — see details for example in refs. [77, 78].

From eq. (183) one can compute differential energy change of the photon field [78]

$$\left.\frac{\partial \rho_\gamma}{\partial \tau}\right|_{\rm CS} \approx 4\theta_e \rho_\gamma \left(1 - \frac{T_e^{\rm eq}}{T_e}\right), \quad T_e^{\rm eq} = \frac{T}{4}\frac{\int x^4 f\,(1+f)\,{\rm d}x}{\int x^3 f {\rm d}x}, \tag{184}$$

where $T_e^{\rm eq}$ is the Compton equilibrium temperature, which is important in distinguishing the direction of energy transfer. If $T_e > T_e^{\rm eq}$, electrons are cooled and photons heated, and vice versa. If the system is in equilibrium, $T_e = T_e^{\rm eq}$, no energy exchange happens. Note that if the photon field is a black-body, $f\,(x) = 1/\left({\rm e}^x - 1\right)$, the photon temperature and the electron equilibrium temperature are equal, $T = T_e^{\rm eq}$. As we expect that the photon spectrum does not deviate greatly from the black-body, we also expect that if the electron temperature T_e is smaller than the photon temperature T, the photons can loose energy and heat up the electrons. This is also seen when due to the expansion of space the temperature of photons and electrons scale differently, which results in electron cooling. This is usually referred to as adiabatic cooling of electrons, and it can lead to creation of observable spectral distortion signal [78, 79].

It is important to know how long can the Compton scattering efficiently thermalize the CMB photons. It is straightforward to show that the Comptonization time-scale (i.e. energy-transfer from electrons to photons) becomes longer than the Hubble expansion time at the redshift $z_{\rm K} \approx 5 \times 10^4$ [77]. This means, that below the redshift $\sim 10^4$, the Compton scattering is inefficient in distributing the energy in the photon-electron system and thus cannot maintain a black-body spectrum in the event of energy injection. The redshift $z \approx z_{\rm K}$ is usually seen as a transition between the μ- and y-type of spectral distortions — see Section 4.1.5.

4.1.4 Bremsstrahlung and Double Compton scattering

The most relevant number-changing processes involving electrons and photons in the early universe plasma are Bremsstrahlung and double Compton scattering. The relevant Bremsstrahlung process is the electron-ion (or proton) interaction

$$e^-\,(k) + H^+\,(l) \rightleftharpoons e\left(p'\right) + H^+\left(l'\right) + \gamma\,(k)\,, \tag{185}$$

where the forward process describes the emission of photon, and backwards process absorption of photon. The double Compton scattering is the first radiative correction to the Compton scattering and has the form

$$e^-\,(k) + \gamma\,(p) \rightleftharpoons e^-\left(k'\right) + \gamma\left(p'\right) + \gamma\,(l)\,. \tag{186}$$

As with the Compton scattering, the derivation of the collisions terms for the BR and DC processes are beyond the scope of this work. The number-changing process part of eq. (181) can be expressed as

$$\left.\frac{\partial f(\tau,x)}{\partial\tau}\right|_{\rm BR}+\left.\frac{\partial f(\tau,x)}{\partial\tau}\right|_{\rm DC}\approx\left(K_{\rm BR}\frac{{\rm e}^{-x_e}}{x_e^3}+K_{\rm DC}\frac{{\rm e}^{-2x}}{x^3}\right)\times\left(1-f\left({\rm e}^{x_e}-1\right)\right), \tag{187}$$

where $K_{\rm BR}$ and $K_{\rm DC}$ are z and momentum/energy dependent functions and $x_e = p/T_e$. The parameters $K_{\rm BR}$ and $K_{\rm DC}$ can be approximated as [78, 79]

$$K_{\rm BR}\approx 1.4\times10^{-6}\left(\frac{\bar{g}_{\rm eff}}{3.0}\right)\left(\frac{\Omega_b h^2}{0.022}\right)(1+z)^{-1/2} \tag{188}$$

$$K_{\rm DC}\approx\frac{16\pi^3}{45}\alpha\theta^2\approx 1.7\times10^{-20}(1+z)^2, \tag{189}$$

where $\bar{g}_{\rm eff}$ is the so-called effective Gaunt factor for the BR process, that encodes different couplings and details of the plasma interactions (see e.g. ref. [78] and references therein), Ω_b is the scaled energy density of baryonic matter, h is the scaled Hubble parameter, α is the fine-structure constant and $\theta = T/m_e$. Comparing BR and DC processes, one finds that at redshifts higher than $z >$ few $\times 10^5$, the double Compton scattering dominates over the Bremsstrahlung [80]. In the computation of the μ-distortion, which is assumed switched off roughly at $z \approx z_{\rm K}$, one usually takes into account only the DC contribution. However, at late times the BR processes need to be taken into account — see for example ref. [79].

4.1.5 Different types of spectral distortion

The final evolution equation for the photon distribution function $f(\tau, x)$ is then obtained by substituting eqs. (183) and (187) to eq. (181). The resulting equation can be solved numerically, and importantly one can also find analytical solutions in certain limiting cases. As discussed above, the inefficiency of Comptonization starts approximately at $z_{\rm K}\approx 5\times10^4$, which marks a transition between the chemical potential type of μ-distortion and the y-distortion, which describes the inefficient energy-transfer between photons and electrons. Let us then next briefly discuss the different eras of spectral distortions.

It can be shown, that at very early times, $z \gtrsim z_{\rm DC}\approx 2\times10^6$, the different processes between electrons and photons are efficient in maintaining the thermodynamic equilibrium. The number-changing processes double Compton scattering and Bremsstrahlung and the energy redistributing Compton scattering are efficient in balancing out any perturbations, and the photon spectrum is to a very high accuracy a black-body spectrum [77]. Below the redshift $z_{\rm DC}\approx 2\times10^6$, the number-changing processes start to become inefficient in maintaining the chemical equilibrium between the electrons and photons in the event of energy-injection or injection of particles, such as diffusion of energy stored in the primordial perturbations or decaying particles. Between the redshifts $5\times10^4 \lesssim z \lesssim$

2×10^6, where the Comptonization is still efficient, the deviation from a black-body is then characterized by a spectrum with a chemical potential μ. The μ-type of spectral distortion cannot be generated at lower redshifts, and therefore is a direct probe of the early universe, pre-recombination, physics [81]. We will discuss the μ-distortion in more detail in next section.

After the Compton scattering has become inefficient, the deviation from a black-body spectrum is described by the y-type spectral distortion. The Compton-y-variable measures the energy transfer between the electrons and photon and is written as (in the limit $|y| \ll 1$) [76]

$$y = \int_0^\tau (\theta_e - \theta)\, \mathrm{d}\tau', \tag{190}$$

where $\theta_{(e)} = T_{(e)}/m_e$, and one assumes that the photon spectrum is initially at $\tau = 0$ a black-body spectrum. We can see that for $\theta_e = \theta \rightarrow T_e = T$, we have $y = 0$.

First studies of formation of y-distortion in our universe were done in the context of photons traveling through clusters of galaxies [82]. The hot free electrons residing in the potential wells of these clusters can scatter of the CMB photons and distort their spectrum. This process is referred to as the thermal Sunyaev-Zeldovich effect [82] (see review of SZ-effect in ref. [83]). In this case $T_e \gg T$, we can write

$$y \approx \int_0^\tau \theta_e \mathrm{d}\tau' \approx \theta_e \tau, \tag{191}$$

as $\theta_e = T_e/m_e$, y-distortion be used to probe the integrated electron pressure of a cluster medium [78]. The thermal SZ effect is independent of redshift, and allows one to track the growth of structures (clusters), and to constrain cosmological parameters and evolution of dark energy — see ref. [83] for more details.

The Compton-y-parameter (190) can have both positive and negative values: if $y > 0$, overall energy is transferred from the electrons to the CMB photons (Comptonization), while for $y < 0$ the energy flows from the CMB photons to the electrons (Compton cooling). Most processes yield a positive y, but the adiabatic cooling of matter in our expanding universe (the electron temperature drops faster than the radiation) can yield a negative y-distortion — see e.g. ref. [78, 79]. This effect is also seen on the μ-distortion side, where most processes yield a positive μ, while the cooling of electrons yields negative-valued μ-distortion [79].

Note that, in reality the transition between the μ- and y-type distortions is not a simple step-function at $z_\mathrm{K} \approx 5 \times 10^4$, but a gradual transition. In the literature, the intermediary distortions are usually referred to as i-distortions (intermediate) or r-distortion (residual). The r-distortion signal, that is seen between redshifts $z \sim 10^4 \ldots 10^5$, can be used to study time-dependency of distortion processes such as decaying particles — see for example refs. [84, 85]. The discussion of the residual distortions is beyond the scope of this work, and in the next sections we will only concentrate on the μ-type spectral distortions.

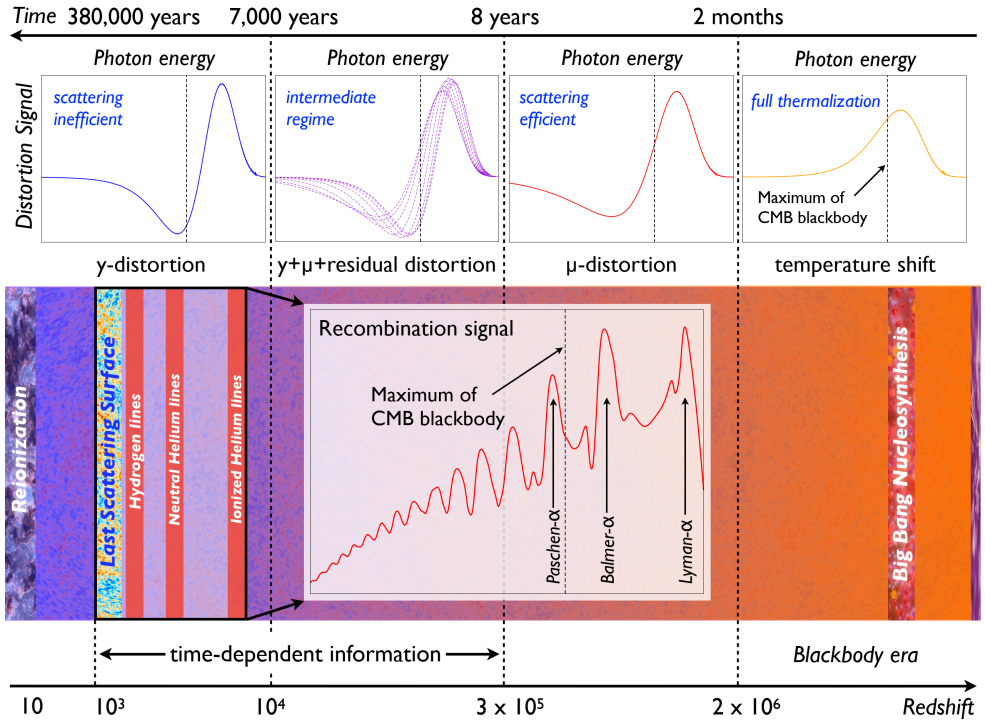

FIGURE 5 Evolution of spectral distortions as a function of redshift and time. The efficient interaction processes between the CMB photons and electrons maintain a black-body spectrum at redshifts $z > 2 \times 10^6$, while at lower redshifts the spectrum distortion can be expressed in terms of a μ-, y- and residual types of distortion. Figure from ref. [75].

4.2 Analytic approximation for μ-distortion

In this section we give a brief review of the formation of μ-distortion and give the analytic approximations for the μ-distortion that are often used in the literature.

4.2.1 Equilibrium solution and distorting the black-body

The equations given in the previous section describe the evolution of the photon spectrum under the different collision terms coupled with the evolution of the electron temperature. In a general case the kinetic equation (181) needs to be solved numerically, but one can find analytical approximations for the evolution depending on what are the dominant effects in the system. Luckily, in the so-called μ-era, the photon spectrum and resulting distortions can be approximated with relatively simple equations. The given presentation in this section mainly follows the treatment presented in refs. [77, 78] and references therein.

We know that in the μ-era the kinetic equilibrium is efficiently maintained by the Compton scattering. If we for now neglect the number-changing absorption and emission processes, i.e. double Compton scattering and Bremsstrahlung,

the efficient Comptonization drives the system to equilibrium and we have that $\partial f/\partial\tau \approx 0$. We then have that the eq. (183) can be written as

$$\frac{\theta_e}{x^2}\frac{\partial}{\partial x}\left\{x^4\left[\frac{\partial f}{\partial x}+\frac{T}{T_e}f\left(1+f\right)\right]\right\}\approx 0. \tag{192}$$

It is straightforward to show that the general solution for eq. (192) is

$$f=\frac{1}{\mathrm{e}^{x_e+\mu_0}-1}, \tag{193}$$

which describes a Bose-Einstein distribution at the electron temperature T_e with dimensionless chemical potential μ_0. We can see that, for positive values, $\mu_0 > 0$, the spectrum (193) is more suppressed than the black-body spectrum at $T = T_e$. This means that there are fewer photons present than in a black-body at T_e, which corresponds to a energy release to the photon side and/or destruction of photons. The negative values corresponds to a surplus of photons, which can be a result of energy extraction from the photon side or a injection of photons [78]. This deviation from the black-body spectrum is then the so-called μ-type spectral distortion. We can derive an expression for the μ_0-parameter by considering small changes in the photon energy and number densities.

Let us then assume that we start from configuration where the initial black-body and electrons are at the same temperature $T_{e,i} = T_{\gamma,i} = T_i$, and we change both the energy and number density of the photon field by

$$\rho_{\gamma,f}=\rho_{\gamma,i}\left(1+\frac{\Delta\rho_\gamma}{\rho_{\gamma,i}}\right) \tag{194}$$

$$n_{\gamma,f}=n_{\gamma,i}\left(1+\frac{\Delta n_\gamma}{n_{\gamma,i}}\right), \tag{195}$$

where the initial photon energy and number density are given by the black-body results in eqs. (171) and (172), i.e. $\rho_{\gamma,i} = \left(\pi^2/15\right) T_i^4$ and $n_{\gamma,i} = 2\left(\zeta(3)/\pi^2\right) T_i^3$.

After the change of energy and number density the Compton scattering drives the system to a kinetic equilibrium, with a final temperature $T_f = T_i + \Delta T$, but not to a chemical equilibrium, and hence the deviation from thermal equilibrium is described by the chemical potential μ_0 [77]. Assuming that both the resulting distortion μ_0 and the change of temperature are small, i.e. $\mu_0 \ll 1$ and $\Delta T \ll T_i$, we can write

$$\rho_{\gamma,f}=\frac{T_f^4}{\pi^2}\int_0^\infty \mathrm{d}x\frac{x^3}{\mathrm{e}^{x+\mu_0}-1}\approx\frac{T_f^4}{\pi^2}I_3\left(1-3\frac{I_2}{I_3}\mu_0\right) \tag{196}$$

$$n_{\gamma,f}\approx\frac{T_f^3}{\pi^2}I_2\left(1-2\frac{I_1}{I_2}\mu_0\right), \tag{197}$$

where $I_n = \int_0^\infty \mathrm{d}x_e\; x_e^n/\left(\mathrm{e}^{x_e}-1\right) = n!\zeta(n+1)$. We find the expression for μ_0 by combining eqs. (194) and (195) with eqs. (196) and (197), and by considering the

quantities μ_0 and ΔT to first order. The result reads

$$\mu_0 \approx \frac{1}{8}\left(\frac{\pi^2}{12\zeta(3)} - \frac{270}{8}\frac{\zeta(3)}{\pi^4}\right)^{-1}\left(3\frac{\Delta\rho_\gamma}{\rho_{\gamma,i}} - 4\frac{\Delta n_\gamma}{n_{\gamma,i}}\right) \tag{198}$$

$$\approx 1.401\left(\frac{\Delta\rho_\gamma}{\rho_{\gamma,i}} - \frac{4}{3}\frac{\Delta n_\gamma}{n_{\gamma,i}}\right). \tag{199}$$

From eq. (199) we can clearly see that the number changing processes can balance the distortion coming from the energy injection, and in the case $\Delta\rho_\gamma/\rho_{\gamma,i} = (4/3)\Delta n_\gamma/n_{\gamma,i}$ the chemical potential is driven to zero and chemical equilibrium is established. In this case the spectrum retains the black-body form, and only its temperature is increased.

4.2.2 Evolution of the distortion and simple analytic approximation for μ

In the previous section we gave the initial value of the μ-distortion as a function of the change of photon energy and number density. However, we did not include any photon production (e.g. double Compton scattering and Bremsstrahlung) in the picture, as we only assumed that it was the Comptonization that changed the photon field. The number-changing processes are however integral for the creation of a black-body spectrum, as these are the processes that can reduce the initial spectral distortion.

As discussed earlier, at higher redshifts ($z \gtrsim 10^4$) the Compton and double Compton scattering dominate over the Bremsstrahlung. This is important for the discussed μ-distortion, and at the early times it is the double Compton scattering that changes the number of photons at the low photon frequencies, while the Compton scattering redistributes these photons in frequency. Obviously, if this process is efficient enough the initial distortion (caused by for example energy-injection) can be reduced greatly. Let us then next briefly discuss the evolution of μ in the early universe and give the analytic approximations that are often used in the literature. More detailed discussion on this matter is given for example in refs. [77, 78, 79, 86].

Let us assume that the non-zero chemical potential μ_0 in eq. (199) characterizes the distortion for the epoch of interest. From eq. (199), we can see that the μ-distortion evolves according to

$$\frac{\mathrm{d}\mu_0}{\mathrm{d}\tau} \approx 1.401\left(\frac{\mathrm{d}\log\left(a^4\rho_\gamma\right)}{\mathrm{d}\tau} - \frac{4}{3}\frac{\mathrm{d}\log\left(a^3 n_\gamma\right)}{\mathrm{d}\tau}\right). \tag{200}$$

As the evolution of the μ_0 depends on the photon energy and number density, one then needs to include the number-changing processes double Compton scattering and Bremsstrahlung. In the literature there are several ways presented how to proceed on defining and calculating the evolution of μ. Here we do not go into details, and follow and quote the results from ref. [78].

The photon heating term in eq. (200) can be parameterized as

$$\frac{\mathrm{d}\log\left(a^4\rho_\gamma\right)}{\mathrm{d}\tau} = \frac{\dot{Q}^*}{\rho_\gamma}, \tag{201}$$

where $\dot{Q}^*$ is the effective heating rate of electrons and baryons (energy release per volume and Thomson scattering time τ) [78, 86]. The rate $\dot{Q}^*$ includes both the effect of electron heating (by the considered process) and the adiabatic cooling of electrons [78, 86].

The photon production term in eq. (200) depends only on the number-changing terms and the source term in eq. (181). One can obtain approximative form for it by expanding eq. (181) in the low the frequency limit, where the double Compton scattering and Bremsstrahlung are more effective than at the higher frequencies, and considering the system to become quasi-stationary, i.e. $\partial f/\partial\tau \approx 0$ [78]. The solution reads

$$\frac{\mathrm{d}\log\left(a^3 n_\gamma\right)}{\mathrm{d}\tau} \approx \frac{x_c\theta}{2\zeta(3)}\mu_0, \tag{202}$$

where x_c is the critical frequency that describes the frequency-dependency of the chemical potential. It comes from the intermediary solution
$\mu(\tau, x) \approx \mu_0(\tau)\,\exp(-x_c(t)/x)$, i.e. for $x \gg x_c$ the chemical potential is constant while for smaller frequencies μ exponentially decreases as the photon absorption/emission processes are efficient there. The computation of the critical frequencies for double Compton and Bremsstrahlung can be found in ref. [86].

We can then write eq. (200) as [1] [78]

$$\frac{\mathrm{d}\mu_0}{\mathrm{d}\tau} \approx 1.401\frac{\dot{Q}^*}{\rho_\gamma} - \frac{2x_c\theta}{3\zeta(3)}\mu_0. \tag{203}$$

By defining the so-called thermalization optical depth

$$\tau_\mu(z) \approx \frac{2}{3\zeta(3)}\int_0^z \theta x_c \frac{\sigma_T n_e}{H(1+z')}\,\mathrm{d}z', \tag{204}$$

and assuming that there is no initial distortion (at very early times), the solution can be written as [78]

$$\mu_0(z) \approx 1.401\int_z^\infty \frac{\dot{Q}^*}{\rho_\gamma}\frac{\mathrm{e}^{-\left(\tau_\mu(z')-\tau_\mu(z)\right)}}{H(1+z')}\,\mathrm{d}z'. \tag{205}$$

It is customary to define the so-called spectral distortion visibility function between the two redshifts z' and z, i.e. $\mathcal{J}_\mu(z', z) \equiv \exp\left(-\left(\tau_\mu(z') - \tau_\mu(z)\right)\right)$ — see for example ref. [78]. The visibility function $\mathcal{J}_\mu(z', z)$ describes the fraction of energy injected at z' that is still visible as a spectral distortion at redshift z. When

[1] In the literature this differential equation is often shown in the form $\mathrm{d}\mu/\,\mathrm{d}t \approx 1.4\dot{Q}^*/\rho_\gamma - \mu/t_{\mathrm{DC,BR}}$, where $t_{\mathrm{DC,BR}}$ is the timescale of the dominant number-changing interaction, see e.g. refs. [80, 87, 88, 89].

$\mathcal{J}_\mu \approx 1$, the distortion has not thermalized, while for $\mathcal{J}_\mu \ll 1$ the initial distortion has mostly thermalized and the energy is converted into the temperature shift that was discussed in the previous section.

Assuming that the dominating number-changing process during the μ-era, i.e. between redshifts $z \approx 2 \times 10^6$ and $z \approx 5 \times 10^4$, is the double Compton scattering, the visibility function can be approximated to be [80]

$$\mathcal{J}_{\mu,\mathrm{DC}}\left(z', z\right) \approx \mathcal{J}_{\mu,\mathrm{DC}}\left(z', 0\right) \approx \mathrm{e}^{-\left(z'/z_{\mathrm{DC}}\right)^{5/2}}, \tag{206}$$

where $z_{\mathrm{DC}} = 4.1 \times 10^5 \left(1 - Y_p/2\right)^{-2/5} \left(\Omega_b h^2\right)^{-2/5} \approx 2 \times 10^6$, where Y_p denotes the primordial helium abundance [88]. This allows us to write the value of μ today as (see e.g. ref. [78])

$$\mu = \mu_0\left(z = 0\right) \approx 1.401 \int_0^\infty \frac{\mathrm{d}}{\mathrm{d}z'}\left(\frac{Q^*}{\rho_\gamma}\right) \mathrm{e}^{-\left(z'/z_{\mathrm{DC}}\right)^{5/2}} \Theta\left(z' - z_{\mathrm{K}}\right) \mathrm{d}z', \tag{207}$$

where we also introduced the step-function $\Theta\left(z' - z_{\mathrm{K}}\right)$ that kills the integral at $z_{\mathrm{K}} \approx 5 \times 10^4$, as below the redshift z_{K} the Comptonization is not efficient enough in redistributing the photon energy, and thus the spectral distortion is not anymore of the chemical potential type. In the calculations one often replaces the upper limit with $z \approx 2 \times 10^6$, as the contribution to μ above $z > z_{\mathrm{DC}}$ is negligible.

Albeit there are plethora of spectral distortion sources, for the interest of our present work we need to take into account only two different sources of μ-distortion: the adiabatic cooling of electrons, which we denote by μ_{cool}, and the dissipation of energy stored in the density fluctuations, i.e. Silk damping of acoustic waves, denoted by μ_{silk}. The latter we will talk in more detail in next section. The detailed study of the former is beyond the scope of this work, and we just briefly describe it here. We know that at high redshifts the Compton scattering couples the electrons and CMB photons, i.e. $T_e \sim T$. Without the efficient Compton scattering, due to the expansion of the universe, the temperatures of the free electrons and CMB photons deviate below $T < m_e$. This means that to counter the effect of expansion, the electrons (or baryonic matter) needs to extract energy from the CMB photons. Consequently, this leads to a unavoidable distortion signal, which is expected to yield negative μ- and y-distortions, both valued roughly at $\mu_{\mathrm{cool}}, y_{\mathrm{cool}} \sim -\text{few} \times 10^{-9}$ — see e.g. refs. [79, 90] for more information. In the computation of the μ-signal, we thus divide the energy injection term in eq. (207) as $Q^* = Q_{\mathrm{cool}} + Q_{\mathrm{silk}}$, resulting in the overall distortion $\mu = \mu_{\mathrm{cool}} + \mu_{\mathrm{silk}}$.

4.3 Distortion from the dissipation of primordial perturbations

As already mentioned in Section 1.2, the diffusion damping of the acoustic oscillations in the CMB, dubbed as the Silk damping, leads to creation of spectral distortions. This is due to the energy release and mixing of the photons of different temperature black-bodies (see e.g. Figure 3 in ref. [91], where the mixing

of photons from different phases of acoustic waves is discussed). Here we give a brief review of the estimation of the energy injection coming from the diffusion of acoustic modes following ref. [90] and references therein. More refined analysis of the dissipation of the energy stored in the energy density perturbations is given in ref. [92].

The comoving energy density $Q_{\rm silk}$ stored in the in acoustic waves in the photon-baryon plasma can be written as [93]

$$Q_{\rm silk} \approx \frac{c_{\rm s}^2}{1+w_\gamma}\,\rho_\gamma \langle \delta_\gamma(\mathbf{x})^2 \rangle, \tag{208}$$

where ρ_γ is the photon energy density and δ_γ is the photon density perturbation and for the radiation we have that the sound speed of photon fluid is $c_{\rm s}^2 \approx 1/3 = w_\gamma$ to first approximation. Note that in eq. (208) we have taken into account the relativistic correction to the classical non-relativistic solution found in the literature, that predicts a factor of $4/3$ larger energy injection (see e.g. [92] for discussion on this matter). We can write the averaged photon density perturbation as

$$\langle \delta_\gamma(\mathbf{x})^2 \rangle = \int \frac{{\rm d}^3\mathbf{k}}{(2\pi)^3}\, P_\gamma\,(k) = \int \frac{{\rm d}^3\mathbf{k}}{(2\pi)^3}\, \Delta_\gamma^2\,(k)\, P_\gamma^i\,(k)\,, \tag{209}$$

where $P_\gamma\,(k)$ is the photon power spectrum, which we further decomposed into two terms: $P_\gamma\,(k) = \Delta_k^2\, P_\gamma^i\,(k)$, where P_γ^i is the initial power spectrum and Δ_γ is the transfer function that describes the diffusion of the modes inside the horizon [90]. The photon power spectrum follows the curvature power spectrum P_ζ according to the following expression [90]

$$P_\gamma^i\,(k) = \frac{4}{\left((2R_\nu/5) + (3/2)\right)^2}\, P_\zeta\,(k) \approx 1.45\, P_\zeta\,(k) \equiv A_\nu P_\zeta\,(k) \tag{210}$$

where $R_\nu = \rho_\nu/(\rho_\gamma + \rho_\nu) \approx 0.4$ [90]. The transfer function can be written as [90]

$$\Delta_\gamma^2\,(k) \approx 9\cos^2\,(k r_{\rm s})\; {\rm e}^{-2k^2/k_{\rm D}^2}, \tag{211}$$

where $r_{\rm s}$ is the sound horizon and $k_{\rm D}$ is the Silk damping diffusion scale. We can see that the perturbations related to the small-scale modes $k \gg k_{\rm D}$ are exponentially damped. The photon damping diffusion scale can be computed to be [94]

$$\frac{1}{k_{\rm D}^2} = \int_z^\infty {\rm d}z' \frac{(1+z')}{6H\,(1+R)\,n_e\,(z')\,\sigma_T} \left(\frac{R_{b,\gamma}^2}{1+R} + \frac{16}{15} \right), \tag{212}$$

where $R_{b,\gamma} = (3\rho_b/4\rho_\gamma)$, σ_T is the Thomson scattering cross-section and n_e is the electron number density, which can be written as $n_e = n_{e,0}\,(1+z)^3$, where the free electron number density before the recombination is given by $n_{e,0} = n_{\rm H,0} +$

$2n_{\mathrm{He},0}$. The solution for eq. (212) during the radiation dominated epoch is then [90]

$$k_D = A_{\mathrm{D}}^{-1/2} \left(1+z\right)^{3/2} \tag{213}$$

$$A_{\mathrm{D}} \approx \frac{8}{135 H_0 \Omega_r^{1/2} \sigma_T} \approx 5.9 \times 10^{10}\ \mathrm{Mpc}^2, \tag{214}$$

where H_0 and Ω_r denote the current Hubble rate and radiation density, respectively.

The energy injection part in eq. (207) is then of the following form

$$\frac{\mathrm{d}}{\mathrm{d}z}\frac{Q_{\mathrm{silk}}}{\rho_\gamma} \approx \frac{1}{4}\int \frac{\mathrm{d}^3\mathbf{k}}{\left(2\pi\right)^3}\, A_\nu P_\zeta\left(k\right) \frac{\mathrm{d}\Delta_\gamma^2\left(k\right)}{\mathrm{d}z} \tag{215}$$

$$\approx \frac{27}{4}\int \frac{\mathrm{d}^3\mathbf{k}}{\left(2\pi\right)^3}\, A_\nu A_{\mathrm{D}} \left(1+z\right)^{-4}\ k^2\ P_\zeta\left(k\right)\ \mathrm{e}^{-2k^2/k_{\mathrm{D}}^2}, \tag{216}$$

where the $\cos^2$-term was replaced with its average value over oscillation of $1/2$ [90]. The value of μ-distortion related to the dissipation of acoustic waves is then approximated by

$$\mu_{\mathrm{silk}} \approx 1.401 \int_{z_1}^{z_2} \mathrm{d}z\, \mathrm{e}^{-\left(z/z_{\mathrm{DC}}\right)^{5/2}} \left(\frac{\mathrm{d}}{\mathrm{d}z}\frac{Q_{\mathrm{silk}}}{\rho_\gamma}\right) \tag{217}$$

$$\approx 0.479 A_\nu A_{\mathrm{D}} \int_{z_1}^{z_2} \mathrm{d}z\, \mathrm{e}^{-\left(z/z_{\mathrm{DC}}\right)^{5/2}} \int_0^\infty \mathrm{d}k\, k^4\ P_\zeta\left(k\right)\ \left(1+z\right)^{-4}\ \mathrm{e}^{-2k^2/k_{\mathrm{D}}^2}, \tag{218}$$

where we set the integration limits to go from $z_1 = 5 \times 10^4$ to $z_2 = 2 \times 10^6$ as discussed in the previous section. We can see that the eq. (218) takes the primordial perturbation power spectrum P_ζ as an input, and therefore we can compute the μ-signal for example in models where the perturbations are sourced by one or two scalar fields.

4.4 Spectral distortions as a constraint on inflationary models

In the previous section we discussed how the dissipation of the energy resided in the acoustic waves of the photon-baryon system allows us to connect the μ-distortion to the initial primordial perturbations power spectrum P_ζ. This unavoidable effect of a distortion signal coming from the perturbations opens up the possibility to constrain the inflationary models via their prediction for the μ-signal.

As the μ-distortion signal originates from the energy dissipation between the redshifts 2×10^6 and 5×10^4, the diffusion damping scale k_{D} in eq. (213) sets the relevant scales probed by the μ-distortion to be $50\ \mathrm{Mpc}^{-1} < k < 10^4\ \mathrm{Mpc}^{-1}$. Importantly, these are much smaller scales than probed by the CMB anisotropies or large-scale structures, i.e. $\mathcal{O}\left(10^{-3}\right)\ \mathrm{Mpc}^{-1} < k_{\mathrm{CMB}} < \mathcal{O}\left(0.1\right)\ \mathrm{Mpc}^{-1}$ and

$\mathcal{O}\left(10^{-2}\right)$ Mpc$^{-1} < k_{\rm LSS} < \mathcal{O}\left(1\right)$ Mpc^{-1}. This means that the spectral distortions can open up an additional window of $\sim 5 \ldots 10$ e-folds into the inflation, roughly doubling the currently probable inflationary physics [95]. While primordial black holes (PBHs) also constrain similar and smaller scales [96], their constraints on the power spectrum are significantly weaker than what can be achieved by proposed future experiments, i.e. PIXIE-like experiments where the sensitivities are of the order of $\mu \sim 10^{-8}$ [75, 81, 97], significantly improving the COBE/FIRAS upper bound $|\mu| \lesssim 10^{-4}$ [8, 9]. This is also illustrated in Figure 6, where the current and future projected constraints for the scalar power spectrum from different sources are plotted.

Let us then estimate the value of the μ-distortion coming from the dissipation of acoustic waves. We will use the standard parametrization of the primordial perturbation power spectrum P_ζ:

$$P_\zeta\left(k\right) = \frac{2\pi^2}{k^3}\mathcal{P}_\zeta\left(k\right) = \frac{2\pi^2}{k^3}\, A_s\, \left(\frac{k}{k_{\rm ref}}\right)^{n_s-1}, \tag{219}$$

where the Planck pivot scale is $k_{\rm ref} = 0.05$ Mpc^{-1}, and we have neglected any higher-order scale-dependencies, such as the running α_s. As eq. (218) takes $P_\zeta\left(k\right)$ as an input, it is easy to compute the μ-distortion from the given spectra. Also, as we can relate the spectral index to the single-field slow-roll parameters, i.e. $n_s = 1 - 6\epsilon_\phi + 2\eta_\phi$, we can in principle compute the μ in terms of the slow-roll parameters or the inflationary potential and its derivatives (at the reference scale).

It is then straightforward to compute the unavoidable μ-type spectral distortion prediction of ΛCDM from eq. (218):

$$\mu_{\rm silk} \approx 1690\,{\rm Mpc}^2 \int_{5\times10^4}^{2\times10^6} {\rm d}z\, \frac{{\rm e}^{-\left(z/z_{\rm DC}\right)^{5/2}}}{\left(1+z\right)^4} \int_0^\infty {\rm d}k\, k\, \left(\frac{k}{k_{\rm ref}}\right)^{n_s-1} {\rm e}^{-2k^2/k_{\rm D}^2(z)} \tag{220}$$

$$\approx 1.9\times10^{-8}, \tag{221}$$

where we used the Planck 2018 best-fit values, $n_s \approx 0.965$ and $A_s \approx 2.09\times10^{-9}$ [4]. The $\mu \approx 10^{-8}$ is a standard prediction of ΛCDM (see e.g. refs. [79, 90]), and is usually assumed to be the target sensitivity for future experiments. As the discussed adiabatic cooling of electrons yields a negative contribution to the μ-signal that is roughly an order of magnitude smaller than $\mu_{\rm silk}$, i.e. $\mu_{\rm cool} \approx \mathcal{O}\left(10^{-9}\right)$, one expects that there is an observable signal without any exotic non-ΛCDM physics. A non-detection at this level could prove to be a problem for the ΛCDM, and might be a hint of new physics [81].

Of course, there is still some leeway for the value of μ: one can extent the scale-dependency in eq. (219) to higher-orders, i.e. include the running of the spectral index α_s and the running of running β_s. However, as the power spectrum parameters are already quite constrained, the affect of inclusion of the running, which is expected to be $\alpha_s \sim \mathcal{O}\left(\left(1-n_s\right)^2\right)$, does greatly not alter the prediction for μ — see for example ref. [98], where the authors studied the ΛCDM + α_s predictions for the μ-distortion.

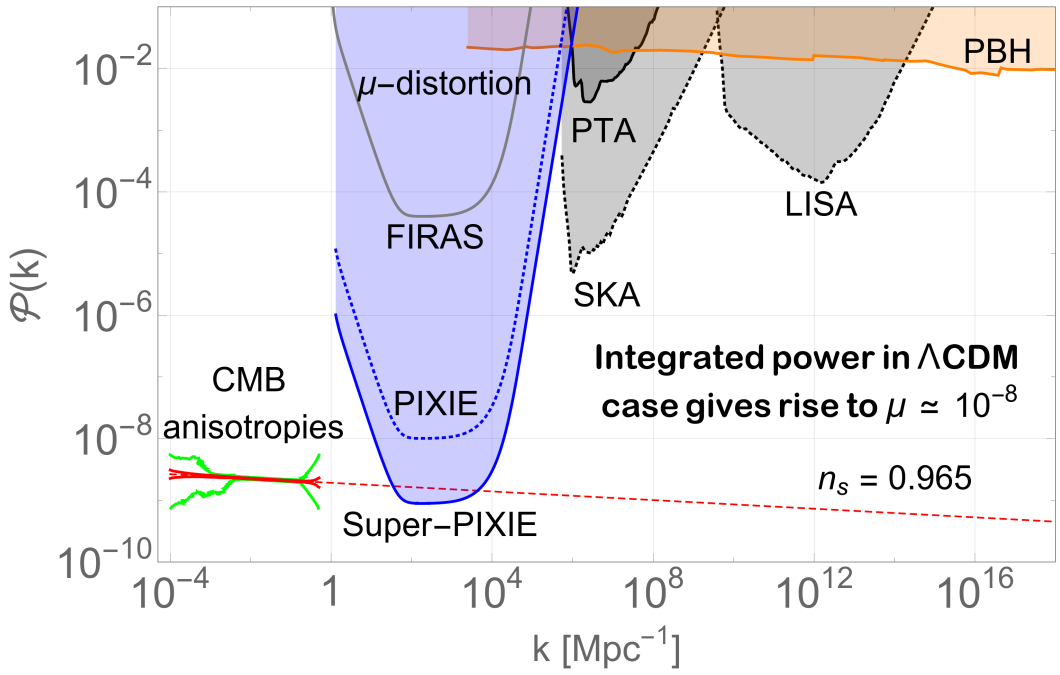

FIGURE 6 Forecast constraints on the primordial perturbation power spectrum $\mathcal{P}_\zeta$ coming from the CMB anisotropies, μ-distortion and PBH studies. The proposed μ-distortion experiments can probe the values $\mu \lesssim \mathcal{O}\left(10^{-8}\right)$, which allows to set constrains on the spectrum $\mathcal{P}_\zeta$ on levels and scales inaccessible to other probes. Figure from ref. [81].

However, a more significant departure from the standard prediction can be achieved, if one considers the primordial perturbations to be sourced by multiple fields. In this case the individual power spectrum parameters (n_i, α_i and β_i) can conspire such that the spectrum is greatly enhanced at the smaller scales sensitive to spectral distortions, while being constrained at the larger scales probed by the CMB anisotropies. We will come back to this scenario in Chapter 5, where we discuss the scientific work [74] related to this thesis.

5 CMB SPECTRAL DISTORTIONS IN GENERIC TWO-FIELD MODELS

So far we have given a review of the standard inflationary cosmology, the production of primordial perturbations and the formation of CMB spectral distortions. These all are needed for the discussion of the scientific work related to this thesis. In this chapter we briefly go through the analysis done in ref. [74], where we studied the formation of the μ-type spectral distortion in two-field inflationary models. The main production mechanism for the μ-distortion is assumed to be the diffusion of the acoustic oscillations, i.e. Silk damping, that was discussed in Chapter 4. As discussed in Sections 4.3 and 4.4, the strength of the μ-signal is related to the primordial power spectrum $\mathcal{P}_\zeta$, which allows the μ-distortion to be used as a constraint on the underlying inflationary model. In the work done in ref. [74], we studied the production of μ-type spectral distortions both in a general two-field setup and in a more specific inflaton-curvaton scenario.

5.1 General parameterization of two-field models

In Section 4.4 we discussed how the CMB spectral distortions can be used to constrain inflationary models. In the context of single-field inflation, it was found in refs. [89, 98, 99] that the future measurements of the μ-distortion could place a significant constraint on the scale-dependence of the spectral index. The spectral distortion predictions in the mixed inflaton-curvaton models have been previously studied for example in ref. [100]. In ref. [74] we studied a general two-field setup, where the spectrum of primordial perturbations is parameterized as

$$\begin{aligned}\mathcal{P}_\zeta &= \mathcal{P}_1 + \mathcal{P}_2 = \frac{A_s}{1+R}\left[\left(\frac{k}{k_{\rm ref}}\right)^{n_1-1+\frac{1}{2}\alpha_1\ln\left(\frac{k}{k_{\rm ref}}\right)+\frac{1}{6}\beta_1\ln^2\left(\frac{k}{k_{\rm ref}}\right)}\right. \\ &\qquad \left. +R\left(\frac{k}{k_{\rm ref}}\right)^{n_2-1+\frac{1}{2}\alpha_2\ln\left(\frac{k}{k_{\rm ref}}\right)+\frac{1}{6}\beta_2\ln^2\left(\frac{k}{k_{\rm ref}}\right)}\right], \qquad (222)\end{aligned}$$

where A_s is the total amplitude of the primordial power spectrum at the reference scale, $A_s = \mathcal{P}_\zeta(k_{\rm ref})$, and R is defined as the ratio of the individual spectrum amplitudes, i.e. $R = \mathcal{P}_2/\mathcal{P}_1$ at the reference scale. The parameters n_i, α_i and β_i, where $i = 1, 2$, are the individual spectral index, the running and the running of the running of the two scalar fields, evaluated at the reference scale $k_{\rm ref} = 0.05\,\mathrm{Mpc}^{-1}$. The phenomenological parametrization (222) can be used to describe two-field configurations such as two-field inflation models and curvaton-type models. As discussed in Section 3.4, in curvaton models the primordial perturbations can be sourced both by adiabatic and isocurvature scalar fields.

In the analysis we set the curvature spectrum amplitude A_s equal to the

observed (Planck 2015) best-fit value $\mathcal{P}_{\rm obs} = 2.19 \times 10^{-9}$ [101]. For the other power spectrum parameters in eq. (222) we chose to have the following prior ranges:

$$n_{1,2} \in [0,2],\ \alpha_{1,2} \in [-0.1, 0.1],\ \beta_{1,2} \in [-0.01, 0.01],\ R \in [0,1]\ . \tag{223}$$

Note that, we chose the ratio R such that $\mathcal{P}_1$ denotes the dominant part of the power spectrum $\mathcal{P}_\zeta$, while the $\mathcal{P}_2$ is chosen as the subdominant part. An obvious requirement is that the Taylor expansion of the power spectrum should hold over the probed scales, i.e. $\mathcal{O}\left(0.05\right) - \mathcal{O}\left(10^4\right)$ Mpc^{-1}. The expansion remains valid in this interval as the priors for the spectral index, its running and the running of the running are chosen such that each successive term is parametrically smaller.

An important feature of the two-field model is that the spectral index n_s, its running α_s and the running of the running β_s are functions of the individual power spectrum parameters. They can be straightforwardly computed from eq. (222), and they read:

$$n_s \equiv 1 + \left.\frac{\mathrm{d}\ln\mathcal{P}_\zeta(k)}{\mathrm{d}\ln(k)}\right|_{k=k_{\rm ref}} = \frac{n_1 + R n_2}{1+R}, \tag{224}$$

$$\alpha_s \equiv \left.\frac{\mathrm{d}n_s}{\mathrm{d}\ln(k)}\right|_{k=k_{\rm ref}} = \frac{\alpha_1 + R\alpha_2}{1+R} + \frac{R(n_2-n_1)^2}{(1+R)^2}, \tag{225}$$

$$\beta_s \equiv \left.\frac{\mathrm{d}^2 n_s}{\mathrm{d}\ln(k)^2}\right|_{k=k_{\rm ref}} = \frac{\beta_1 + R\beta_2}{1+R} + \frac{3R(n_2-n_1)(\alpha_2-\alpha_1)}{(1+R)^2} + \frac{R(1-R)(n_2-n_1)^3}{(1+R)^3}\ . \tag{226}$$

Note that, the difference between the spectral indices $n_1 \neq n_2$, induces both running α_s and running of the running β_s of the spectral index, even if the individual running parameters are negligible or zero. This is an important feature, that allows the spectrum and the μ-distortion signal to be enhanced compared to the single-field case. We can also see, that the configurations for which the power spectrum parameters are equal are degenerate with the single-field configuration with $R = 0$.

5.1.1 Analysis of the distortion constraints on the models

In the analysis of ref. [74], we scanned over the seven model parameters (223), and proceeded to first compute the spectral index n_s, its running α_s, running of the running β_s according to the eqs. derived in the previous section, and then the spectral μ-distortion coming from the dissipation of the primordial perturbations from eq. (218) derived in Section 4.3. We also took into account the small negative μ-distortion generated by the adiabatic cooling of electrons, as discussed in Section 4.2.2. As constraints, we imposed the Planck 2015 bounds on n_s, α_s and β_s [101], and the COBE/FIRAS upper bound on the spectral μ-distortion, i.e. $|\mu| < 9 \times 10^{-5}$ [8, 9]. We also compared the computed μ-distortion signals to the sensitivity of the future PIXIE-like experiment ($\Delta\mu = 1 \times 10^{-8}$ [97]) which was discussed in Section 4.4. In the analysis we performed a scan over 5 000 000

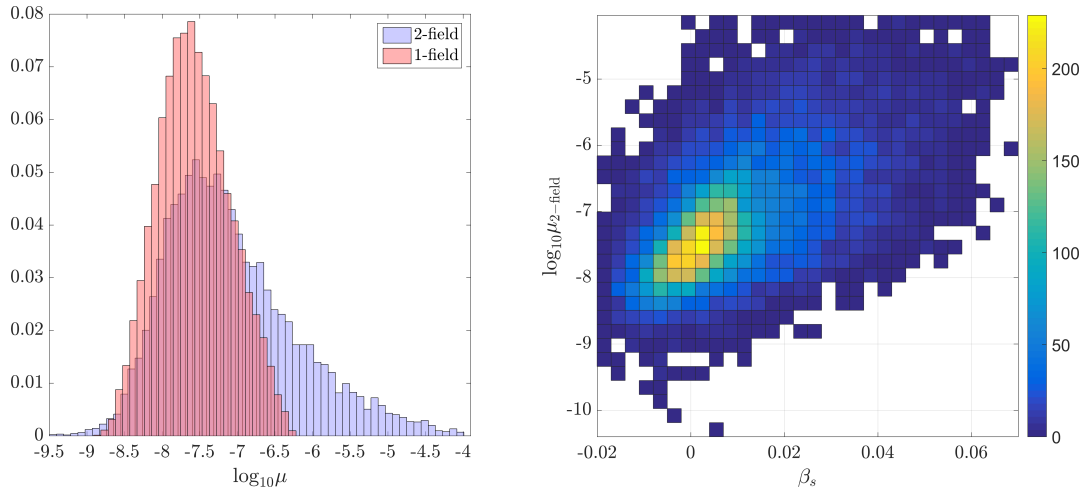

FIGURE 7 Left panel: distribution of μ-values compatible with the Planck constraints at 99 % C.L. in the single-field (red) and two-field (blue) cases. Right panel: the distribution of the running of the running β_s and μ-distortion in the two-field model. Figure reproduced from ref. [74] with permission.

parameters sets in the prior range (223), of which 12 628 generated sets were compatible with the imposed constraints. Here we only briefly summarize the main results of ref. [74], and refer the article for a more detailed discussion.

The key outcome is seen in the left-panel of Figure 7[1]. The histogram shows the μ-value distributions for the single-field ($R = 0$) and two-field models that satisfy the imposed constraints. In ref. [74], we argued that the wider spread of μ-distortion values in the two-field configuration originates from the fact that the second field allows a more significant scale-dependency, while still being consistent with the Planck 2015 bounds on $(n_s,\ \alpha_s, \beta_s)$ at the reference scale $k = 0.05\ \mathrm{Mpc}^{-1}$. We found three different structures leading to enhanced distortion signal: large tilt n_2 of the subdominant field, large difference between the tilts n_1 and n_2, discussed already in ref. [102], and large difference between the runnings α_1 and α_2. Due to the scale-dependency of the spectrum, the second field can arise to give a dominant contribution at smaller scales, while still being subdominant at the observed CMB scales. This can happen especially, if the spectral index n_2 is blue-tilted on the scales probed by μ-distortion. As mentioned, the enhancement of the μ-signal is due to the difference in the spectral indices or runnings, which can induce large positive running α_s and running of the running β_s.

The right-panel of Figure 7 shows correlation between the running of the running β_s and the μ-distortion for the two-field setups. Interestingly, in our analysis the distribution seems to be centered around $\beta_s = 0$, and does not lie within the Planck 2015 best-fit value for $\beta_s = 0.025 \pm 0.013$ [101].

[1] In ref. [74], we also plotted the correlations of the different spectrum parameters n_i, α_i and β_i with each-other as a function of the predicted μ-signal, which allows (albeit somewhat weakly) to constrain the two-field model parameter space.

5.2 A specific example: mixed inflaton-curvaton case

We have now seen, that in a general two-field setting the individual power spectrum parameters can conspire such that the μ-signal is greatly enhanced while still fulfilling the Planck constraints. It is then interesting to study a more specific setup, where the constraints on the power spectrum parameters can be turned into constraints onto the model-dependent parameters, i.e. slow-roll parameters that depend on the specific potential of the inflationary model. As a concrete two-field model example, in ref. [74] we studied the mixed inflaton-curvaton scenario, which was already briefly discussed in Section 3.4.3.

In ref. [74], we assumed that the inflationary scalar potential is separable and is given by

$$V(\phi,\chi) = V_1(\phi) + V_2(\chi), \tag{227}$$

where ϕ is the inflaton field and χ is now the curvaton field. As we studied the curvaton scenario, we assumed that the field is subdominant during inflation, i.e. $V_1(\phi) \approx 3H^2M_{\rm Pl}^2 \gg V_2(\chi)$. Furthermore, as in ref. [74] we probed the parameter space on the level of the individual running of the running, we need to consider the higher order slow-roll parameters than we have previously discussed in this work. In ref. [74], we argued that the relevant slow-roll parameters are

$$\epsilon_\phi = \frac{M_{\rm Pl}^2}{2}\left(\frac{V_{,\phi}}{V}\right)^2,\ \eta_\phi = M_{\rm Pl}^2\frac{V_{,\phi\phi}}{V},\ \eta_\chi = M_{\rm Pl}^2\frac{V_{,\chi\chi}}{V},\ \xi_\phi = M_{\rm Pl}^4\frac{V_{,\phi}V_{,\phi\phi\phi}}{V^2}, \tag{228}$$

$$\xi_\chi = M_{\rm Pl}^4\frac{V_{,\chi}V_{,\chi\chi\chi}}{V^2} \simeq 0,\ \sigma_\phi = M_{\rm Pl}^6\frac{V_{,\phi}^2V_{,\phi\phi\phi\phi}}{V^3},\ \sigma_\chi = M_{\rm Pl}^6\frac{V_{,\chi}^2V_{,\chi\chi\chi\chi}}{V^3} \simeq 0. \tag{229}$$

Note that, we assumed that that the slow-roll parameters ξ_χ and σ_χ are either zero or negligible. This was discussed in Section 3.4, where we argued that in the curvaton scenario potential needs to be flat enough that $V_{,\chi} \simeq 0$, which indicates that the curvaton is close to the isocurvature field space direction. As we mentioned in Section 3.4, this is fulfilled in the case of a quadratic curvaton scenario.

As discussed in Sections 3.3.4 and 3.4, the spectrum of the primordial curvature perturbations is given in the ΔN formalism as

$$\mathcal{P}_\zeta(k) = N_{,\phi}^2\mathcal{P}_\phi(k) + N_{,\chi}^2\mathcal{P}_\chi(k), \tag{230}$$

where the leading-order slow-roll result reads

$$\mathcal{P}_\phi(k) = \mathcal{P}_\chi(k) = \left(\frac{H}{2\pi}\right)^2_{k=aH},\ N_{,\phi} = \left(M_{\rm Pl}\sqrt{2\epsilon_\phi}\right)^{-1}. \tag{231}$$

Note that $N_{,\chi}$ depends on the exact details of the curvaton model, as was discussed in Section 3.4. If we define

$$R = \frac{N_{,\chi}^2(k_{\rm ref})}{N_{,\phi}^2(k_{\rm ref})}, \tag{232}$$

the two-field power spectrum (230) coincides with the phenomenological spectrum (222) discussed in the previous section. Note that, unlike in the general parametrisation of the previous section, here we let the ratio R to be $R \in [0, \infty[$. If $R = 0$, the inflaton dominates the curvature spectrum at the reference scale, while for $R \gg 1$ the primordial perturbations are sourced by the dominant curvaton.

As in the previous section, we want to find the spectral index n_s, its running α_s and running of the running β_s, which are given by the derived eqs. (224), (225) and (226), where the individual parameters are now replaced by $n_1 = n_\phi$, $n_2 = n_\chi$ etc. These individual power spectrum parameters are straightforward to compute, and they read

$$\begin{aligned} n_\phi &= 1 - 6\epsilon_\phi + 2\eta_\phi \,, \\ n_\chi &= 1 - 2\epsilon_\phi + 2\eta_\chi \,, \\ \alpha_\phi &= -24\epsilon_\phi^2 + 16\epsilon_\phi\eta_\phi - 2\xi_\phi \,, \\ \alpha_\chi &= -8\epsilon_\phi^2 + 4\epsilon_\phi\eta_\phi + 4\epsilon_\phi\eta_\chi \,, \\ \beta_\phi &= 2\sigma_\phi - 8\epsilon_\phi(4\eta_\phi^2 + 3\xi_\phi) + 2\eta_\phi\xi_\phi + 192\epsilon_\phi^2\eta_\phi - 192\epsilon_\phi^3 \,, \\ \beta_\chi &= -64\epsilon_\phi^3 - 8\epsilon_\phi\eta_\phi(\eta_\phi + \eta_\chi) + 8\epsilon_\phi^2(7\eta_\phi + 3\eta_\chi) - 4\epsilon_\phi\xi_\phi \,. \end{aligned} \tag{233}$$

In the analysis we also used the constraints on the tensor-to-scalar ratio r, that was discussed in Section 3.2.2, to constrain the available parameter space. As the spectrum of tensorial modes, i.e. gravitational waves, can be written as $\mathcal{P}_T = 8H^2/(4\pi^2 M_{\rm Pl}^2)$, the spectrum (230) can be recast in the form

$$\mathcal{P}_\zeta\left(k_{\rm ref}\right) = \mathcal{P}_T\left(k_{\rm ref}\right)\ \frac{1+R}{16\epsilon_\phi\left(k_{\rm ref}\right)}, \tag{234}$$

which allows us to write the tensor-to-scalar ratio at the reference scale as

$$r = \frac{\mathcal{P}_T\left(k_{\rm ref}\right)}{\mathcal{P}_\zeta\left(k_{\rm ref}\right)} = \frac{16\epsilon_\phi\left(k_{\rm ref}\right)}{1+R}, \tag{235}$$

i.e. we can turn the constraint on r to constraints on the $\left(\epsilon_\phi, R\right)$ plane.

5.2.1 Analysis and results

Again, in ref. [74], we fixed the observed spectrum amplitude value as $\mathcal{P}_\zeta = 2.19 \times 10^{-9}$ [101]. As we also included the computation of tensor-to-scalar ratio r in this section, we also imposed the Planck 2015 + BICEP2/KECK bound $r < 0.07$ (at 95 % CL) [103] in addition to the already discussed Planck 2015 and COBE/FIRAS constraints. We then proceeded to scan over the five slow-roll parameters $\epsilon, \eta_\phi, \eta_\chi, \xi_\phi, \sigma_\phi$ and the spectrum amplitude ratio R with the chosen prior ranges

$$\begin{aligned} &\epsilon_\phi \in [0, 0.1], \qquad \eta_\phi, \eta_\chi \in [-0.1, 0.1], \qquad \xi_\phi \in [-0.01, 0.01], \\ &\sigma_\phi \in [-0.001, 0.001], \qquad R \in [0.01, 100] \,. \end{aligned} \tag{236}$$

We argued that the prior range for R for all practical purposes describes the configurations from the inflaton domination to the curvaton dominated limit. In the analysis we performed a scan over the generated 3 000 000 models, of which 121 086 models (roughly 4 percent) were compatible with the imposed Planck and COBE/FIRAS bounds. Again, here we only recap the main results of ref. [74], and refer there to a more detailed discussion.

As one might expect from the previous two-field model findings, we found that the mixed inflaton-curvaton setup also allows a more wider spread of μ-values compared to the pure inflaton case. This is again due to the fact that the two sources can conspire such that the runnings of the spectral index are enhanced.

In terms of the curvaton parameter space, the main result of ref. [74] is shown in Figure 8, where the the dependence of μ-distortion on the curvaton parameters η_χ and R is depicted. If the tensor-to-scalar ratio bound is not imposed, the μ-values are heavily degenerate on the curvaton parameter (η_χ, R) plane (this is depicted in the first panel). For large R values (i.e. curvaton dominated part), the large negative and positive η_χ values are excluded, as they yield a too small or large spectral index. As seen in the second panel: imposing the tensor-to-scalar ratio bound $r < 0.07$, has the effect of removing parameter combinations which yield large μ-values in the inflaton dominated limit, $R \ll 1$, where the curvaton contribution is small. In this regime the r-bound constrains the positive η_ϕ values, which give a positive enhancement to α_s and β_s and thus correlate with large μ-distortions. When the inflaton and the curvaton contributions to the power spectrum are of the same order at the pivot scale, i.e. $R \sim 1$, the curvaton slow-roll parameter values $\eta_\chi \gtrsim 0.05$ are cut out, as the constraints would require $\eta_\phi < -0.1$ which is excluded by our choice of priors.

Figure 8 also shows the effect of tighter tensor bounds that could be expected from future data. As we decreased the tensor-to-scalar ratio (depicted in the the two lower panels), we saw that the size of the cut-out region further increased. It is however important to note that, the two depicted curvaton parameters, η_χ and R, do not completely fix the value of μ-distortion. The μ-distortion continues to depend on the inflaton slow-roll parameters even in the curvaton dominated limit. In ref. [74], we argued that while the degeneracy was present, the obtained results indicated that the measurement of μ-distortion in conjunction with the improving bounds on tensor-to-scalar ratio r could reduce and place interesting constraints on the curvaton parameter space, thus allowing to break the parameter degeneracies in the curvaton sector. For example, taking $\mu < 0.5 \times 10^{-8}$ and $r < 0.01$ as sample values of futuristic bounds, our results would suggest that there are two different outcomes for the curvaton sector. Either the curvaton contribution vanishes, or the curvaton dominates the primordial perturbations. In the latter case, the curvaton slow-roll parameter η_χ is constrained to have values between $-0.007 < \eta_\chi < 0.045$. This goes some way in demonstrating that the constraints on the μ-distortion originating from the diffusion of acoustic waves are compelling observable especially with the forthcoming next-generation polarization probes (see e.g. ref. [104]) that can give strong

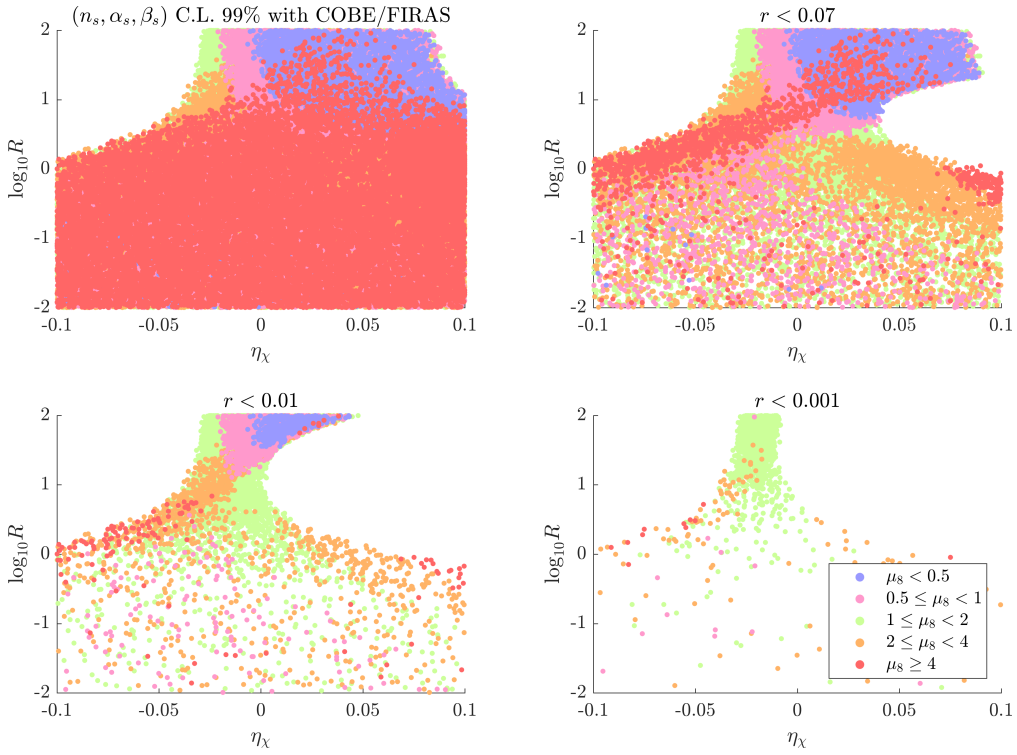

FIGURE 8 The mixed inflaton-curvaton μ-signal predictions as function of the curvaton parameters η_χ and R. Figure reproduced from ref. [74] with permission.

bounds on the tensor-to-scalar ratio r.

6 CONCLUSIONS

In this thesis we have reviewed the primordial perturbations generated by scalar fields during inflation: how they are generated and how they can be related to observational quantities. We have discussed the preliminaries of the ΛCDM cosmology, the inflationary paradigm, the cosmological perturbation theory and the formation of the CMB spectral distortions. We have concentrated on scalar field models, where the primordial perturbations are sourced by multiple fields, whereas in the standard single-field slow-roll inflation both the inflationary dynamics and the density perturbations are sourced by the inflaton field.

Due to the efficient thermalization, the CMB is remarkably close to a perfect black-body spectrum, with deviations, dubbed as spectral distortions, at most to one part in 10^5 allowed. These spectral distortions can be created when the thermalization of the disturbances in the primordial plasma, in form of energy or particle injections, is not efficient enough. The deviations from thermal equilibrium can be caused by many different early universe processes, e.g. exotic processes like decaying dark matter particles or evaporating primordial black holes. However, in the ΛCDM there is an unavoidable source of distortions: the diffusion of energy stored in the primordial density perturbations due to the Silk damping. This effect allows one to connect the μ-type spectral distortions to the primordial power spectrum $\mathcal{P}_\zeta$.

In ref. [74], we studied the μ-distortion predictions in generic two-field models, where two uncorrelated sources can contribute to the primordial curvature power spectrum. We studied both a more general phenomenological model, where the underlying model be can be for example two-field inflation, and also a more specific model, a mixed inflaton-curvaton model. We found that in the two-field setups the μ-signal can be greatly enhanced compared to the expected single-field model value, i.e. $\mu \approx \mathcal{O}\left(10^{-8}\right)$. The second field can be subdominant at the observed CMB scales, and thus fulfilling the observational constraints, while still giving a major contribution to the primordial power spectrum on the smaller scales probed by the spectral distortions. In the mixed inflaton-curvaton case, we showed that at the sensitivity levels of the proposed spectral distortion measurements, in conjunction with the bounds on the tensor-to-scalar ratio, can efficiently probe the values of the curvaton model parameter space. In the analysis done in ref. [74], we neglected the discussion of correlating μ-distortions with various other observables, such as non-Gaussianities, which we expect to further improve the efficiency of the spectral distortions as tests for the abundant inflationary models.

REFERENCES

[1] D. W. Hogg *et al.*, "Cosmic Homogeneity Demonstrated with Luminous Red Galaxies," ApJ **624** (2005) 54-58 doi:10.1086/429084 [arXiv:411197 [astro-ph]].

[2] M. I. Scrimgeour *et al.*, "The WiggleZ Dark Energy Survey: the transition to large-scale cosmic homogeneity," Mon. Not. Roy. Astron. Soc. **425** 1 116-134 (2012) doi: 10.1111/j.1365-2966.2012.21402.x [arXiv:1205.6812 [astro-ph]].

[3] S. M. Carroll, "Spacetime and Geometry: An Introduction to General Relativity," Pearson International (2013), ISBN: 978-1-29-202663-3.

[4] N. Aghanim *et al.* [Planck Collaboration], "Planck 2018 results. VI. Cosmological parameters," [arXiv::1807.06209 [astro-ph]].

[5] D. Baumann, "Advanced Cosmology," Lecture Notes, [url: http://cosmology.amsterdam/education/advanced-cosmology/].

[6] D. Baumann, "Cosmology," Lecture Notes, [url: http://cosmology.amsterdam/education/cosmology/].

[7] S. Dodelson, "Modern Cosmology," Academic Press (2003), ISBN: 978-0-12-219141-1, doi:10.1016/B978-0-12-219141-1.X5019-0 .

[8] D. J. Fixsen, E. S. Cheng, J. M. Gales, J. C. Mather, R. A. Shafer and E. L. Wright, "The Cosmic Microwave Background Spectrum from the Full COBE* FIRAS Data Set," ApJ **473** (1996) 002 doi:10.1086/178173 [arXiv:9605054 [astro-ph]].

[9] J. C. Mather *et al.* "Measurement of the cosmic microwave background spectrum by the COBE FIRAS instrument," ApJ **420** (1994) 002 doi:10.1086/173574

[10] Y. Akrami *et al.* [Planck Collaboration], "Planck 2018 results. I. Overview and the cosmological legacy of Planck," [arXiv::1807.06205 [astro-ph]].

[11] S. M. Carroll and J. Chen, "Spontaneous Inflation and the Origin of the Arrow of Time," [arXiv:0410270 [hep-th]].

[12] S. M. Carroll and J. Chen, "Spontaneous Inflation and the Origin of the Arrow of Time," Int. J. Mod. Phys. D **14** (2005) doi:10.1142/S0218271805008054 [arXiv:0505037 [gr-qc]].

[13] D. Baumann, "TASI Lectures on Inflation," Lecture Notes, [arXiv:0907.5424 [hep-th]].

[14] A. H. Guth, "Inflationary universe: A possible solution to the horizon and flatness problems," Phys. Rev. D **23**, 347 (1981) doi:10.1103/PhysRevD.23.347

[15] A. Linde, "A new inflationary universe scenario: A possible solution of the horizon, flatness, homogeneity, isotropy and primordial monopole problems," Phys. Lett. B **108** 6 389-393 (1982) doi:10.1016/0370-2693(82)91219-9

[16] A. Linde, "Scalar field fluctuations in the expanding universe and the new inflationary universe scenario," Phys. Lett. B **116** 5 335-339 (1982) doi:10.1016/0370-2693(82)90293-3

[17] A. A. Albrecht and P. J. Steinhardt "Cosmology for Grand Unified Theories with Radiatively Induced Symmetry Breaking," Phys. Rev. Lett. **48**, 1220 (1982) doi:10.1103/PhysRevLett.48.1220

[18] A. A. Starobinsky, "A new type of isotropic cosmological models without singularity," Phys. Lett. B **91** 1 99-102 (1980) doi:10.1016/0370-2693(80)90670-X

[19] A. A. Starobinsky, "Dynamics of phase transition in the new inflationary universe scenario and generation of perturbations," Phys. Lett. B **117** 3-4 175-179 (1982) doi:10.1016/0370-2693(82)90541-X

[20] P. A. R. Ade *et al.* [Planck Collaboration], "Planck 2015 results. XIII. Cosmological parameters," Astron. Astrophys. **594**, A13 (2016) doi:10.1051/0004-6361/201525830 [arXiv:1502.01589 [astro-ph]].

[21] E. W. Kolb and M. S. Turner "The Early Universe," Westview Press (1994), ISBN: 978-0-20-162674-2.

[22] D. J. E. Marsh, "Axion Cosmology," Physics Reports. **643** (2016) 0370-1573 doi:10.1016/j.physrep.2016.06.005 [arXiv:1510.07633 [astro-ph]].

[23] A. R. Liddle, P. Parsons and J. D. Barrow "Formalizing the slow-roll approximation in inflation," Phys. Rev. D **50**, 7222 (1994) doi:10.1103/PhysRevD.50.7222 [arXiv:9408015 [astro-ph]]

[24] A. Riotto, "Inflation and the Theory of Cosmological Perturbations," Lectures Notes (2002, updated 2017), [arXiv:0210162 [hep-ph]].

[25] H. Kurki-Suonio, "Cosmological Perturbation Theory, part 1 & 2," Lectures Notes (2015, 2020), [url: http://www.courses.physics.helsinki.fi/teor/cpt/].

[26] S. Nurmi, "Cosmology,", Lecture Notes (2019), [url: http://users.jyu.fi/~satunurm/Cosmology/public_html/].

[27] T. Jacobson, "Introduction to Quantum Fields in Curved Spacetime and the Hawking Effect," Lecture Notes,CECS School on Quantum Gravity, (2002), [arXiv:0308048 [qr-qc]].

[28] T. S. Bunch and P. C. W. Davies, "Quantum Field Theory in de Sitter Space: Renormalization by Point Splitting," Proc. Roy. Soc. Lond. A **A360** 117-134 (1978) doi:10.1098/rspa.1978.0060

[29] A. A. Starobinsky, "Stochastic de Sitter (Inflationary) Stage in the Early Universe," Lect. Notes Phys. **246** 107-126 (1986) doi:10.1007/3-540-16452-9_6

[30] K. Nakao, Y. Nambu and M. Sasaki, "Stochastic Dynamics of New Inflation," Prog. Theor. Phys. **80** 6 1041-1068 (1988) doi:10.1143/PTP.80.1041

[31] A. Albrecht *et al.* "Inflation and squeezed quantum states," Phys. Rev. D **50**, 4807 (1994) doi:10.1103/PhysRevD.50.4807 [arXiv:9303001 [astro-ph]].

[32] D. H. Lyth, K. A. Malik and M. Sasaki, "A general proof of the conservation of the curvature perturbation," JCAP **0505**, 004 (2005) doi:10.1088/1475-7516/2005/05/004 [arXiv:0411220 [astro-ph]].

[33] D. S. Salopek and J. R. Bond, "Nonlinear evolution of long-wavelength metric fluctuations in inflationary models," Phys. Rev. D **42**, 3936 (1990) doi:10.1103/PhysRevD.42.3936

[34] G. I. Rigopoulos and E. P. S. Shellard "The Separate Universe Approach and the Evolution of Nonlinear Superhorizon Cosmological Perturbations," Phys. Rev. D **68**, 123518 (2003) doi:10.1103/PhysRevD.68.123518

[35] D. H. Lyth and D. Wands, "Conserved cosmological perturbations," Phys. Rev. D **68**, 103515 (2003) doi:10.1103/PhysRevD.68.103515 [arXiv:0306498 [astro-ph]].

[36] T. Moroi and T. Takahashi, "Effects of cosmological moduli fields on cosmic microwave background," Phys. Lett. B **522** (2001) 215 [arXiv:0110096 [hep-ph]]

[37] K. Enqvist and M. S. Sloth, "Adiabatic CMB perturbations in pre - big bang string cosmology," Nucl. Phys. B **626** (2002) 395 doi:10.1016/S0550-3213(02)00043-3 [arXiv:0109214 [hep-ph]].

[38] D. H. Lyth and D. Wands, "Generating the curvature perturbation without an inflaton," Phys. Lett. B **524** 1-2 (2002) 5-14 doi:10.1016/S0370-2693(01)01366-1 [arXiv:0110002 [hep-ph]].

[39] D. H. Lyth and A. R. Liddle, "The primordial density perturbation: Cosmology, inflation and the origin of structure," Cambridge University Press (2009) ISBN: 978-0-51-181920-9 doi:10.1017/CBO9780511819209

[40] J. M. Bardeen, "Gauge-invariant cosmological perturbations," Phys. Rev. D **22**, 1882 (1980) doi:10.1103/PhysRevD.22.1882

[41] V. F. Mukhanov, "Gravitational instability of the universe filled with a scalar field," Pisma Zh.Eksp.Teor.Fiz.**41** (1985) 402-405 JETP Lett. **41** (1985) 493-496

[42] M. Sasaki, "Large Scale Quantum Fluctuations in the Inflationary Universe ," Prog. Theor. Phys. **76** 5 (1986) 1036-1046 doi:10.1143/PTP.76.1036

[43] D. Wands, K. A. Malik, D. H. Lyth and A. R. Liddle, "New approach to the evolution of cosmological perturbations on large scales," Phys. Rev. D **62**, 043527 (2000) doi:10.1103/PhysRevD.62.043527 [arXiv:0003278 [astro-ph]].

[44] S. Weinberg, "Adiabatic Modes in Cosmology," Phys. Rev. D **67**, 123504 (2003) doi:10.1103/PhysRevD.67.123504, [arXiv:0302326 [astro-ph]].

[45] S. Weinberg, "Adiabatic Modes in Cosmology," Phys. Rev. D **70**, 043541 (2004) doi:10.1103/PhysRevD.70.043541, [arXiv:0401313 [astro-ph]].

[46] C. Gordon, D. Wands, B. A. Bassett and R. Maartens, "Adiabatic and entropy perturbations from inflation," Phys. Rev. D **63**, 023506 (2000) doi:10.1103/PhysRevD.63.023506 [arXiv:0009131 [astro-ph]].

[47] J. M. Maldacena, "Non-Gaussian features of primordial fluctuations in single field inflationary models," JHEP **05** 013 (2003) doi:10.1088/1126-6708/2003/05/013 [arXiv:0210603]

[48] Y. Akrami *et al.* [Planck Collaboration], "Planck 2018 results. X. Constraints on inflation," [arXiv::1807.06211 [astro-ph]].

[49] D. H. Lyth and Y. Rodriguez, "The inflationary prediction for primordial non-gaussianity," Phys. Rev. Lett. **95**, 121302 (2005) doi:10.1103/PhysRevLett.95.121302 [arXiv:0504045 [astro-ph]].

[50] R. L. Arnowitt, S. Deser and C. W. Misner, "The Dynamics of general relativity," Gen. Rel. Grav. **4** 1997-2027 (2008) doi:10.1007/s10714-008-0661-1 [arXiv:0405109 [gr-qc]]

[51] J. Silk and M. S. Turner, "Double Inflation," Phys. Rev. D **35**, 419 (1987) doi:10.1103/PhysRevD.35.419

[52] K. Enqvist, S. Nurmi, T. Tenkanen and K. Tuominen, "Standard Model with a real singlet scalar and inflation," JCAP **1408**, 035 (2014) doi:10.1088/1475-7516/2014/08/035 [arXiv:1407.0659 [astro-ph]].

[53] S. Nurmi, T. Tenkanen and K. Tuominen, "Inflationary Imprints on Dark Matter," JCAP **1511**, 001 (2015) doi:10.1088/1475-7516/2015/11/001 [arXiv:1506.04048 [astro-ph]].

[54] T. Markkanen, A. Rajantie and T. Tenkanen, "Spectator Dark Matter," Phys. Rev. D **98**, 123532 (2018) doi:10.1103/PhysRevD.98.123532 [arXiv:1811.02586 [astro-ph]].

[55] B. A. Bassett, S. Tsujikawa and D. Wands, "Inflation Dynamics and Reheating," Rev. Mod. Phys. **78** 537-589 (2006) doi:10.1103/RevModPhys.78.537 [arXiv:0507632 [astro-phh]].

[56] C. T. Byrnes and D. Wands, "Curvature and isocurvature perturbations from two-field inflation in a slow-roll expansion," Phys. Rev. D **74**, 043529 (2006) doi:10.1103/PhysRevD.74.043529 [arXiv:0605679 [astro-ph]].

[57] K. Enqvist, S. Nurmi, G. Rigopoulos, O. Taanila and T. Takahashi, "The Subdominant Curvaton," JCAP **0911**, 003 (2009) doi:10.1088/1475-7516/2009/11/003 [arXiv:0906.3126 [astro-ph]].

[58] V. Vennin, K. Koyama and D. Wands, "Encyclopaedia Curvatonis," JCAP **1511**, 008 (2015) doi:10.1088/1475-7516/2015/11/008 [arXiv:1507.07575 [astro-ph]].

[59] C. T. Byrnes, K. Enqvist, S. Nurmi and T. Takahashi, "Strongly scale-dependent polyspectra from curvaton self-interactions," JCAP **1111**, 011 (2011) doi:10.1088/1475-7516/2011/11/011 [arXiv:1108.2708 [astro-ph]].

[60] D. H. Lyth, C. Ungarelli and D. Wands, "Primordial density perturbation in the curvaton scenario," Phys. Rev. D **67**, 023503 (2003) doi:10.1103/PhysRevD.67.023503 [arXiv:0208055 [astro-ph]].

[61] C. T. Byrnes, M. Cortes and A. R. Liddle, "Comprehensive analysis of the simplest curvaton model," Phys. Rev. D **90**, 023523 (2014) doi:10.1103/PhysRevD.90.023523 [arXiv:1403.4591 [astro-ph]].

[62] K. Enqvist, S. Nurmi, O. Taanila and T. Takahashi, "Non-Gaussian Fingerprints of Self-Interacting Curvaton," JCAP **1004**, 009 (2010) doi:10.1088/1475-7516/2010/04/009 [arXiv:0912.4657 [astro-ph]].

[63] D. Langlois and F. Vernizzi, "Mixed inflaton and curvaton perturbations," Phys. Rev. D **70**, 063522 (2004) [arXiv:astro-ph/0403258];

[64] G. Lazarides, R. R. de Austri and R. Trotta, "Constraints on a mixed inflaton and curvaton scenario for the generation of the curvature perturbation," Phys. Rev. D **70**, 123527 (2004) [hep-ph/0409335].

[65] T. Moroi, T. Takahashi and Y. Toyoda, "Relaxing constraints on inflation models with curvaton," Phys. Rev. D **72**, 023502 (2005) [arXiv:hep-ph/0501007];

[66] T. Moroi and T. Takahashi, "Implications of the curvaton on inflationary cosmology," Phys. Rev. D **72**, 023505 (2005) [arXiv:0505339 [astro-ph]];

[67] K. Ichikawa, T. Suyama, T. Takahashi and M. Yamaguchi, "Non-Gaussianity, Spectral Index and Tensor Modes in Mixed Inflaton and Curvaton Models," Phys. Rev. D **78**, 023513 (2008) [arXiv:0802.4138 [astro-ph]].

[68] J. Fonseca and D. Wands, "Primordial non-Gaussianity from mixed inflaton-curvaton perturbations," JCAP **1206**, 028 (2012) [arXiv:1204.3443 [astro-ph]].

[69] K. Enqvist and T. Takahashi, "Mixed Inflaton and Spectator Field Models after Planck," JCAP **1310** (2013) 034 [arXiv:1306.5958 [astro-ph]].

[70] V. Vennin, K. Koyama and D. Wands, "Encyclopaedia curvatonis," JCAP **1511**, 008 (2015) [arXiv:1507.07575 [astro-ph]].

[71] K. Ichikawa, T. Suyama, T. Takahashi and M. Yamaguchi, "Primordial Curvature Fluctuation and Its Non-Gaussianity in Models with Modulated Reheating," Phys. Rev. D **78**, 063545 (2008) [arXiv:0807.3988 [astro-ph]].

[72] T. Suyama, T. Takahashi, M. Yamaguchi and S. Yokoyama, "On Classification of Models of Large Local-Type Non-Gaussianity," JCAP **1012**, 030 (2010) [arXiv:1009.1979 [astro-ph]].

[73] T. Fujita, M. Kawasaki and S. Yokoyama, "Curvaton in large field inflation," JCAP **1409**, 015 (2014) doi:10.1088/1475-7516/2014/09/015 [arXiv:1404.0951 [astro-ph]].

[74] K. Kainulainen, J. Leskinen, S. Nurmi and T. Takahashi, "CMB spectral distortions in generic two-field models," JCAP **1711**, no. 11, 002 (2017). © IOP Publishing Ltd and Sissa Medialab Srl. All rights reserved. doi:10.1088/1475-7516/2017/11/002 [arXiv:1707.01300 [astro-ph]].

[75] J. Chluba *et al.*, "Spectral Distortions of the CMB as a Probe of Inflation, Recombination, Structure Formation and Particle Physics," [arXiv:1903.04218 [astro-ph]].

[76] J. Chluba, "Future Steps in Cosmology using Spectral Distortions of the Cosmic Microwave Background," Lecture Notes (Varenna, 2018), [arXiv:1806.02915 [astro-ph]].

[77] W. Hu, "Wandering in the Background: A CMB Explorer," PhD thesis (1995), [arXiv:9508126 [astro-ph]].

[78] J. Chluba, "Science with Spectral Distortions of the Cosmic Microwave Background," CUSO Lectures (2014), [url: http://www.chluba.de/science].

[79] J. Chluba and R. A. Sunyaev, "The evolution of CMB spectral distortions in the early Universe," Mon. Not. Roy. Astron. Soc. **419** (2012) 1294 doi:10.1111/j.1365-2966.2011.19786.x [arXiv:1109.6552 [astro-ph]].

[80] L. Danese and G. De Zotti, "Double Compton process and the spectrum of the microwave background," Astronomy & Astrophysics, **107** (1982).

[81] J. Chluba *et al.*, "New Horizons in Cosmology with Spectral Distortions of the Cosmic Microwave Background," [arXiv:1909.01593 [astro-ph]].

[82] Y. B. Zeldovich and R. A. Sunyaev, "The interaction of matter and radiation in a hot-model universe," Astrophys Space Sci **4** 301-316 (1969) doi:10.1007/BF00661821

[83] J. E. Carlstrom, G. P. Holder and E. D. Reese, "Cosmology with the Sunyaev-Zeldovich effect," Ann. Rev. Astron. Astrophys. **40** 643-680 (2002) doi:10.1146/annurev.astro.40.060401.093803 [arXiv:0208192 [astro-ph]]

[84] R. Khatri and R. A. Sunyaev, "Beyond y and μ: the shape of the CMB spectral distortions in the intermediate epoch, $1.5x10^4 < z < 2x10^5$," JCAP **1209** (2012) 016 doi:10.1088/1475-7516/2012/09/016 [arXiv:1207.6654 [astro-ph]].

[85] J. Chluba and D. Jeong, "Teasing bits of information out of the CMB energy spectrum ," Mon. Not. Roy. Astron. Soc. **438** 3 2065-2082 (2014) doi:10.1093/mnras/stt2327 [arXiv:1306.5751 [astro-ph]]

[86] J. Chluba,, "Refined approximations for the distortion visibility function and ÎŒ-type spectral distortions," Mon. Not. Roy. Astron. Soc. **440**, 2544 (2014) doi:10.1093/mnras/stu414 [arXiv:1312.6030 [astro-ph]].

[87] W. Hu and J. Silk, "Thermalization and spectral distortions of the cosmic background radiation," Phys. Rev. D **48** (1993) 485. doi:10.1103/PhysRevD.48.485

[88] W. Hu, D. Scott and J. Silk, "Power Spectrum Constraints from Spectral Distortions in the Cosmic Microwave Background," ApJ **430** (1994) 001 doi:10.1086/187424

[89] J. B. Dent, D. A. Easson and H. Tashiro, "Cosmological constraints from CMB distortion," Phys. Rev. D **86**, 023514 (2012) doi:10.1103/PhysRevD.86.023514 [arXiv:1202.6066 [astro-ph]].

[90] R. Khatri, R. A. Sunyaev and J. Chluba, "Does Bose-Einstein condensation of CMB photons cancel μ distortions created by dissipation of sound waves in the early Universe?," Astron. Astrophys. **540**, A124 (2012) doi:10.1051/0004-6361/201118194 [arXiv:1110.0475 [astro-ph]].

[91] J. Chluba, R. Khatri and R. A. Sunyaev, "Mixing of blackbodies: entropy production and dissipation of sound waves in the early Universe," Astronomy & Astrophysics, **543**, A136 (2012) doi:10.1051/0004-6361/201219590 [arXiv:1205.2871 [astro-ph]].

[92] J. Chluba, R. Khatri and R. A. Sunyaev, "CMB at 2x2 order: The dissipation of primordial acoustic waves and the observable part of the associated energy release," Mon. Not. Roy. Astron. Soc. **425**, 1129 (2012) doi:10.1111/j.1365-2966.2012.21474.x [arXiv:1202.0057 [astro-ph]].

[93] E. Pajer and M. Zaldarriaga, "A hydrodynamical approach to CMB μ-distortion from primordial perturbations," JCAP **1409**, 036 (2013) doi:10.1088/1475-7516/2013/02/036 [arXiv:1206.4479 [astro-ph]].

[94] S. Weinberg, "Cosmology," Oxford University Press (2008), ISBN: 978-0-19-852682-7, doi:10.1007/s10714-008-0728-z .

[95] R. Khatri, "Mixing of blackbodies: Increasing our view of inflation to 17 e-folds with spectral distortions from Silk damping," [arXiv:1302.5633 [astro-ph]].

[96] C. T. Byrnes, P. S. Cole and S. P. Patil, "Steepest growth of the power spectrum and primordial black holes," JCAP **1906** (2019) 028 doi:10.1088/1475-7516/2019/06/028 [arXiv:1811.11158 [astro-ph]].

[97] A. Kogut *et al.* [PIXIE Collaboration], JCAP **1107** (2011) 025 doi:10.1088/1475-7516/2011/07/025

[98] G. Cabass, A. Melchiorri and E. Pajer, "μ distortions or running: A guaranteed discovery from CMB spectrometry," Phys. Rev. D **93**, no. 8, 083515 (2016) doi:10.1103/PhysRevD.93.083515 [arXiv:1602.05578 [astro-ph]].

[99] S. Clesse, B. Garbrecht and Y. Zhu, "Testing inflation and curvaton scenarios with CMB distortions," JCAP **1410** (2014) 046 doi:10.1088/1475-7516/2014/10/046 [arXiv:1402.2257 [astro-ph]].

[100] K. Enqvist, T. Sekiguchi and T. Takahashi, "Mixed Inflaton and Spectator Field Models: CMB constraints and μ distortion," JCAP **1604**, no. 04, 057 (2016) doi:10.1088/1475-7516/2016/04/057 [arXiv:1511.09304 [astro-ph]].

[101] P. A. R. Ade *et al.* [Planck Collaboration], "Planck 2015 results. XX. Constraints on inflation," Astron. Astrophys. **594**, A20 (2016) doi:10.1051/0004-6361/201525898 [arXiv:1502.02114 [astro-ph]].

[102] W. H. Kinney, A. Moradinezhad Dizgah, B. A. Powell and A. Riotto, "Inflaton or curvaton? Constraints on bimodal primordial spectra from mixed perturbations" Phys. Rev. D **86** (2012) no.2, 023527 doi:10.1103/PhysRevD.86.023527 [arXiv:1203.0693 [astro-ph]].

[103] P. A. R. Ade *et al.* [BICEP2 and Keck Array Collaborations], "Improved Constraints on Cosmology and Foregrounds from BICEP2 and Keck Array Cosmic Microwave Background Data with Inclusion of 95 GHz Band," Phys. Rev. Lett. **116**, 031302 (2016) doi:10.1103/PhysRevLett.116.031302 [arXiv:1510.09217 [astro-ph]].

[104] D. Barron *et al.*, "Optimization Study for the Experimental Configuration of CMB-S4," [arXiv:1702.07467 [astro-ph]].

ORIGINAL PAPERS

PI

"CMB SPECTRAL DISTORTIONS IN GENERIC TWO-FIELD MODELS"

by

Kimmo Kainulainen, Juuso Leskinen, Sami Nurmi and Tomo Takahashi

JCAP **1711**, 11, 002 (2017).

 doi: 10.1088/1475-7516/2017/11/002.